FLEXURAL BEHAVIOR OF A GLASS FIBER REINFORCED WOOD FIBER COMPOSITE,

by

Stephen John Smulski

Dissertation submitted to the Faculty of the
Virginia Polytechnic Institute and State University
in partial fulfillment of the requirements for the degree of

DOCTOR OF PHILOSOPHY

in

Forestry and Forest Products

APPROVED:

G. Ifju, Chairman

W. G. Glasser

J. P. Wightman

F. A. Kamke

H. F. Brinson

December, 1985

Blacksburg, Virginia

FLEXURAL BEHAVIOR OF A GLASS FIBER REINFORCED WOOD FIBER COMPOSITE

by

Stephen John Smulski

Committee Chairman: Geza Ifju

Forest Products

(ABSTRACT)

The static and dynamic flexural properties of a wood fiber matrix internally reinforced with continuous glass fibers were investigated. When modelled as a sandwich composite, the static flexural modulus of elasticity (MOE) of glass fiber reinforced hardboard could be successfully predicted from the static flexural MOE of the wood fiber matrix, and the tensile MOE and effective volume fraction of the glass fiber reinforcement. Under the same assumption, the composite modulus of rupture (MOR) was a function of the reinforcement tensile MOE and effective volume fraction, and the matrix stress at failure. The composite MOR was predicted on this basis with limited success.

The static flexural modulus of elasticity, dynamic modulus of elasticity, and modulus of rupture of glass fiber reinforced hardboard increased with increasing effective reinforcement volume fraction. The logarithmic decrement of the composite decreased with increasing effective reinforcement volume fraction. Excellent linear correlation found among flexural properties determined in destructive static tests

and nondestructive dynamic tests demonstrated the usefulness of dynamic test methods for flexural property evaluation.

The short-term flexural creep behavior of glass fiber reinforced hardboard was accurately described by a 4-element linear viscoelastic model. Excellent agreement existed between predicted and observed creep deflections based on nonlinear regression estimates of model parameters.

ACKNOWLEDGEMENTS

The author wishes to extend his sincere gratitude and appreciation to the following individuals for guidance and materials provided:

Georgia Pacific Corp.

Georgia Pacific Corp.

Burlington Glass Fabrics Co.

Burlington Glass Fabrics Co.

Burlington Glass Fabrics Co.

Owens Corning Fiberglas Corp.

Masonite Corp.

Masonite Corp.

I wish to thank past and present committee members for their critique of this work, and for the numerous suggestions offered to me:

Dr. Wolfgang Glasser	Forest Products
Dr. Fred Kamke	Forest Products
Dr. Al DeBonis, formerly	Forest Products
Dr. Greg Moore, formerly	Forest Products
Dr. James Wightman	Chemistry
Dr. Hal Brinson	Engineering Science and Mechanics

The technical assistance of of the Thomas Brooks Forest Products Center is appreciated.

Lastly, I would like to gratefully acknowledge the guidance and support provided to me by my major professor, Dr. Geza Ifju.

TABLE OF CONTENTS

TABLE OF CONTENTS cont.

TABLE OF CONTENTS cont.

TABLE OF CONTENTS cont.

LIST OF FIGURES

LIST OF FIGURES cont.

LIST OF FIGURES cont.

LIST OF FIGURES cont.

LIST OF TABLES

LIST OF TABLES cont.

LIST OF SUBSCRIPTS AND SYMBOLS

Subscripts

c	composite
f	glass fiber reinforcement
hyp	hypothetical
m	wood fiber matrix
obs	observed
prd	predicted

Symbols

a	distance between support and point load (in)
A_i	cross sectional area of lamina i (in^2)
b	width (in)
d	depth (in)
D_i	distance from neutral axis to centroid of lamina i (in)
E	true modulus of elasticity (psi)
E_e	instantaneous modulus of elasticity (psi)
E_d	delayed modulus of elasticity (psi)
E'	dynamic modulus of elasticity (psi)
E"	loss modulus (psi)
E*	complex modulus (psi)
f_r	fundamental resonant frequency of vibration (Hz)
f_1, f_2	frequency at $1/\sqrt{2}$ times maximum amplitude of vibration (Hz)
G	in-plane modulus of rigidity (psi)
I	moment of inertia about neutral axis (in^4)

LIST OF SUBSCRIPTS AND SYMBOLS cont.

I'	transform moment of inertia (in^4)
i	$\sqrt{-1}$
l	test span (in)
L	length (in)
MOE	apparent modulus of elasticity (psi)
MOR	modulus of rupture (psi)
M	applied moment (in-lb)
n	ratio of E/G
N	shear stiffness (lbs)
P	load (lbs)
t	time (hr)
v	volume (in^3)
V	volume fraction
w	weight (lbs)
x	distance from neutral axis (in)
x_m	distance from neutral axis to extreme tension fiber of matrix (in)
y	center point deflection (in)
α	level of statistical significance
δ	angle of phase lag between stress and strain (o)
$\tan \delta$	loss tangent
Δ	logarithmic decrement
ε	strain (in in^{-1})
η_d	delayed coefficient of viscosity (psi-hr)

LIST OF SUBSCRIPTS AND SYMBOLS cont.

η_v	viscous coefficient of viscosity (psi-hr)
σ	bending stress (psi)
τ	retardation time (hr)

INTRODUCTION

Hardboard has seen limited use in structural applications. The high interlaminar shear strength of hardboard has permitted its use where loads will act parallel to its surface. Hence, it is used as a shear-web in box and I-beams. Inadequate flexural stiffness and strength, however, have precluded hardboard from applications where loads will act normal to its surface. A method for enhancing the flexural properties of hardboard is needed if its present structural use-spectrum is to be broadened.

Significant enhancement of the flexural properties of solid wood, plywood and particleboard has been accomplished by bonding glass fiber reinforced polymer overlays to their surfaces. It was hypothesized that a similar strengthening effect could be achieved by incorporating a woven glass fiber fabric within the hardboard matrix. Further, it was assumed that the flexural behavior of glass fiber reinforced hardboard could be explained using composite material concepts. The reinforced wood fiber/glass fiber composite envisioned may then compete in the structural panels market, from which hardboard is virtually excluded.

OBJECTIVES

The first objective of this investigation was to examine the effect of reinforcement volume fraction on the static and dynamic flexural properties of a hardboard matrix internally reinforced with continuous glass fibers. The properties examined were the static modulus of elasticity, the modulus of rupture, the dynamic modulus of elasticity, and the logarithmic decrement.

A second objective was the identification of predictive equations relating certain constituent properties and composite static flexural modulus of elasticity and modulus of rupture. The constituent properties considered included the static modulus of elasticity and the modulus of rupture of the hardboard matrix, and the tensile modulus of elasticity and volume fraction of the glass fiber reinforcement.

A third objective was to identify empirical relationships between flexural properties obtained from nondestructive dynamic and destructive static test methods. Relationships between the static modulus of elasticity and the dynamic modulus of elasticity, the modulus of rupture and the dynamic modulus of elasticity, and the modulus of rupture and the static modulus of elasticity were examined.

A fourth objective was to investigate the effect of reinforcement volume fraction and load level on the short-term creep behavior of glass fiber reinforced hardboard within the elastic limit. A subordinate objective was to estimate the parameters of a four-element

linear viscoelastic creep model chosen to represent the composite's creep behavior.

Auxilary objectives included identification of the mechanism of stress transfer between matrix and reinforcement, and discernment of the mode of composite failure.

REVIEW OF LITERATURE

Composite Materials

A composite material is composed of two or more distinct substances, which when combined, produce a material with structural or functional properties not found in any one component. The properties of a composite are a function of the relative amounts, spatial distribution and properties of the composing elements, as well as the interactions between them. Composites afford a more efficient use of materials, as in their design, strength can be added where needed, and deleted where unnecessary. Directional properties can be tightly controlled so that highly anisotropic composites able to resist stresses differing in direction, magnitude and type are possible. A small variation in property values between composites of identical construction is typical. In general, multi-component materials offer increased efficiency of design, control of properties and surety of performance over most mono-component materials. Agarwal and Broutman (1980) present an extended discussion of composite material concepts.

Wood Composites

At present, there exist many composites whose dominant comprising element is wood. Wood elements may be of fiber, particle, strand, flake, wafer, veneer or lumber form. Individual elements are conjoined with adhesive resins or mechanical fasteners to produce the

composite. Hardboard, particleboard, oriented strandboard, flakeboard, waferboard, plywood and laminated timbers are common wood composites. These primary composites may be further combined to produce secondary composites such as particleboard overlaid with veneer, or box and I-beams of plywood webs fastened to structural lumber flanges.

There also exist many less common composite wood products in which wood may or may not be the dominant element. Exemplary products include wood/metal and wood/cement building components, wood flour filled polymer molding compounds, polymer impregnated wood, wood fiber reinforced polymers, mineral filled paper products and chemically modified wood.

Wood/metal composites for structural use have generated the greatest interest. The reader is referred to a review by Bulleit (1984) for a comprehensive treatment of the topic.

Wood/Glass Fiber Composites

The configuration of wood/glass fiber composites is varied, and influences the form of both the glass fiber and wood components. Lumber, veneer and reconstituted wood particle panels typify the wood component. Parallel, continuous strands of glass fiber embedded in a polymer matrix are available in ribbon and sheet form. They are commonly used as a surface reinforcement in composite beams because of their anisotropy. Continuous glass fibers woven into fabric, and discontinuous glass fibers randomly felted into mats are both

essentially isotropic and have seen use in both beam and panel applications. Short, chopped glass fibers find use in reconstituted panel products where they can be dispersed among the wood particles.

Glass fiber must be placed on or near the composite surface to take best advantage of its great tensile strength. A viable glass fiber/wood adhesive bond is required to effect load sharing between the two. Epoxy and phenolic resins have demonstrated compatibility with both substrates. Difunctional amino silane coupling agents have also been used to promote adhesion. One terminal group of the linear molecule is designed to react with the reinforcement; the other with the matrix. Silane selection is made in consideration of the reactive functional groups present in the reinforcement and matrix.

An up-to-date survey of research conducted on wood/glass fiber composites is next presented. The survey is organized first according to the form of the wood component: pole, solid or laminated beam, plywood, particleboard and hardboard. Within each wood form category, individual investigations are reviewed in chronological order.

Mark and Zuckerman (1958) described one of the earliest applications of glass fiber in the wood products industry. Viz., glass fiber reinforced polymer overlays used to impart water imperviousness and decay immunity to wood and plywood used in marine applications.

Mark et al. (1968) and Tang and Adams (1973) applied the concept to wood transmission poles which were jacketed with multiple plies of unidirectional glass fiber reinforced polymer. They observed an

increase of 12 to 21 percent in flexural modulus of elasticity (E) of full size reinforced poles over that of nonreinforced controls. Good agreement existed between the observed stress distribution in the pole composite when flexed as a cantilever beam and that calculated from a theoretical elasticity solution (Adams et al. 1967).

Wangaard (1964) bonded unidirectional glass fiber reinforced epoxy polymer to the tension and compression surfaces of solid wood beams with epoxy resin. Two theoretical approaches were employed to predict the apparent flexural modulus of elasticity (MOE) of the composite beams. The first ignored shear deformation of the wood core. The stiffness of the composite beam (i.e., E times moment of inertia, I) was calculated as the sum of the stiffnesses of its components, as described by Dietz (1949). Values of MOE predicted by this method were 6 to 14 percent higher than observed values over a core wood specific gravity (sp gr) range of 0.40 to 0.93. A second method adapted from Kuenzi (1959) in which the composite beams were treated as structural sandwiches, accounted for shear deformation of the wood core. The stiffness of the composite beam was calculated as before, except that E replaces MOE. An apparent deflection representing deformation due to both bending and shear was calculated based on beam stiffness. MOE was obtained by using the apparent deflection in the usual formula for calculating MOE when shear effects are ignored. (A detailed mathematical explanation of this technique is presented in the Modulus of Elasticity of Glass Fiber Reinforced Hardboard chapter.) Values for MOE predicted when deflection due to

shear was accounted for were 2 to 8 percent lower than observed values over the same core wood specific gravity range.

Wangaard noted that the greatest gains in observed MOE of composite beams versus controls were made at the lower core wood specific gravities, and decreased dramatically as core wood specific gravity increased. The observed MOE of balsa (sp gr 0.09) core composite beams was four times that of the core itself, for example, while no increase in MOE was observed for hickory (sp gr 0.93) core composite beams.

Biblis (1965), who participated in Wangaard's study, reanalyzed the data in verification of a method he proposed for predicting bending moment at both the load at proportional limit and the load at 90 percent of ultimate. The complexity of the method precludes it from being described completely here; the reader is referred to the original publication. The method is based on the customary flexure formula, and accounts for shear deformation of the wood core. The actual composite beam cross section is represented by an equivalent all-wood fictitious cross section of identical width, but with a "vertically transformed depth". The "vertically transformed depth" is the depth of a fictitious beam in which the glass fiber reinforced polymer faces have been replaced by equivalent core wood. As the observed MOE of wood varies considerably with the test span-to-depth ratio, Biblis' method can be used only when this relationship is known. Predicted values for bending moment at the load at proportional limit and the load at 90 percent of ultimate were

respectively, 1 to 8 percent and 1 to 18 percent lower than observed values over a core wood specific gravity range of 0.45 to 1.14. Composite beams failed in tension in the wood core, except at the highest wood specific gravities (0.93 and 1.14) where compression failure of the core occurred.

Woven glass fiber fabric was wrapped around the exterior of laminated wood beams and bonded in place by Theakston (1965). The load-carrying capacity of the beams was increased by 30 to 60 percent. He noted that the glass fiber reinforcement continued to support a substantial load even after the wood core had failed.

Spaun (1981) evaluated wood/glass fiber composite beams of a finger-jointed solid wood core overlaid on the tension and compression surfaces with veneer. Either 3.5 or 7 percent unidirectional glass fiber reinforcement by volume was embedded in the phenol-resorcinol bondline between core and veneer. The MOE of beams with 3.5 or 7 percent glass fiber as determined in static bending was 15 and 24 percent greater than the control MOE, respectively. When tested in tension, increases in tensile strength of 9 and 22 percent, respectively, over that of the controls were realized. Spaun used the method of transformed sections in which the composite beam is replaced by an equivalent all-wood beam of larger cross section to "predict" its MOE. The necessary wood cross sectional area to be substituted is found by multiplying the actual cross sectional area of glass fiber by the ratio of the moduli of glass fiber and wood. The actual I of the composite beam is thus transformed to that of a larger, all-wood beam.

The transformed I is then used in the usual formula for calculating MOE. "Predicted" values were in excellent agreement with those empirically observed.

Five-ply laminated wood beams with two plies of unidirectional glass fiber embedded in each bondline were tested in static bending by Rowlands et al. (1982). The reinforcement volume fraction was 0.18. A 21 percent increase in beam stiffness over that of the controls was realized. The tensile strength and modulus of small coupons cut from the reinforced beams were on average 85 and 28 percent higher than those of nonreinforced controls. Tensile E as predicted by the rule of mixtures, in which the composite property is equal to the sum of the products of each component property and its volume fraction, were in poor agreement with experimental values.

The American Plywood Association has done extensive testing of plywood overlaid with glass fiber reinforced polymer (APA 1972, Poplis and Mitzner 1973, Mitzner 1973). Two plies of unidirectional glass fiber laid at right angles to one another, or a single ply of either bidirectional woven glass fabric or randomly felted discontinuous glass fibers are used to produce essentially isotropic surface reinforced plywood panels.

Methods for predicting the stiffness and maximum moment capacity of reinforced panels based on the same properties of the plywood and glass fiber reinforced plastic overlay were given. Essentially, the composite is treated as a structural sandwich. The data from which predictive equations are derived were generated by subjecting the

panels to pure bending moment. Predicted values of stiffness and maximum moment capacity are in excellent agreement with experimental results.

Boehme and Schulz (1974) analyzed plywood and particleboard panels overlaid with bidirectional woven glass fiber reinforced polymer as structural sandwiches. The authors presented graphical data in which the composite stiffness, modulus of rupture (MOR) and tensile and compressive strengths were plotted against overlay thickness for several core thicknesses. Each property increased with increasing overlay thickness for all core thicknesses. The greatest gains in bending stiffness and MOR were made with the largest core thickness, illustrating the importance of placing the reinforcement as far as possible from the neutral axis. The smallest core thickness, however, exhibited the greatest increase in tensile and compressive strengths. At the smallest core thickness the percentage of the composite cross sectional area occupied by high strength glass fiber increased rapidly as overlay thickness increased. The result is a concurrent rapid increase in composite tensile and compressive strengths.

Boehme (1976a) compared the experimental results of the above study with those predicted by a theoretical analysis in which the flexural and tensile E and MOR were expressed as functions of the overlay thickness. Good agreement was shown to exist between calculated and observed flexural MOR and tensile E, but theoretical values for flexural E and tensile MOR were unsatisfactory.

Boehme (1976b) next reported the creep behavior of the sandwich panels used in the 1974 study. The author loaded in flexure both reinforced and nonreinforced particleboard and plywood panels to one-third of ultimate load and subjected them to cyclic relative humidity. Control particleboard and plywood panels failed in 28 and 17 weeks, respectively. The corresponding total creep deflections were 13 and 11 times the initial deflections upon loading. Over the same time intervals, reinforced particleboard and plywood panels exhibited a total creep only 3 and 2 times their intial deflections, respectively, regardless of overlay thickness. When overlaid panels were unloaded at 57 weeks, total creep had increased negligibly beyond that observed at failure of the controls. Boehme also noted that the moisture content of reinforced panels was considerably less than that of the controls, and attributed this to the impervious overlay.

Extruded dimension lumber beams composed of urea formaldehyde-bonded wood wafers, and reinforced throughout the cross section with continuous glass fibers, were produced by Saucier and Holman (1975). The MOE of reinforced particlebeams was twice that of nonreinforced controls, while the MOR of experimental members was one and one-half to two and one-half times that of the controls. The authors noted that no specific attempt was made to bond the glass fibers to the wood particles. Load sharing between matrix and reinforcement probably was effected only by frictional forces due to mechanical entrapment of glass fibers.

Bulleit (1981) bonded continuous unidirectional glass fiber mats impregnated with a phenol-resorcinol resin to the surfaces of particleboard. The dynamic modulus of elasticity and in-plane modulus of rigidity (G) of the particleboard, and the tensile and compressive moduli, strengths, and Poisson's ratios of both the particleboard and reinforcement were empirically determined. Reinforced particleboard beams were modelled first as structural sandwiches using the method of transformed sections, and secondly as laminated plate strips. Beam stiffness predicted by either method underestimated that experimentally observed by only 3.5 percent. The stiffness and ultimate moment capacity of reinforced beams were 3.4 and 2.8 times greater than those of the nonreinforced particleboard, respectively.

Bulleit also studied the flexural behavior of reinforced particleboard plates modelled as laminated composite plates. The predicted center deflection of unidirectionally reinforced plates under a point or uniform load was 9 to 17 percent and 29 to 33 percent less than that empirically observed, respectively. Center deflections predicted for bidirectionally reinforced plates underestimated observed values by 1 and 31 percent under the same conditions. Bulleit attributed the wider departure in predicted versus observed values for uniformly loaded plates to a shortcoming in experimental procedure.

Cavlin and Back (1968) blended 5 or 10 percent by weight chopped glass fiber into a wet-process hardboard furnish to enhance its dimensional stability. Their work represents the first reported wood

fiber/glass fiber composite. Panels ranging in specific gravity from 0.2 to 1.0 were isothermally cycled through a 30 to 100 percent relative humidity environment. Linear expansion of composite panels was reduced by 40 percent compared to that of the controls. Thickness swelling, permanent dimensional change and hygroscopicity of composite panels were slightly reduced with the addition of glass fibers. All effects were greater in panels at the higher glass fiber volume fraction, and were most pronounced in the 0.2 to 0.6 specific gravity range. Glass fibers in a hardboard matrix inhibit the swelling of those wood fibers to which they are bonded, thereby reducing the magnitude of the overall panel volumetric change.

Nishikawa et al. (1974) added from 5 to 50 percent by weight chopped glass fiber to a wet-process hardboard furnish. The trends in panel dimensional stability and hygroscopicity mirrored those reported by Cavlin and Back (1968). No further enhancement of dimensional stability occurred at greater than 15 percent glass fiber addition. Flexural, tensile, impact and internal bond strengths of the composite at 5 percent glass fiber addition were slightly higher than those of the controls. With greater addition of reinforcement, however, all composite properties decayed rapidly. Short-fiber composites may exhibit strength-reduction with increasing addition of reinforcement due to low interfacial shear strength which prohibits transfer of significant stress to the fibers. At high stress levels, the short fibers may act more like voids and simply reduce the effective composite cross section (Agarwal and Broutman 1980).

Nishikawa et al. (1975) expanded their original study to examine the effect of reinforcement form and fiber type on wet-process hardboard properties. Hardboard reinforced with chopped glass fibers, rock-wool, glass-wool, slug-wool and asbestos fibers was produced. All reinforcement forms and fiber types produced similar increases in hardboard dimensional stability and decreases in hygroscopicity. Again, flexural, tensile, impact and internal bond strengths deteriorated with increasing reinforcement. The authors concluded that use of chopped glass fiber optimized composite properties on a cost/benefit basis.

Essentially unidirectional woven glass fiber fabric treated with phenolic resin was bonded to the surfaces of dry-process hardboard *in situ* by Steinmetz (1977). The flexural MOE and MOR and tensile strength of panels of 0.80 sp gr were respectively, 29, 37 and 31 percent higher than that of the controls. Linear expansion was reduced by 40 percent; compressive strength was unaffected. The corresponding increases for panels of 0.95 sp gr were 49, 45 and 31 percent. Linear expansion was reduced by 70 percent; again, compressive strength was unaffected. Steinmetz noted that the reinforced composite failed on the tension side during flexure, while nonreinforced controls failed on the compression side as normally occurs in dry-process hardboard.

Summary

Virtually all of the wood/glass fiber composites described above were successful in the laboratory in terms of property enhancement. Few, however, have seen commercial success owing to the superior economics of competing materials. Plywood overlaid with glass fiber reinforced polymer is the exception. Wide use is made of it in the trucking and containerized shipping industries owing to its high strength to weight ratio, durability and repairability. Laufenberg et al. (1984) concluded that laminated veneer lumber reinforced with continuous unidirectional glass fibers could be profitable under existing market conditions.

It is evident that judicious reinforcement of wood components with glass fibers yields a composite material of superior mechanical performance. Wood/glass fiber composites show typically, enhanced flexural properties as well as a marked reduction of creep deflection under sustained loading. Optimal property enhancement is achieved by bonding glass fiber to wood, and by placing the glass fiber as far as possible from the composite's neutral axis.

It has been demonstrated that the flexural properties of certain wood/glass fiber composites can be accurately predicted from the material properties of their components when modelled as a structural sandwich or laminated composite.

Hardboard Stiffness and Strength

The mechanical and physical properties typical of commercial hardboard at normal temperature and humidity are presented in Table 1. A discussion of the factors influencing hardboard properties follows.

Stillinger and Coggan (1956) investigated the influence of moisture content on the flexural MOE and MOR of 25 commercial hardboards and found the trend similar to that for solid wood; viz., that both properties are lowest at the highest moisture content, and increase with decreasing moisture content. Hardboard properties deviate from those of solid wood at moisture contents in equilibrium with relative humidities of 30 to 0 percent. In this range, wood continues to increase in MOE and MOR, becoming greatest near 0 percent equilibrium moisture content. Hardboard panels showed a maximum in MOE and MOR at equilibrium moisture contents attained under 30 to 10 percent relative humidity. At lower relative humidities, MOE and MOR values became erratic, with some panels increasing in strength, while others decreased or showed no change in strength. Work to maximum load was smallest for oven dry panels, and increased to a maximum in panels exposed to the highest relative humidities. This is unlike the trend for solid wood, in which work to maximum load is essentially constant as moisture content increases.

McNatt (1974) also investigated the effect of equilibrium moisture content on hardboard mechanical properties. Hardboard is less hygroscopic than solid wood; under the same relative humidity and

Table 1. Typical mechanical properties of commercial hardboards.[a]

Property	Unit	Medium-density hardboard	High-density hardboard	Tempered hardboard
Density	pcf	33-50	50-80	60-80
Specific gravity	---	0.53-0.80	0.80-1.28	0.93-1.28
Modulus of elasticity (bending)	1,000 psi	325-700	400-800	650-1,100
Modulus of rupture	psi	1,900-6,000	3,000-7,000	5,600-10,000
Tensile strength parallel to surface	psi	1,000-4,000	3,000-6,000	3,600-7,800
Tensile strength perpendicular to surface	psi	40-200	75-400	160-450
Compressive strength parallel to surface	psi	1,000-3,500	1,800-6,000	3,700-6,000
Shear strength (in plane of board)	psi	100-475	300-600	430-850
Shear strength (across plane of board)	psi	600-2,500	2,000-3,000	2,800-3,400
24-hour water absorption	pct. by wt.	5-20	3-30	3-20
Thickness swelling, 24-hour soaking	pct.	2-10	10-25	8-15
Linear expansion from 50-90% rel. humidity	pct.	0.2-0.4	0.15-0.45	0.15-0.45
Thermal conductivty at mean temp. of 75°F	$\frac{Btu\ in/hr}{ft^2\ ^oF}$	0.54-0.75	0.75-1.40	0.75-1.50

[a] Forest Products Laboratory (1974)

temperature conditions hardboard will attain, on average, an equilibrium moisture content only 50 to 60 percent of that of solid wood. Like wood, it too exhibits an adsorption/desorption hysteresis. The flexural MOE and MOR, and tensile, compressive and shear strengths of hardboard increase as panel moisture content decreases. Interlaminar shear shows the greatest change in moving from 0 to 90 percent relative humidity; MOR is least affected.

The flexural MOE and MOR of hardboard are directly proportional to panel specific gravity, as illustrated in a study of 36 commercial hardboards by Hofstrand (1958). He found strong empirical correlation between specific gravity and MOE and MOR for each hardboard tested. Variation in panel formation parameters such as wood species, resin binder and processing pressure and temperature, precluded development of a general predictive equation relating specific gravity and flexural MOE and MOR.

The effect of temperature on the MOE and MOR of hardboard at constant moisture content over the range of 0 to 200 ^{o}F was investigated by Haygreen and Sauer (1969). The MOR of both wet- and dry-process hardboard was a maximum at 0 ^{o}F and decreased linearly with rising temperature. The trend for MOE was similar, except that the decay with temperature was curvilinear.

Moslemi (1967) measured the dynamic modulus of elasticity and the logarithmic decrement of hardboard over the moisture content range of 0 to 16 percent. Logarithmic decrement, a measure of a material's damping capacity, increased with increasing moisture content, while

dynamic modulus decreased. The ratio of dynamic and static moduli of elasticity remained essentially constant over all moisture contents.

Hardboard Dimensional Stability

Hardboard, like all wood-based materials, shrinks and swells with the desorption or adsorption of water. Although its in-plane dimensional changes are small when compared to solid wood, panel thinness and the fact that in use panels are typically restrained often combine to induce out-of-plane buckling deflections. Suchsland (1964) discusses the mechanics of the buckling phenomenon.

Spalt and Sutton (1968) modelled hardboard strips fastened to wood frames as Euler columns and showed that buckling deflection of restrained hardboard is dependent upon only panel thickness and the length of the unsupported span. McNatt (1973) also studied hardboard buckling behavior and found that it could be also related to panel specific gravity.

Hardboard Creep Behavior

Like solid wood and other wood composites, hardboard is viscoelastic in nature and exhibits mechanosorptive behavior (Grossman 1976). Its creep and stress relaxation behaviors are highly dependent upon panel moisture content and specific gravity, and magnitude and duration of load. Viscous deformation under constant load continues to increase with time so that prolonged loading even at low load

levels may induce failure. Based on the results of tensile creep studies, Lundgren (1957) recommended that only 15 percent of the strength shown by short term tests should be used as an estimate of strength for prolonged loading.

The linear viscoelastic nature of hardboard was demonstrated by Moslemi (1964a). He showed that the ratio of load to deflection was constant among specimens loaded in flexure from 10 to 60 percent of ultimate load. Numerical estimates for the parameters of a hardboard creep model comprising elastic, viscoelastic and viscous components were also presented.

Moslemi (1964b) monitored creep deflection in hardboard at three moisture contents loaded in flexure for two hours to 10, 30 or 60 percent of ultimate load. Deflection measured one minute after loading was assumed to represent the instantaneous elastic response. At all moisture contents, hardboard deflection increased with increasing load level and time. Creep rate and deflection were greatest for hardboard of high moisture content (16 to 19 percent), followed by panels of low moisture content (1 to 2 percent), and were least for hardboard at intermediate moisture content (6 to 8 percent) for all load levels. A plot of creep deflection with time became linear after approximately 1 hour for all load levels, except at the highest moisture content where it remained decidedly curvilinear. Moslemi estimated the stress relaxation behavior of hardboard from his creep data using Hansen's method (Hansen 1964). The trend in relaxation behavior was similar to that for creep: the least amount

of load relaxed at intermediate moisture contents, the greatest at high moisture contents.

Sauer and Haygreen (1968) investigated the effect of moisture adsorption and desorption on the creep deflection of hardboard loaded in flexure to 30 or 50 percent of ultimate load for 48 hours. The deflection measured one minute after application of load was assumed to represent instantaneous elastic deformation. Hardboard at 5 percent moisture content was loaded in flexure and allowed to isothermally adsorb until an equilibrium moisture content of 10 percent was achieved. Similarly, hardboard at 10 percent moisture content was allowed to desorb until a 5 percent equilibrium moisture content was attained. Creep deflection during adsorption and desorption was greater than that for hardboard at constant moisture content. Creep during adsorption for example, was twice as great as that during desorption and 2.6 times that at a constant 10 percent moisture content at 30 percent of ultimate load. Creep deflection was observed to increase with both temperature and load level.

Haygreen and Sauer (1969) developed predictive equations for creep deflection and rupture stress of hardboard as a function of time based on the results of static bending tests performed at temperatures ranging from 0 to 200 ^{o}F. The MOR of hardboard decreased linearly with increasing temperature. Hardboard MOE decreased in a curvilinear fashion with increasing temperature. A temperature-time equivalence as per that developed by Goldfein (1960) for creep and stress rupture in polymers was invoked. Data from static bending tests were used to

construct a master modulus curve from which the time-to-failure for any stress level and temperature combination can be determined. The stress required to induce flexural failure in hardboard decreased exponentially with time. Creep deflection with time increased exponentially.

McNatt (1970) investigated the effect of rate and duration of single and cyclic loading on the strength of oil-tempered hardboard. The observed strength of hardboard decreased with a decreased rate of loading. An approximate 8 percent reduction in strength was observed for each tenfold increase in time to maximum load. Hardboard subjected to constant stress showed an increase in magnitude of time to failure of 10 with each 8 percent decrease in load level. The fatigue strength of hardboard after 10 million cycles of stress was approximately 45 percent of the static strength in tension and shear. It was concluded that the behavior of hardboard under different rates and durations of loading was similar to that of solid wood.

The effect of moisture cycling on hardboard creep behavior was investigated by Armstrong and Grossman (1972). Hardboard at 6 and 18 percent moisture content was stressed in flexure under constant load for 40 days. Creep deflection was greatest at the higher moisture content. Creep deflection of hardboard at the lower moisture content increased steadily for 10 days, with little additional deflection accruing over the duration of the test. Creep deflection of hardboard at 18 percent moisture content increased steadily over the entire 40 days' duration, and was ultimately 4 times that of the lower moisture

content material. The moisture content of hardboard initially at 7 percent was gradually raised to 17 percent and then returned to 7 percent with the specimen under constant load. The rate of creep during adsorption exceeded that during desorption. Hardboard initially at 21 percent moisture content was subjected to cyclic desorption and adsorption under constant load. The rate of creep during desorption was greater than during adsorption.

It was concluded that the greatest increases in rate of creep occur during desorption, and that during adsorption the rate of creep is lower, except when adsorption is the first step of moisture cycling. This behavior is similar to that of solid wood. The largest increases in creep deflection in hardboard under constant load occur during the initial moisture change of moisture content cycling, whether it is adsorption or desorption. During subsequent moisture content changes, the greatest increase in creep deflection occurs during desorption, with smaller deflection occurring during adsorption.

Sutula and Moslemi (1973) examined the creep behavior of hardboard under constant load. They reported only that creep deflection increased with increasing moisture content.

Chow and Hanson (1979) evaluated a sandwich composite consisting of a hardboard core overlaid on both faces with oak veneer. Hardboard of four thicknesses, with three different specific gravities per thickness, and veneer of four different thicknesses were combined to produce twelve hardboard/veneer combinations. Composite beams were

loaded to a low, medium or high percentage of ultimate load and their creep deflection monitored over three weeks. Creep deflection decreased with both increasing hardboard specific gravity and increasing veneer thickness. Higher load levels produced greater creep deflections for all core specific gravity/overlay thickness combinations.

Hardboard Property Enhancement

Presently, several methods for enhancing hardboard properties are commercially practiced (Maloney 1977). Many material and processing parameters interact to influence hardboard properties. Wood species and specific gravity, fiber acidity and moisture content are among the most important (Mataki 1972, Nelson 1973, Myers 1977). Two to 4 percent adhesive resin is usually added to the wood fiber furnish in promotion of interfiber bonding. The strength and stiffness of hardboard increase as the degree and tenacity of interfiber bonding increases.

Specific gravity is the greatest determinant of hardboard strength and stiffness. There exists through the thickness of a hardboard panel a specific gravity profile. The panel shell is of higher specific gravity than the core, owing to the shell's direct contact with the hot press platens during manufacture. Wood fiber at the surface is heated, plasticized and compressed while that in the core is still relatively cool and incompressible. Adhesive resin near

the surface cures first, holding the wood fiber at a higher specific gravity. Eventually, the temperature of the core rises to allow compaction of the wood fiber, which now sets at a lower specific gravity. In this sense, hardboard is a sandwich material with higher strength (i.e., higher specific gravity) faces atop a lower strength core.

Commercial hardboard is mildly anisotropic due to an aligning of wood fibers parallel to the direction of material flow that occurs during felting of the furnish. Mechanical properties are sometimes reported for specimens oriented in both the machine and cross directions. Laboratory-sized specimens lack this anisotropy, as they are generally felted manually. Alignment of wood fibers increases panel MOE, MOR and dimensional stability in the direction of alignment (Steinmetz and Polley 1974, Woodson 1977).

The water resistance of hardboard can be increased by the addition of 0.5 to 1.0 percent wax emulsion to the wood furnish. Wax serves only to retard the uptake of liquid water; water vapor is adsorbed unimpeded. Dimensional stability is improved only slightly. A greater improvement in dimension stability can be achieved by coating hardboard surfaces with an impermeable resin (Steinmetz and Fahey 1968). Exposing hardboard to temperatures of 300 to 400 ^{o}F for several hours induces covalent bond formation between wood fibers, which enhances dimensional stability (Klinga and Back 1964). Oil-tempered hardboard has excellent dimensional stability. Hardboard is

dipped in linseed oil, then removed to a drying oven where the oil is polymerized. Small gains in flexural properties also result.

The addition of fire retardants and preservatives to hardboard often has the effect of increasing its hygroscopicity due to the additive's hydrophilic nature. Hardboard properties, however, decay at a much faster rate with increasing moisture content than those of solid wood (Sauer and Haygreen 1968).

Summary

Nearly 8 billion square feet (one-eighth inch basis) of hardboard was consumed in the United States in 1979 (Ulrich 1981). Annual consumption is expected to rise slowly through the turn of the century. Virtually all hardboard produced is used in nonload-bearing applications owing to its limited flexural properties when compared to plywood or solid wood of comparable dimensions. Inadequate stiffness, excessive creep under load and dimensional instability are in descending importance, its greatest liabilities. Currently, major nonstructural hardboard applications include its use as exterior siding and roofing, door and furniture panels, wall paneling, automobile, truck, and trailer panels, laboratory bench tops and outdoor signs.

The high interlaminar shear strength of hardboard permits its use as a shear-web in box and I-beams. England, West Germany and Sweden have published allowable design loads for structural use of hardboard

(Lundgren 1969, Chan 1977, McNatt 1980). Hardboard-webbed roof rafters, floor joists and framing members have been used in residential and light commercial construction there, as well as in Australia, Czechoslovakia, Java and the United States. Typically, oil-tempered hardboard is used because of its superior strength and water resistance. Hardboard, when used as a shear-web in box and I-beams, is a viable structural material. However, hardboard-webbed beams exhibit excessive deflection, and wrinkling and buckling of the hardboard webs during prolonged exposure to high relative humidities (Superfesky and Ramaker 1978, McNatt and Superfesky 1983).

With the exception of oil-tempering, the gains made in hardboard strength, stiffness and dimensional stability using existing enhancement methods are small. Increasing the flexural properties of hardboard to a level where it can compete with other structural panel materials can be brought about only by combination with a high modulus reinforcing material.

MATERIALS

Wood Fiber

Thermomechanical wood fiber consisting of mixed oak, maple, beech and birch fibers with 2.5 percent by weight phenolic resin and petrolatum additives was obtained from Masonite Corporation. The fiber was refined from green chips in an Asplund single disc defibrator under 110 psi steam pressure at a temperature in excess of 260 ^{o}F. Under these conditions, individual wood cells are separated at the middle lamella as the lignin composing this region softens and fails in shear against the rotating disc. Thermomechanical wood fiber consists of about 60 percent fiber bundles, 40 percent individual fibers and some fiber fines and fragments. Fiber surfaces show in some areas the unoriented cellulose microfibrils composing the primary cell wall, and in others a smooth layer of amorphous middle lamella lignin (Koran 1970, Spalt 1977, Short 1981). The thermal softening properties of lignin are again exploited as wood fibers become autoadhesive when compressed under high pressures at elevated temperatures during hardboard manufacture.

Glass Fiber

A leno-weave bidirectional E-glass fiber fabric with 20 warp and 10 fill yarns per inch (10 X 10 visual) was obtained from Burlington Glass Fabrics Company (Figure 1). Each warp yarn is composed of 408

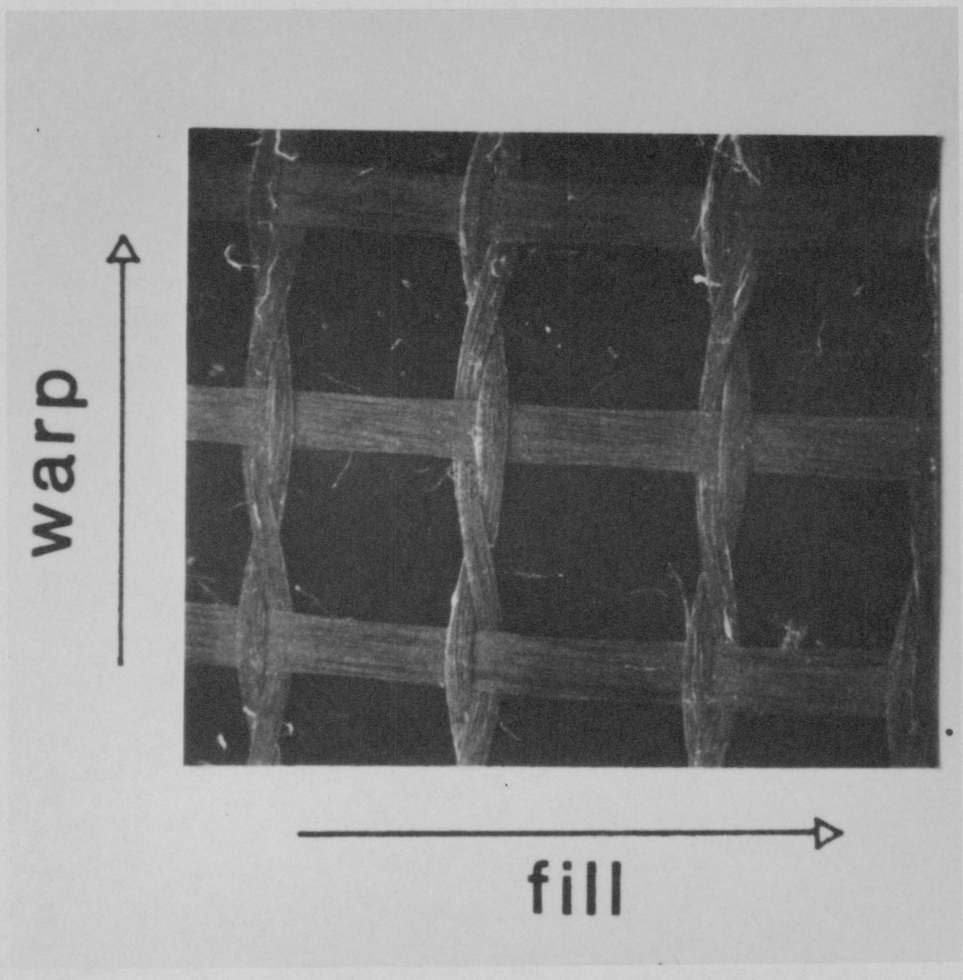

Figure 1. Glass fiber fabric. SEM 12X.

individual glass filaments 3.6×10^{-4} inches in diameter. Fill yarns are composed of 816 individual filaments of identical diameter. Warp yarns alternately pass over and under fill yarns so that proper spacing is maintained. As a result, fabric strength in the fill direction is greater. Fabric tensile moduli of elasticity and rupture were determined using 1 inch wide strips and a 3 inch gauge length. Observed values for both the as-received greige fabric, to which only a vegetable starch sizing has been applied to improve processability, and for fabric coated with a phenolic resin (see below) are presented in Table 2. A tensile stress/strain plot is found in Appendix 1. The specific gravity of glass fiber is 2.5.

Adhesive Resin

A powdered phenol-formaldehyde novolac resin supplied by Georgia-Pacific Corporation was used to bond glass fiber to wood fiber. The resin has commercially demonstrated compatibility with both substrates. The manufacturer's product information sheet is found in Appendix 2.

Panelmaking

Square hardboard panels 25 cm on a side and 6.35 mm thick with 0, 1, 2 or 3 plies of glass fiber fabric at 0.25 mm intervals below each surface were made using wood fiber at 6 percent moisture content. The wood fiber matrix target specific gravity was 0.95. Wood fiber layer

Table 2. Estimated glass fiber and hardboard properties.

Property	Glass Fiber Fabric[a]				Hardboard[b]
	Greige		Resin-Coated		
	Warp	Fill	Warp	Fill	
E[c]	2,492,000	3,245,000	2,589,000	3,272,000	450,900
	(57,000)	(59,200)	(129,700)	(26,300)	
MOR[c]	73,100	103,000	104,800	135,600	3,360
	(4,100)	(5,800)	(2,800)	(3,100)	
G[c]	---	---	---	---	34,700
failure strain[d]	0.029	0.033	0.039	0.041	0.012

[a] tension

[b] flexure

[c] psi; (std. dev.)

[d] in in^{-1}

thickness was controlled by felting the necessary weight of wood fiber as calculated from panel dimensions, specific gravity, wood fiber moisture content and glass fiber volume. Thirty percent powdered adhesive by weight of glass fiber held by electrostatic charge, was applied to cut-to-size plies as they were swirled about in a tray containing adhesive. Panels were laid up in a teflon-lined forming box by the air-felting of wood fiber drawn across a 6 mm mesh screen, and manual placement of resin-coated glass fiber plies. The felted mat was consolidated to one-third of target specific gravity in a cold prepress. The mat was removed to a hot press with a platen temperature of 405 ^{o}F, and consolidated under a maximum 475 psi for 4.5 minutes. Panels were hot-stacked upon removal from the press. After attaining an average 3.5 percent moisture content, test specimens were cut from only the central portion of each panel to eliminate edge effects. Macro- and microscope views of glass fiber *in situ* are presented in Figure 2.

Moduli of Elasticity and Rigidity of Hardboard

Load and deflection at proportional limit data from static bending tests were used in conjunction with load and deflection data from creep tests to estimate the true flexural moduli of elasticity and rigidity of hardboard. Test procedures are detailed in the Modulus of Elasticity of Glass Fiber Reinforced Hardboard chapter, and in the Creep Behavior of Glass Fiber Reinforced Hardboard chapter,

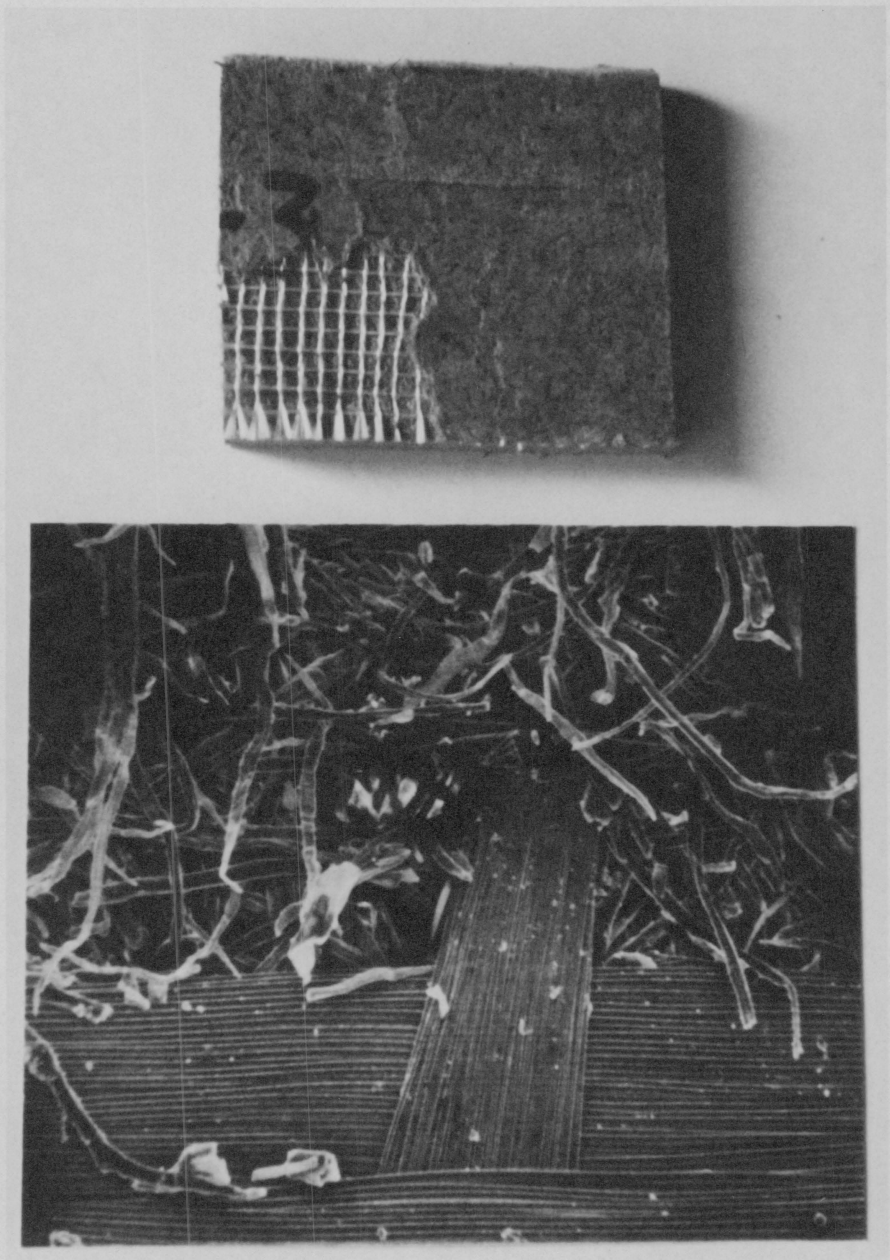

Figure 2. Glass fiber fabric in situ.
Upper: actual size.
Lower: SEM 120X.

respectively. Simply supported, homogeneous hardboard beams were deflected under single-point and two-pointing loading, respectively. Due to a difference in rate of loading between the two, viscoelastic effects on observed deflection must be accounted for. Under ramp loading, the deflection at proportional limit of static bending specimens consists of a bending, shear and creep component. In the present case, proportional limit was attained after approximately 35 seconds under an average applied moment of 14.0 inch-pounds. The deflection of creep specimens at 30 seconds after instantaneous application of a 13.6 inch-pound moment was used in the following calculations in compensation for time-dependent effects present in static bending.

The deflection of a simply supported homogenous beam under single-point or two-point loading derived by elastic strain energy methods is, respectively (Timoshenko and Gere 1972):

$$y = \frac{Pl^3}{48EI} + \frac{0.3Pl}{bdG} \qquad [1]$$

$$y = \frac{Pa(3l^2-4a^2)}{48EI} + \frac{0.6Pa}{bdG} \qquad [2]$$

The former term in each represents deflection due to bending moment; the latter, deflection due to shear. It is assumed that the ratio of material properties, E/G, is equal to a constant, n. Making the

appropriate substitution into Equations [1] and [2] and rearranging yields:

$$E = \frac{Pl^3}{48Iy} + n\left(\frac{0.3Pl}{bdy}\right) \qquad [3]$$

$$E = \frac{Pa(3l^2-4a^2)}{48Iy} + n\left(\frac{0.6Pa}{bdy}\right) \qquad [4]$$

Estimates of the flexural moduli of elasticity and rigidity are obtained by equating Equations [3] and [4] and solving first for n, then E and G. Empirical estimates of E and G for the hardboard matrix compare favorably with those of Werren and McNatt (1975) and are found in Table 2.

MODULUS OF ELASTICITY OF GLASS FIBER REINFORCED HARDBOARD

Introduction

A method for predicting the modulus of elasticity of glass fiber reinforced hardboard is presented. When modelled as a sandwich construction, the composite modulus is expressed as a function of the modulus of the hardboard matrix and the modulus and effective volume fraction of glass fiber reinforcement.

Theoretical

The stiffness of a sandwich composite symmetric about its neutral axis (Figure 3a) as given by Kuenzi (1959) is:

$$E_c I_c = E_m \frac{bd_m^3}{12} + E_f \frac{b(d_c^3 - d_m^3)}{12} \qquad [5]$$

With $I_c = bd_c^3/12$, Equation [5] reduces to:

$$E_c = E_m \frac{d_m^3}{d_c^3} + E_f \left(1 - \frac{d_m^3}{d_c^3}\right) \qquad [6]$$

Equation [6] can be expressed in terms of the volume fraction occupied by the reinforcing faces by recognizing that:

$$V_m = \frac{v_m}{v_c} = \frac{d_m}{d_c} \qquad [7]$$

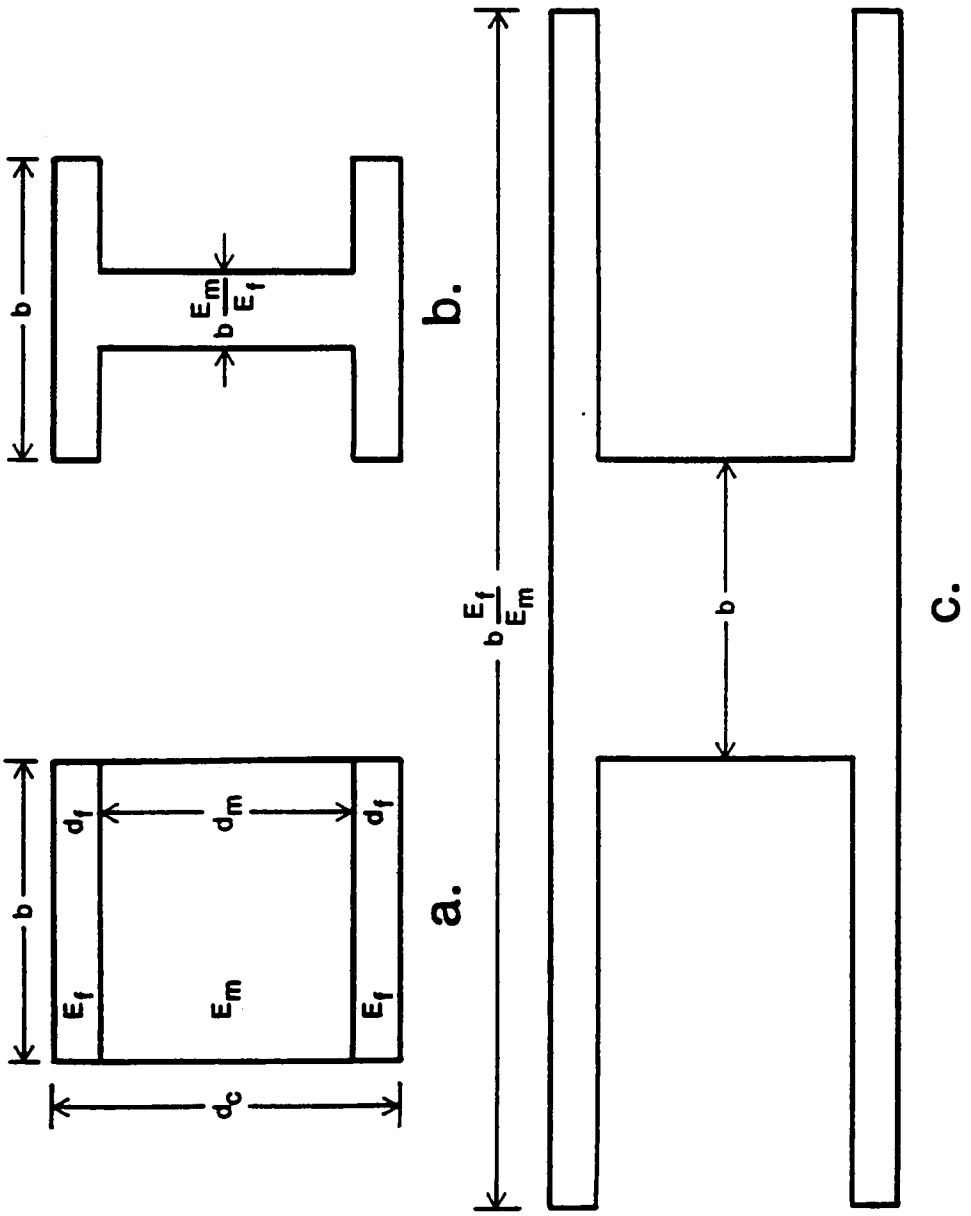

Figure 3a. Sandwich composite cross section.

3b. Equivalent all-face material transformed section.

3c. Equivalent all-core material transformed section.

and

$$V_m + V_f = 1 \qquad [8]$$

Substituting Equations [7] and [8] into Equation [6] and reducing yields an expression for predicting the composite modulus based on the moduli of its components and the volume fraction of reinforcement:

$$E_c = E_f + (1 - V_f)^3 (E_m - E_f) \qquad [9]$$

Here, E_c represents the true modulus of the composite.

The observed MOE_c, obtained when shear deflection is ignored, is estimated as follows:

The deflection of a simply supported sandwich beam under a point load at its center is:

$$y = \frac{Pl^3}{48E_cI_c} + \frac{Pl}{4N} \qquad [10]$$

Shear stiffness, N, is equal to:

$$N = \left(\frac{d_c + d_m}{2}\right) bG \qquad [11]$$

An estimate of observed MOE_c is made by substituting the total deflection, y, from Equation [10] into the expression normally used to calculate MOE for a homogeneous beam when shear deflection is ignored:

$$MOE = \frac{Pl^3}{48I_cy} \qquad [12]$$

Assumptions

When viewed in cross section, the composite is not by strict definition of sandwich construction (Figure 4a). Several assumptions are invoked in modelling the composite as a true sandwich. Individual yarns of the woven fabric are considered en masse, and are modelled as a solid lamina of glass fiber of identical cross sectional area acting in the same plane (Figure 4b). Wood fiber composing the composite surface and the 0.25 mm-thick layers separating glass fiber plies is ignored. The core wood fiber matrix thickness is unchanged, and glass fiber plies act directly upon its surface (Figure 4c).

The effective reinforcement volume fractions based on this model sandwich cross section for 1, 2 or 3 plies of glass fiber at each surface are 0.0073, 0.0158 and 0.0260, respectively. Only that glass fiber stressed parallel to its length is considered. Perfect bonding between wood fiber and glass fiber is assumed so that matrix and reinforcement at the interface experience equal strain. Two assumptions from ordinary bending theory also apply: no shifting of the neutral axis occurs, and the E-moduli in tension and compression are equal.

Experimental

Static bending tests as per ASTM D 1037, Standard Methods of Evaluating the Properties of Wood-Base Fiber and Particle Panel Materials (ASTM 1981) were performed on 15 specimens for each of three

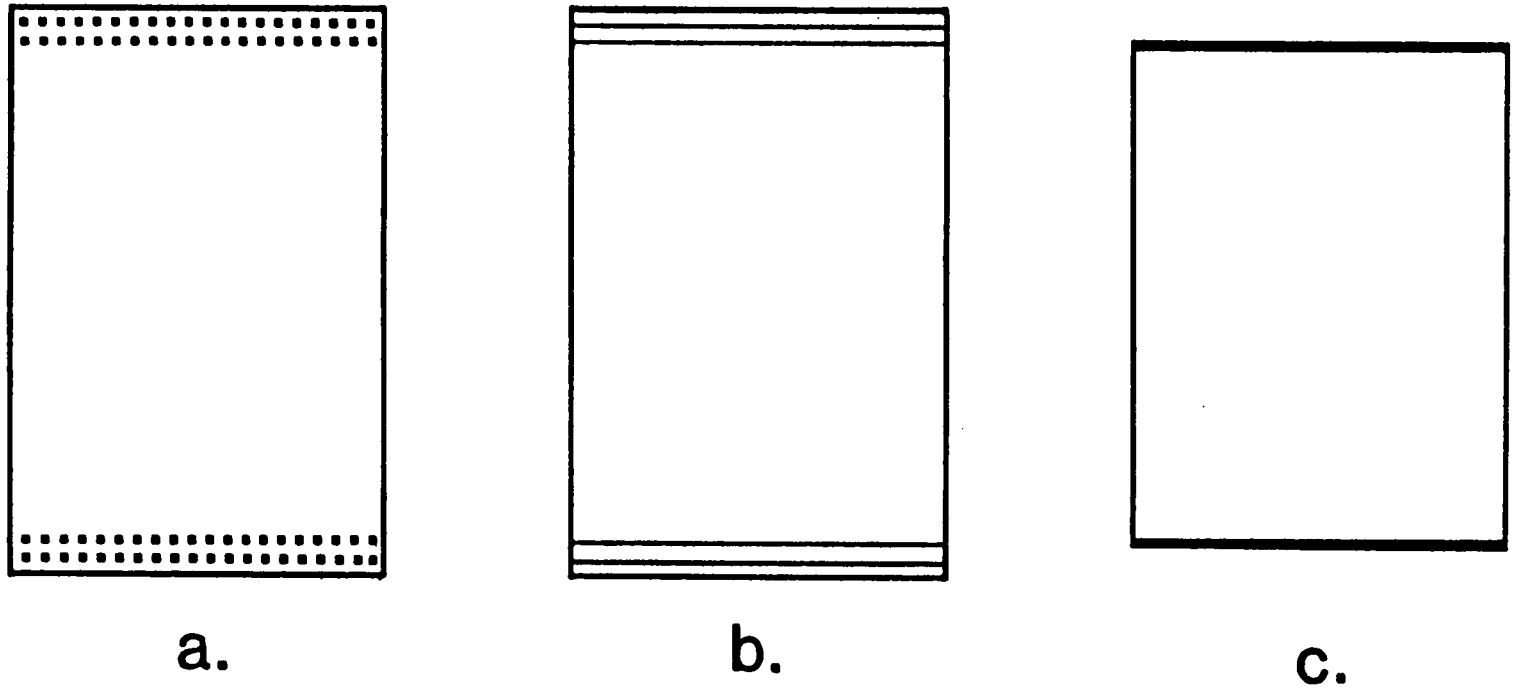

Figure 4a. Glass fiber reinforced hardboard cross section (effective reinforcement volume fraction equals 0.0158).

4b. Glass fiber yarns modelled as laminae of equal cross sectional area.

4c. Glass fiber reinforced hardboard modelled as a sandwich composite.

reinforcement volume fractions. Glass fiber fabric was oriented within the composite such that fill yarns were stressed in tension and compression parallel to their length during flexure. The observed MOE was calculated using the customary expression:

$$MOE = \frac{Pl^3}{48Iy} \qquad [13]$$

The predicted composite flexural modulus, E_c, is computed using the effective reinforcement volume fractions as previously given, and the E values for the hardboard matrix and resin-coated fill yarns as per Table 2.

Results and Discussion

The modulus of elasticity of glass fiber reinforced hardboard was observed to increase in a curvilinear fashion with increasing effective reinforcement volume fraction (Table 3). The mean and range of observed values, and the 95 percent confidence interval for each mean are plotted versus effective reinforcement volume fraction in Figure 5. Individual observed values of MOE are listed in Appendix 3. A one-way analysis of variance (ANOVA) was performed on the mean values of observed MOE over all effective reinforcement volume fractions. Inequality among means at $\alpha = 0.01$ was found. Duncan's multiple range test (DMRT) subsequently showed that each mean is unique, also at $\alpha = 0.01$. ANOVA and DMRT results are summarized in Appendix 4.

Table 3. Observed and predicted flexural modulus of elasticity of glass fiber reinforced hardboard.[a]

Effective V_f	Predicted		Observed	
	E	MOE	MOE	MOE Δ %[b]
0	450,900	439,400	439,500	-0.04
			(23,360)	
0.0073	512,100	501,400	524,900	-4.48
			(21,260)	
0.0158	582,700	570,900	597,300	-4.42
			(28,800)	
0.0260	665,000	652,000	664,800	-1.92
			(29,780)	

[a] psi; (std. dev.)

[b] $\Delta\% = \frac{\text{prd-obs}}{\text{obs}}$

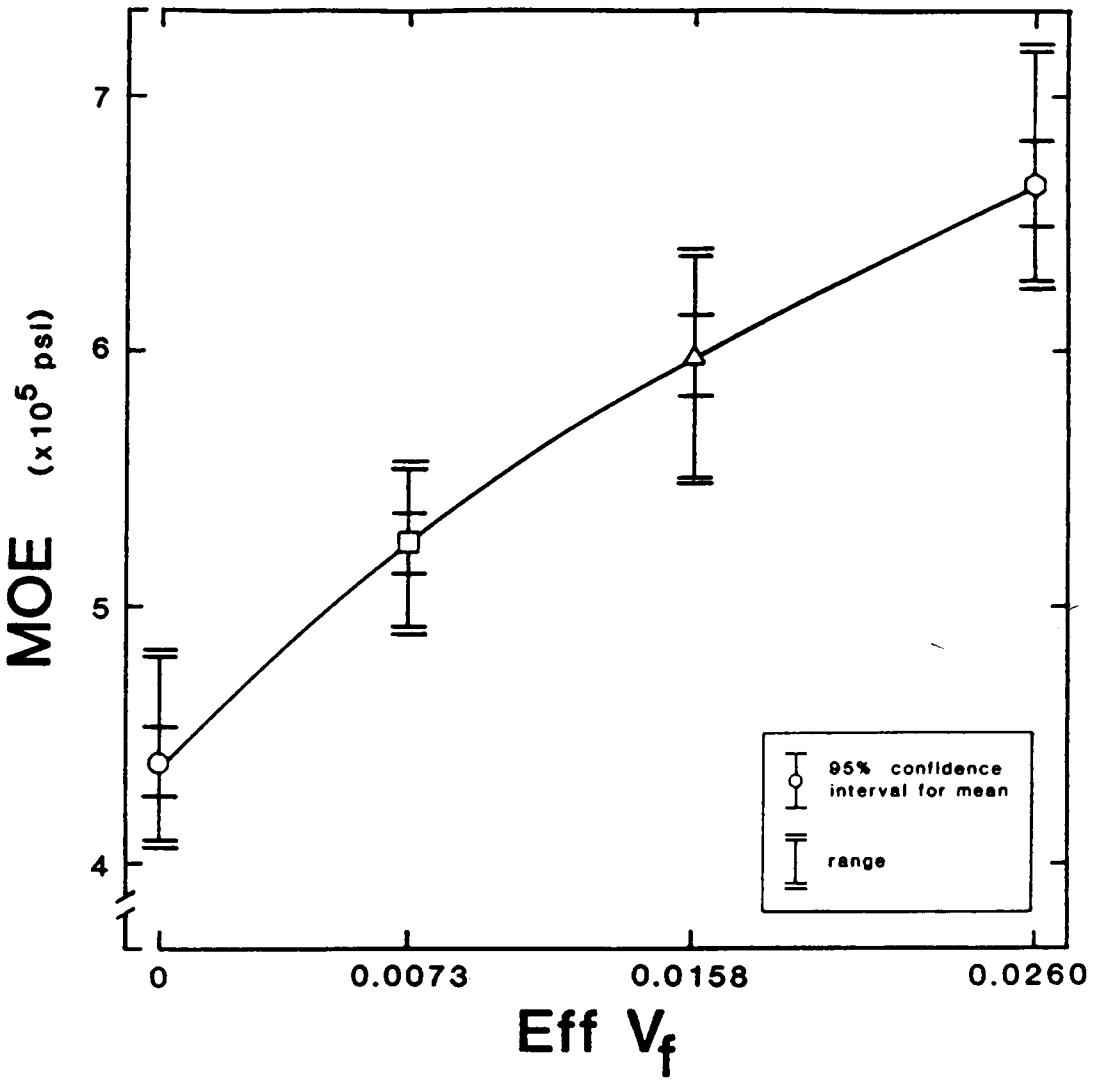

Figure 5. Influence of effective reinforcement volume fraction (Eff V_f) on the flexural modulus of elasticity (MOE) of glass fiber reinforced hardboard.

Close agreement exists between the predicted and observed mean values of MOE of glass fiber reinforced hardboard when analyzed as a sandwich composite (Table 3, Figure 6). For comparative purposes, the difference between mean observed and predicted values is expressed as a percentage of the observed value throughout this report. The predicted composite MOE underestimates the mean observed MOE by less than 5 percent over all effective reinforcement volume fractions.

Predicted MOE is computed using the appropriate values from Table 2 for the matrix and reinforcement, and the average dimensions and load and deflection at proportional limit of 15 flexure specimens at each effective reinforcement volume fraction (Appendix 3).

The conservative nature of predicted values owes possibly to a wood fiber/resin/glass fiber interaction that is unaccounted for. The characteristic drape of the uncoated glass fiber fabric, for example, is absent in resin-coated fabric. After adhesive cure the fabric is instead, stiff and inflexible. Also, surface wood fiber and that composing the layers separating glass fiber plies, although ignored in the model, may have a minor influence on the composite MOE. These effects are discussed in detail in the Results and Discussion section of the Modulus of Rupture of Glass Fiber Reinforced Hardboard chapter.

A hypothetical predicted deflection at proportional limit is calculated with the present method owing to the assumption in which wood fiber composing the composite surface and the layers intervening glass fiber plies is ignored. The effective moment of inertia of the model sandwich cross section, I_c, is considerably smaller than that of

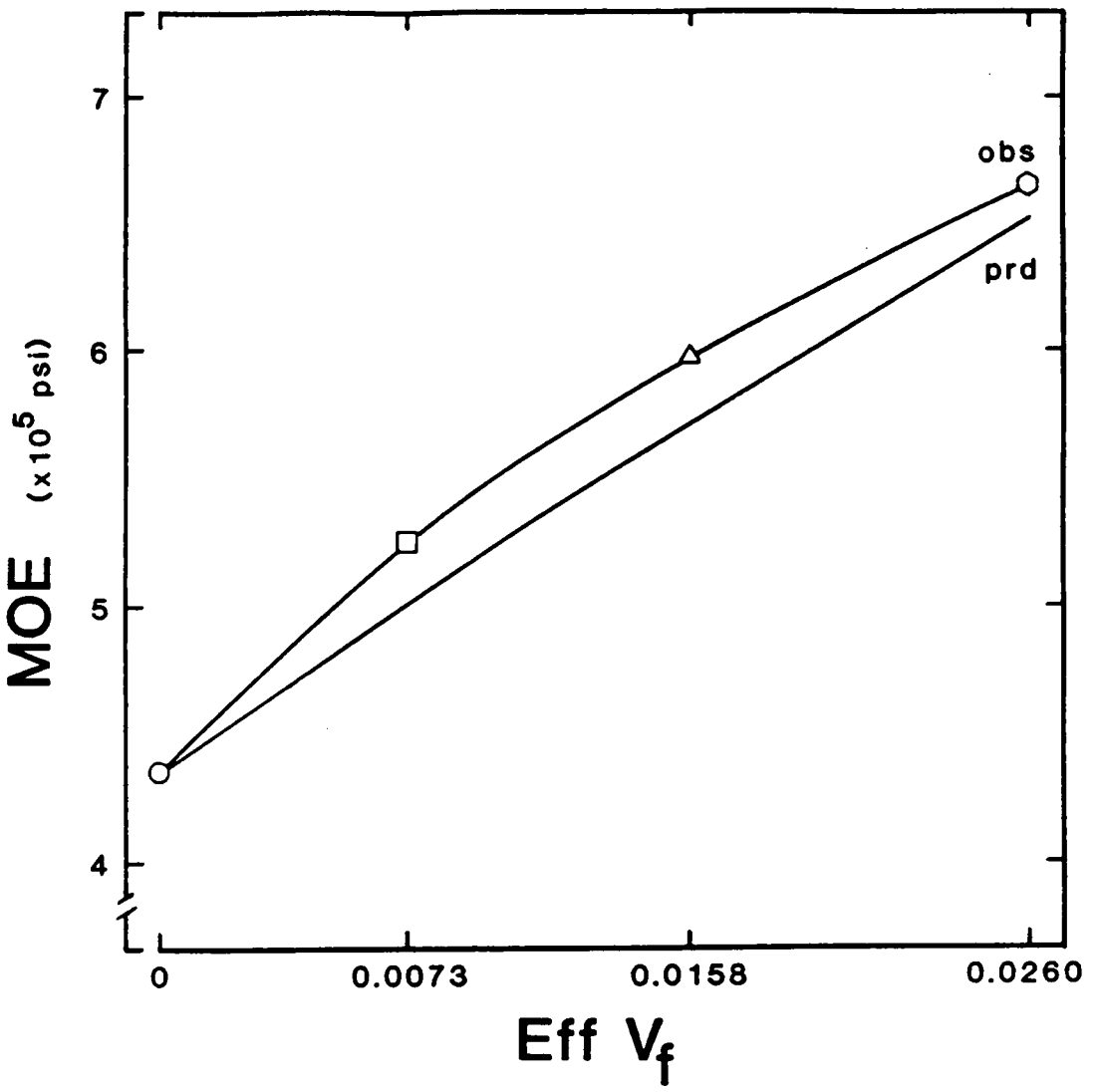

Figure 6. Influence of effective reinforcement volume fraction (Eff V_f) on the observed and predicted flexural modulus of elasticity (MOE) of glass fiber reinforced hardboard.

the actual composite cross section, I_{obs}. The component of deflection due to bending, and ultimately, the total deflection as per Equation [10] are thus inflated in compensation. The true deflection of the composite can be estimated by substituting I_{obs} of the actual composite cross section for I_c (Table 4). The observed and predicted deflections for the hardboard controls are in excellent agreement. Those for the reinforced composites exhibit a small departure. The flexural modulus of the reinforced composite is underestimated by Equation [9]. Thus, the bending component of deflection and total deflection are subsequently overestimated in Equation [10].

Conclusions

The modulus of elasticity of glass fiber reinforced hardboard increased with increasing effective reinforcement volume fraction in a curvilinear manner. The mean observed MOE at each effective reinforcement volume fraction was statistically unique at $\alpha = 0.01$. The flexural modulus of elasticity of glass fiber reinforced hardboard can be successfully predicted from the moduli of its components and effective reinforcement volume fraction when modelled as a sandwich construction. Shear deflection of the hardboard core must be accounted for. The predicted composite MOE underestimates observed values by less than 5 percent at all effective reinforcement volume fractions, while the predicted deflection at proportional limit exceeds observed values by at most 7 percent.

Table 4. Observed and predicted deflection at proportional limit of glass fiber reinforced hardboard.

Effective V_f	Moment of Inertia[a]		Total Deflection at Proportional Limit[b]			
	I_{obs}	I_c	y_{obs}	y^c_{hyp}	y^d_{prd}	$\Delta\%$[e]
0	2.497	2.497	0.076	0.076	0.076	0
0.0073	2.510	1.998	0.079	0.105	0.084	+6.3
0.0158	2.521	1.567	0.084	0.141	0.089	+6.0
0.0260	2.528	1.201	0.084	0.183	0.089	+6.0

[a] $\times 10^{-3}$ in^4

[b] in

[c] using I_c in Eq [10]

[d] using I_{obs} in Eq [10]

[e] $\Delta\% = \frac{prd-obs}{obs}$

MODULUS OF RUPTURE OF GLASS FIBER REINFORCED HARDBOARD

Introduction

The nature of failure and the ultimate strength of glass fiber reinforced hardboard are discussed. When modelled as a structural sandwich, the composite MOR is a function of the elastic moduli of its components, the effective reinforcement volume fraction, and the matrix ultimate stress.

Theoretical

The bending stress distribution through the depth of a beam of rectangular cross section is given by the flexure formula:

$$\sigma = \frac{Mx}{I} \qquad [14]$$

Implicit in its use are the restrictions that bending deformations are small, and that sections plane before bending remain plane after bending. Strain must be linearly proportional to stress, and E-moduli in tension and compression are assumed equal (Bodig and Jayne 1982).

The flexure formula applies only to homogeneous beams. Thus, the cross section of a composite beam must be represented by an equivalent hypothetical homogeneous cross section. Composite beam components lying in the same horizontal plane are assumed to experience equal strain by virtue of the bond between them. Under load, the stress

developed in each component is thus proportional to its elastic modulus.

Based on the equal strain concept, the sandwich beam cross section of Figure 3a can be represented as a homogeneous cross section using the method of transformed sections. An equivalent beam composed wholly of face material is created by reducing the core width by the factor E_m/E_f (Figure 3b). Similarly, by increasing the width of the faces by E_f/E_m, an equivalent cross section of core material is produced (Figure 3c).

Failure is initiated in a composite beam when the ultimate stress (or strain) of any one of its components is exceeded. The maximum moment that can be resisted by a component is dependent upon its stress at ultimate, and the distance from the neutral axis to its extreme fiber. Composite failure is expected to initiate in the component exhibiting the smallest resisting moment. Each component is assumed to act within the composite as it would alone.

Failure of the sandwich beam of Figure 3a is assumed to occur as a tensile fracture of the core at its extreme fiber. The beam's maximum moment capacity can be predicted by applying Equation [14] to its transformed section (Figure 3c):

$$M_{prd} = \sigma_m I' \left(\frac{2}{d_m} \right) \qquad [15]$$

The observed modulus of rupture, however, is based on the moment of inertia calculated from the actual dimensions of the composite (Figure 3a):

$$MOR = \frac{M\left(\frac{d_c}{2}\right)}{I_{obs}} \qquad [16]$$

Substitution of the expression for M_{prd} into Equation [16] yields:

$$MOR_{prd} = \frac{\sigma_m I' \left(\frac{d_c}{d_m}\right)}{I_{obs}} \qquad [17]$$

The moment of inertia of the actual and transformed cross sections are, respectively:

$$I_{obs} = \frac{bd_c^3}{12} \qquad [18]$$

and

$$I' = \frac{b}{12}\left[\frac{E_f}{E_m}(d_c^3 - d_m^3) + d_m^3\right] \qquad [19]$$

Substitution of Equations [18] and [19] into Equation [17] yields upon reduction:

$$MOR_{prd} = \sigma_m \left(\frac{d_c}{d_m}\right)\left[\frac{E_f}{E_m}\left(1 - \left(\frac{d_m}{d_c}\right)^3\right) + \left(\frac{d_m}{d_c}\right)^3\right] \qquad [20]$$

Equation [20] can be expressed in terms of the volume fraction of the composite occupied by the reinforcing faces by recognizing that:

$$V_m = \frac{v_m}{v_c} = \frac{d_m}{d_c} \qquad [21]$$

and

$$V_m + V_f = 1 \qquad [22]$$

Substitution of Equations [21] and [22] into Equation [20] yields an expression for predicting the composite modulus of rupture based on the elastic moduli of its components, the reinforcement volume fraction, and the matrix ultimate stress:

$$MOR_{prd} = \sigma_m (1-V_f)^{-1} \left[\frac{E_f}{E_m} (1-(1-V_f)^3) + (1-V_f)^3 \right] \qquad [23]$$

Restrictions governing use of the flexure formula are also in effect for Equation [23]. The technique is designated MOR I. For a composite beam of fixed width and depth, reinforcement volume fraction influences the moment of inertia of the transformed section, and ultimately, the composite modulus of rupture.

Assumptions

All assumptions invoked in prediction of the composite modulus of elasticity are again in effect. The flexure formula is applied under the limitations noted. Composite tensile and compressive E-moduli for the composite are assumed equal, so that shifting of the neutral axis is precluded.

Experimental

Data for the composite modulus of rupture are derived from the static bending tests described previously. The observed MOR is:

$$MOR = \frac{3Pl}{2bd^2} \qquad [24]$$

The wood fiber matrix of the failed composite was removed via sulfuric acid to assess damage to the reinforcement.

Results and Discussion

At all effective reinforcement volume fractions, glass fiber reinforced hardboard fails by tensile fracture of the extreme fiber of the hardboard core. The adjacent wood fiber/glass fiber interface remains viable, indicating good interfacial adhesion. Upon acid-dissolution of the hardboard matrix, the resin-coated glass fiber fabric is recovered intact, with no fiber tensile failure evident.

Composite failure due to tensile fracture of the matrix occurs in particulate-filled systems, in continuous fiber composites with small reinforcement volume fractions, in composites with low interfacial shear strength, and in fiber reinforced materials in which the reinforcement strain at failure exceeds matrix strain at failure. Steel-fiber-reinforced concrete and glass-fiber-reinforced gypsum plaster, for example, exhibit the latter behavior (Ali and Grimer 1979, Allen 1971, Aveston et al. 1972).

The strain at failure of the tension face of hardboard controls was estimated from static bending deflection to be 0.012 in in^{-1}. Tensile testing of the glass fiber fabric showed a strain at failure of 0.041 in in^{-1}. Glass fiber is considered to be a Hookean solid.

In the present investigation, glass fiber strain was linearly proportional to stress to approximately 90 percent of ultimate stress (Appendix 1).

The MOR of a composite with a low-strain-at-failure matrix increases with reinforcement volume fraction even though the reinforcement never fails. The matrix will fail at a given strain regardless of whether it is a homogeneous beam, or part of a composite. For a given load, the strain in the matrix of a composite is less than it would be in a homogeneous beam of identical geometry. This arises because the work performed in deforming the composite is distributed as strain energy among its components. Total strain energy owes in part to the matrix, and in part to the reinforcement. Thus, a greater load is required to develop the necessary fracture strain in the matrix when it is part of a composite.

Static bending stress-strain curves representing the average behavior of 15 replications at each effective reinforcement volume fraction are presented in Figure 7; the associated MOR values are summarized in Table 5.

The area under a stress-strain curve represents the work-to-failure performed in deforming a material. Assuming that energy is conserved, work-to-failure is equal to the strain energy of the deformed material. The proportion of composite total strain energy owing to the reinforcement increases as its effective volume fraction increases. A concurrent increase in the composite MOR results. The work-to-failure per unit volume of glass fiber reinforced hardboard

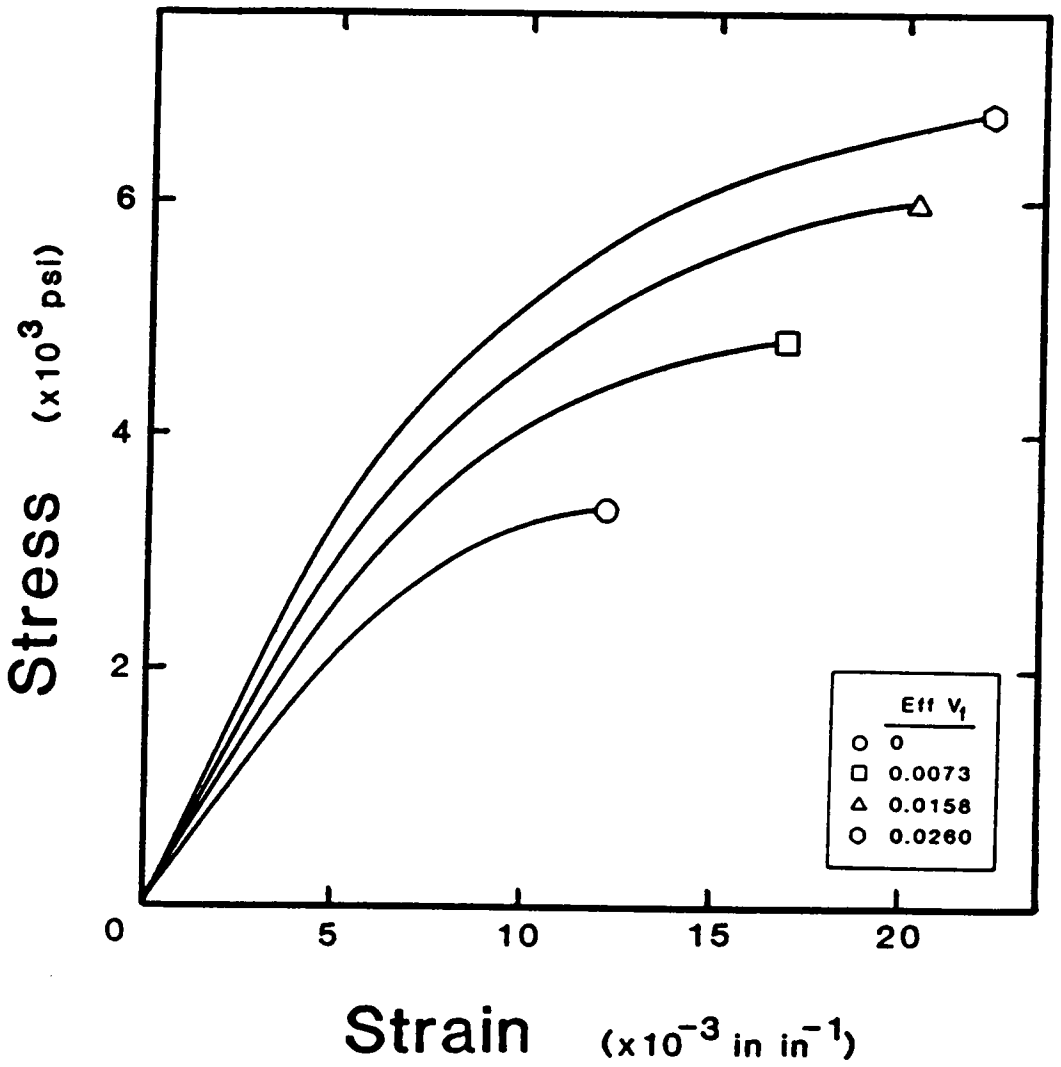

Figure 7. Influence of effective reinforcement volume fraction (Eff V_f) on the flexural stress-strain response of glass fiber reinforced hardboard.

Table 5. Work-to-failure and observed modulus of rupture of glass fiber reinforced hardboard.

Effective V_f	Work-to-failure[a]	MOR_{obs}[b]
0	8.6	3,360 (270)
0.0073	17.5	4,800 (280)
0.0158	26.3	5,970 (330)
0.0260	33.1	6,740 (410)

[a] in-lb in^{-3}

[b] psi; (std. dev.)

increases with increasing effective reinforcement volume fraction, as shown in Figure 8 (see also Table 5). The marked non-linearity of the composite stress-strain trace shows that energy is not conserved.

The modulus of rupture of glass fiber reinforced hardboard was observed to increase with increasing effective reinforcement volume fraction in a curvilinear manner (Table 5). The mean and range of observed values, and the 95 percent confidence interval for each mean are plotted versus effective reinforcement volume fraction in Figure 9. Individual observed values of MOR are listed in Appendix 3. The results of ANOVA performed on the means over all effective reinforcement volume fractions showed inequality among them at $\alpha = 0.01$. Using DMRT, each mean value of MOR is shown to be unique at $\alpha = 0.01$. A summary of ANOVA and DMRT results is found in Appendix 5.

Values for the composite MOR predicted using Equation [23] - MOR I - underestimate observed mean values by 20 to 26 percent (Figure 10, Table 6). The discrepancy is due in part to simplifying assumptions made concerning the spatial distribution of composite constituents.

Although modelled as such, the composite is not by strict definition of sandwich construction (Figure 11a). The sandwich model assumes that wood fiber composing the composite surface and that separating glass fiber plies contributes negligibly to composite properties, and can be ignored (Figure 11b). Satisfactory results are obtained under this assumption in predicting the composite MOE, for example. At loads approaching ultimate load, however, the contribution to moment of inertia made by wood fiber overlying and

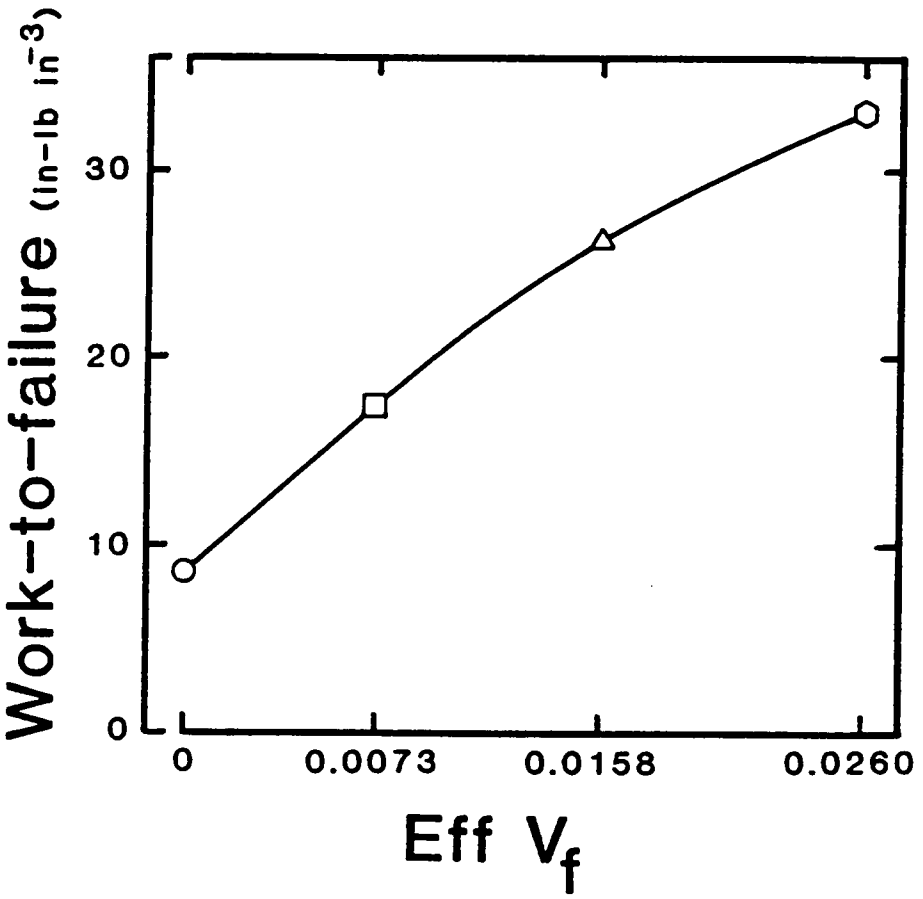

Figure 8. Influence of effective reinforcement volume fraction (Eff V_f) on the flexural work-to-failure of glass fiber reinforced hardboard.

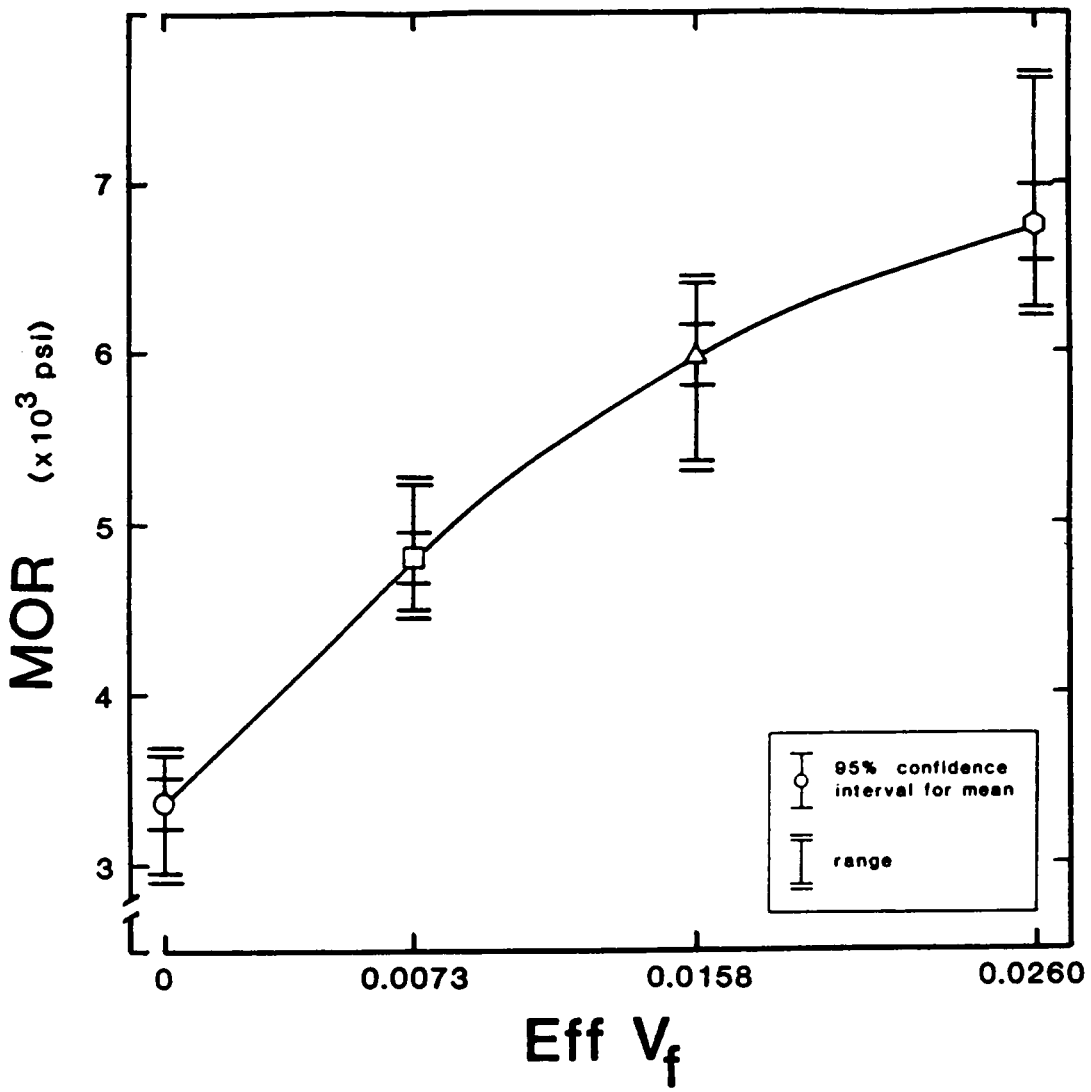

Figure 9. Influence of effective reinforcement volume fraction (Eff V_f) on the flexural modulus of rupture (MOR) of glass fiber reinforced hardboard.

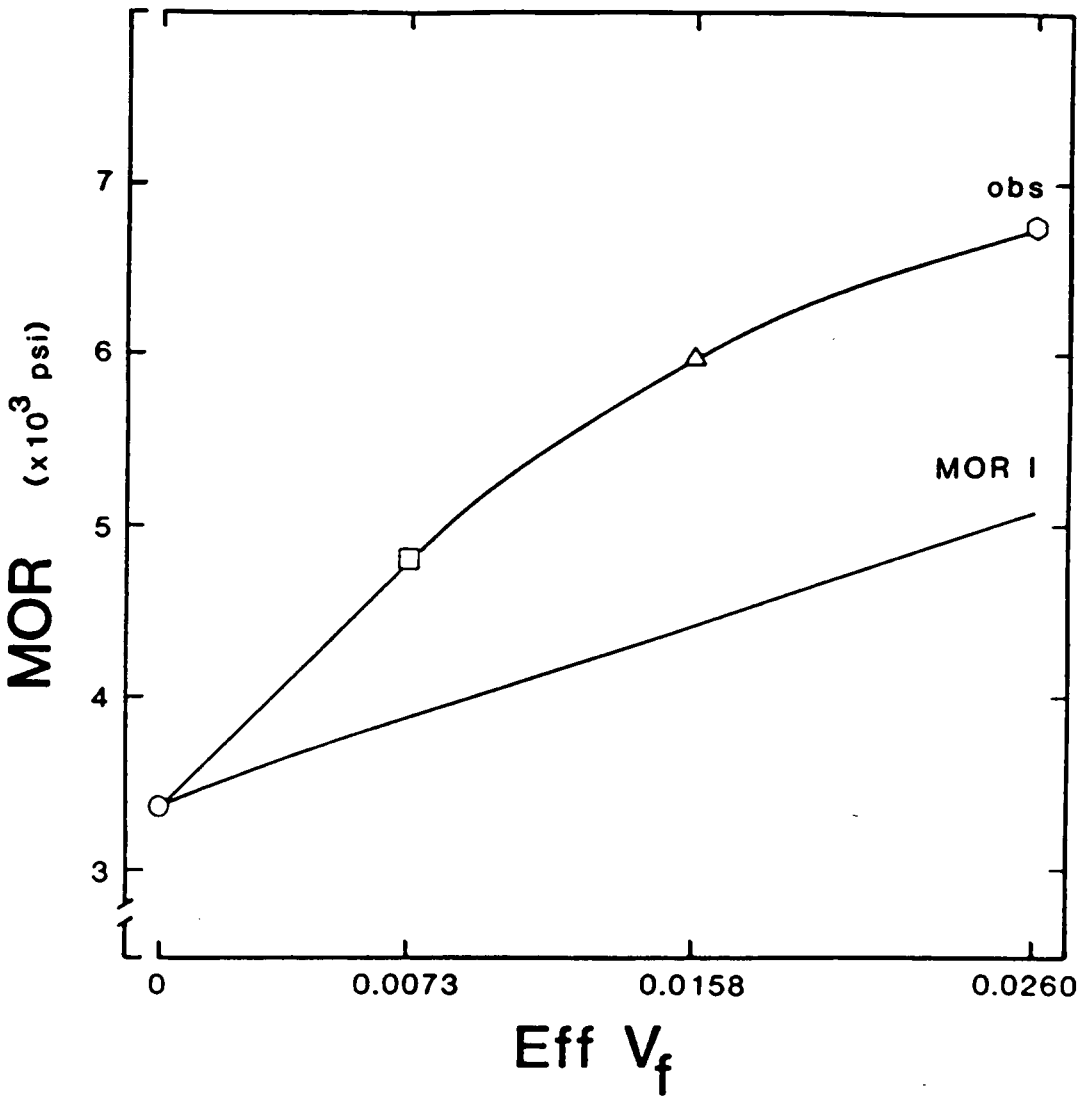

Figure 10. Influence of effective reinforcement volume fraction (Eff V_f) on the observed and predicted flexural modulus of rupture (MOR) of glass fiber reinforced hardboard using MOR I analysis.

Table 6. Observed and predicted modulus of rupture of glass fiber reinforced hardboard.[a]

Effective V_f	MOR_{obs}	MOR I	$\Delta\%$[b]	MOR II	$\Delta\%$[b]
0	3,360	3,360	0	3,360	0
0.0073	4,800	3,840	-19.9	4,050	-15.6
0.0158	5,970	4,410	-26.1	4,790	-19.8
0.0260	6,740	5,090	-24.5	5,620	-16.6

[a] psi

[b] $\Delta\% = \frac{prd-obs}{obs}$

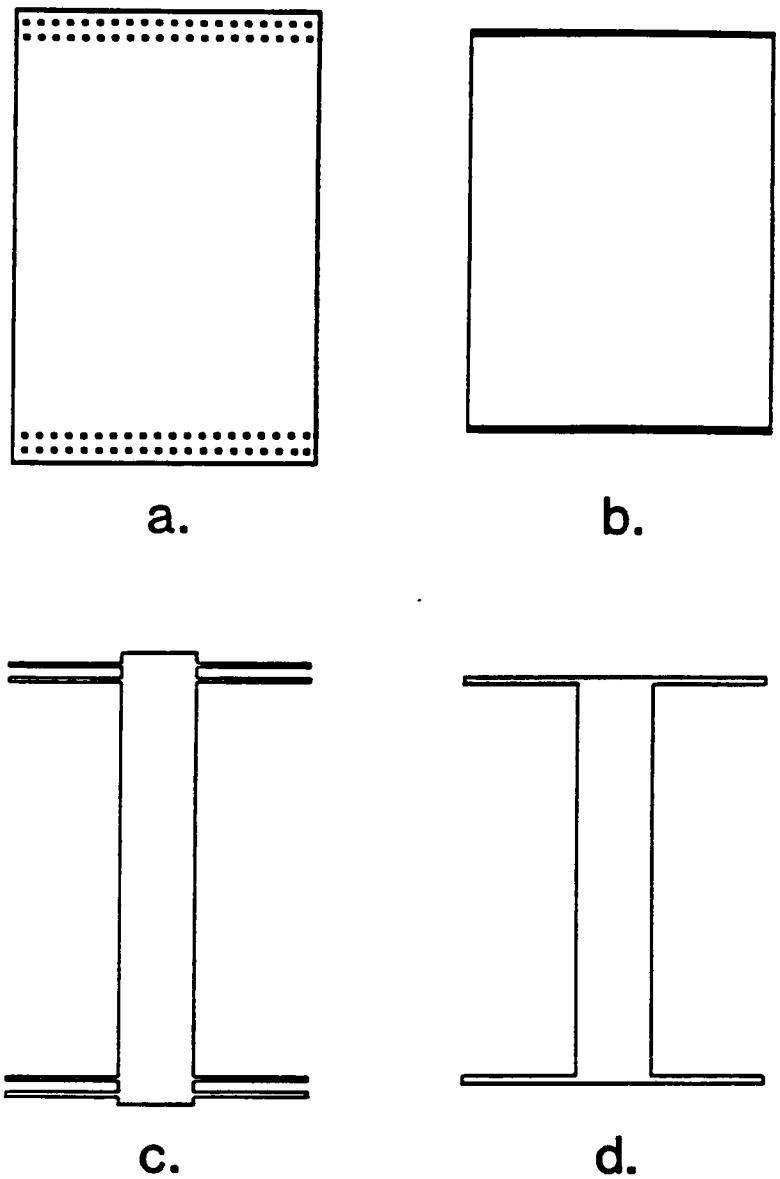

Figure 11a. Glass fiber reinforced hardboard cross section (effective reinforcement volume fraction 0.0158).

11b. Glass fiber reinforced hardboard modelled as a sandwich composite.

11c. Equivalent all-glass fiber transformed section of 11a. using MOR II analysis.

11d. Equivalent all-glass fiber transformed section of 11b. using MOR I analysis.

separating glass fiber plies becomes significant. By ignoring this contribution, the moment of inertia of the transformed sandwich section is conservative at all effective reinforcement volume fractions (Figure 11d). An underestimation of the composite MOR follows.

A second mechanism which further reduces the transformed sandwich moment of inertia operates when more than one ply of glass fiber is present below each surface of the composite. The sandwich model assumes that multiple plies of glass fiber are collapsed into a single ply of appropriate thickness. This hypothetical ply acts directly upon the surface of the wood fiber core. The moment arm from the neutral axis to the actual centroid of the glass fiber plies is thus shortened. A further underestimation of the transformed sandwich moment of inertia, and subsequently, the composite MOR, results. The effect becomes greater as effective reinforcement volume fraction increases.

The above effects can be removed by calculating the moment of inertia of a transformed section in which all layers present in the composite cross section are accounted for in their actual position, as in Figure 11c. The analysis is designated MOR II.

The predicted maximum moment capacity of the composite is again given by Equation [15]. The moment of inertia of the transformed section of Figure 11c, for use in Equation [15] with MOR II, is calculated as:

$$I' = \sum_{i=1}^{n} \left(I_i + A_i D_i^2 \right) \qquad [25]$$

The composite modulus of rupture is predicted using:

$$MOR_{prd} = \frac{M_{prd}\ (\frac{d}{2})}{I_{obs}} \qquad [26]$$

Actual dimensions of the composite are used to calculate d/2 and I_{obs}.

Observed mean and predicted values for composite MOR using MOR I and II are plotted versus effective reinforcement volume fraction in Figure 12 (see also Table 6). An improvement of 4 to 8 percent in property prediction is seen with the latter method. Values predicted for the composite modulus of rupture when the effect of all layers is accounted for underestimate observed values by 16 to 20 percent. Two additional effects which may account for the remaining disparity between observed and predicted values are discussed below.

The tensile MOE and MOR of hardboard are 4 and 15 percent higher than its corresponding compressive properties (Werren and McNatt 1975). It is likely that the glass fiber increases composite tensile strength, without affecting its compressive strength. Further, the reinforcement stress-strain response at composite failure is Hookean, while that of the matrix is markedly nonlinear.

A downward shifting of the neutral axis from its assumed position at the mid-depth of the composite is implied. With progressive descent of the neutral axis, the moment of inertia of the transformed section of the composite slowly decreases, while the distance from the neutral axis to the extreme tension fiber of the hardboard core

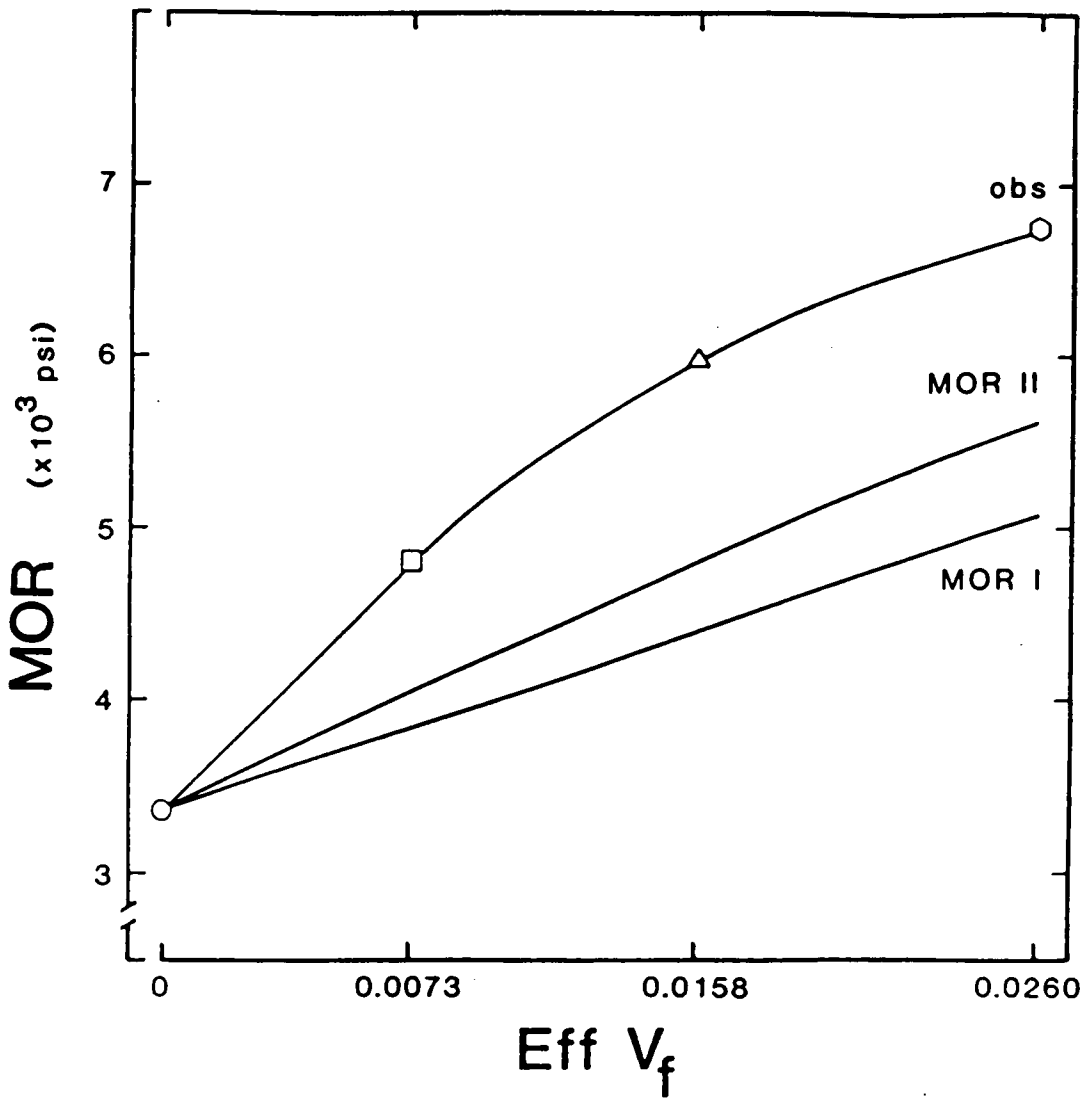

Figure 12. Influence of effective reinforcement volume fraction (Eff V_f) on the observed and predicted flexural modulus of rupture (MOR) of glass fiber reinforced hardboard using MOR I and MOR II analyses.

decreases rapidly. Inspection of Equations [15] and [26] shows that a downward shifting of the neutral axis produces a greater predicted value for both maximum moment and modulus of rupture.

The distance by which the neutral axis must descend to account for the disparity between observed and predicted values of modulus of rupture using MOR II has been estimated at each effective reinforcement volume fraction in support of the above. A trial and error procedure was employed in positioning the neutral axis. Equation [15] is modified to reflect the observed composite failure mode, viz., tensile fracture of the hardboard core at its extreme fiber:

$$M_{prd} = \frac{\sigma_m I'}{x_m} \qquad [27]$$

The moment of inertia of the transformed section, and the composite modulus of rupture are calculated as per Equations [25] and [26], respectively. At failure, the composite neutral axis is estimated to lie on average, 0.015 inches below the mid-depth of the composite at each effective reinforcement volume fraction (Table 7).

It has been assumed that each component acts within the composite as it would alone. In addition to an apparent shifting of the neutral axis of the composite, a wood fiber/resin/glass fiber synergy is proposed. Two possible effects are acknowledged. First, the specific gravity profile that normally exists in hardboard - higher at the surface and lower in the core - may be accentuated by the presence of

Table 7. Estimated shift of neutral axis of glass fiber reinforced hardboard during static bending.

Effective V_f	Estimated neutral axis shift[a]	Maximum Moment[b]		MOR[c]	
		Estimated	Observed	Estimated	Observed
0.0073	0.0148	98.5	98.6	4,820	4,800
0.0158	0.0164	122.4	122.4	5,970	5,970
0.0260	0.0134	139.2	139.2	6,770	6,740

[a] in

[b] in-lbs

[c] psi

the subsurface glass fiber. Secondly, the phenolic resin used to bond reinforcement to matrix may stiffen and strengthen wood fiber at the interface. Both phenomena act at the composite's surface where their combined effect will exert the greatest influence on composite stiffness and strength.

Conclusions

The apparent failure of glass fiber reinforced hardboard occurred as a tensile fracture of the extreme fiber of the hardboard core. Slight wrinkling of the composite compression surface immediately adjacent to the load head preceded tensile failure. Glass fiber reinforcement remained intact. The observed failure mode was due to a strain at failure for the hardboard matrix that was significantly less than that of the glass fiber reinforcement. Failure mechanism notwithstanding, the composite MOR increased with increasing effective reinforcement volume fraction in a curvilinear manner. The mean observed MOR at each effective reinforcement volume fraction was statistically unique at $\alpha = 0.01$. Greater work-to-failure is performed on the composite in deforming an increasingly larger cross sectional area of glass fiber as effective reinforcement volume fraction increases.

When modelled as a sandwich construction, the composite MOR can be expressed as a function of the elastic moduli of its components, the effective reinforcement volume fraction, and the matrix ultimate

stress. Predicted values underestimate observed values by 20 to 26 percent using this model. The departure owes to simplifying assumptions made in the modelling process which unfavorably alter the spatial distribution of composite constituents. When the actual spatial distribution of components is considered, a 4 to 8 percent improvement in composite MOR prediction is realized. Predicted values, however, still underestimate observed values by 16 to 20 percent.

The discrepancy appears to owe to a downward shifting of the composite's neutral axis that is unaccounted for. Probable contributing factors include a violation of the assumption of equal tensile and compressive E-moduli, and a Hookean stress-strain response for the reinforcement at composite failure versus a decidedly nonlinear stress-strain response for the matrix. Trial and error estimates on average, place the neutral axis at failure 0.015 inches below the mid-depth of the composite at all effective reinforcement volume fractions. A possible wood fiber/resin/glass fiber synergy which favorably alters the composite surface stiffness and strength is also acknowledged.

STRESS TRANSFER IN GLASS FIBER REINFORCED HARDBOARD

Introduction

A viable adhesive bond between reinforcement and matrix is paramount to enhanced property development in composite materials. Stress transfer from a lower modulus matrix to a higher modulus reinforcement is effected by the development of shear stress at the adhesive interface. Poor interfacial adhesion cannot promote an adequate level of stress transfer, thus limiting the percentage of an applied load that can be transferred to and borne by the reinforcement.

Experimental

Hardboard panels in which no adhesive was applied to the single ply of glass fiber fabric just below each surface were prepared. The flexural MOE and MOR of 9 specimens were determined as before.

Results and Discussion

The creation of a reinforcement/matrix adhesive bond significantly increases the stiffness and load-carrying capacity of glass fiber reinforced hardboard (Figure 13). The mean MOE and MOR of hardboard containing unbonded reinforcement were only 4.5 and 6.8 percent greater than that of nonreinforced controls, respectively (Table 8). The difference in both properties is statistically

significant at $\alpha = 0.05$ (Appendix 6). The slight property increase most likely arises from the development of frictional forces due to entrapment of reinforcement within the matrix. In contrast, panels in which the same reinforcement volume fraction was adhesively bonded showed a mean MOE and MOR 19.4 and 42.9 percent greater than that of nonreinforced controls, respectively. Individual observed values of the MOE and MOR of glass fiber reinforced hardboard with unbonded glass fiber are listed in Appendix 3.

Significant stress transfer from a lower modulus matrix to a higher modulus reinforcement has the greatest probability of occurrence when the two are linked by an interfacial zone of intermediate modulus. This zone serves to minimize the development of localized stress concentrations that could cause separation of the reinforcement from the matrix. It is likely that the phenolic resin applied to the glass fiber created a resin-rich zone of wood fiber at the interface whose modulus is intermediate between that of the reinforcement and the bulk matrix.

Conclusions

The role of a phenolic resin in promoting stress transfer between matrix and reinforcement has been demonstrated. Frictional forces between reinforcement and matrix are sufficient to promote a slight increase in the stiffness and strength of glass fiber reinforced hardboard. Although not investigated, the possibility of a stiffening and strengthening effect by addition of phenolic resin alone to the

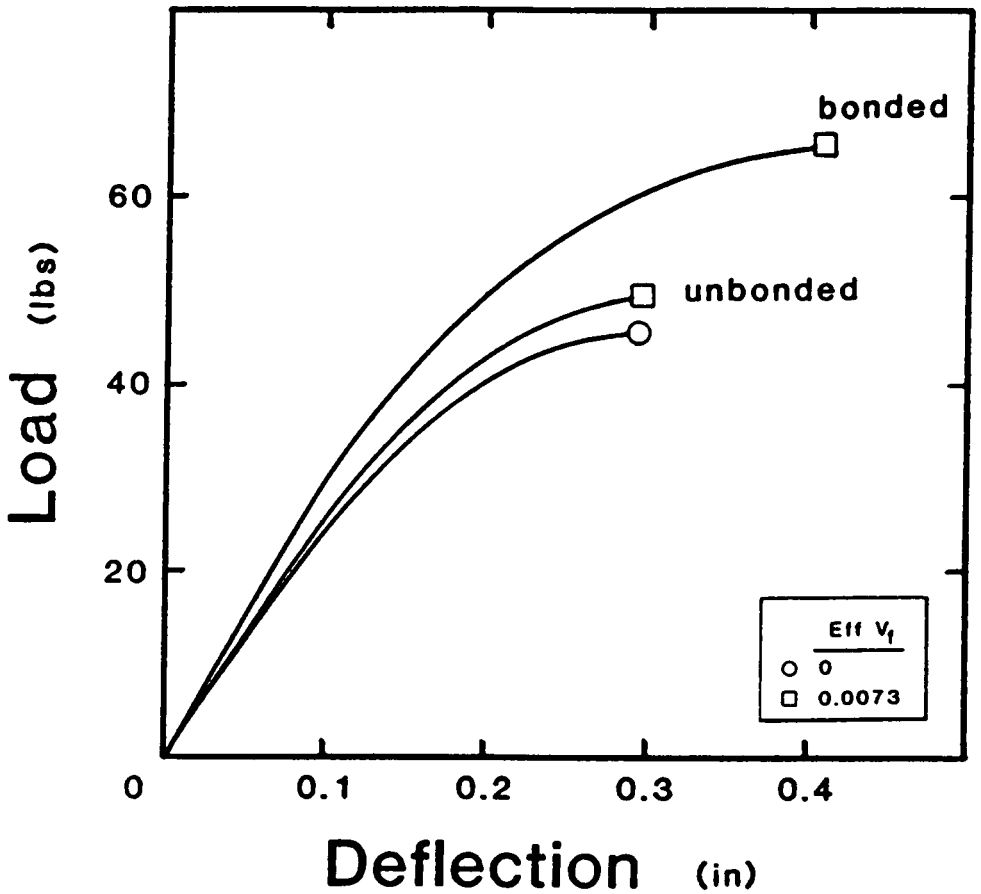

Figure 13. Influence of bonded and unbonded glass fiber on the flexural load-deflection response of glass fiber reinforced hardboard at an effective reinforcement volume fraction (Eff V_f) of 0.0073.

Table 8. Observed modulus of elasticity and modulus of rupture of glass fiber reinforced hardboard using bonded and unbonded glass fiber.

	Effective V_f			$\Delta\%$[a]	
	0	0.0073 unbonded	0.0073 bonded	unbonded	bonded
MOE[a]	439,500 (23,360)	459,200 (19,700)	524,900 (21,260)	+4.5	+19.4
MOR[a]	3,360 (270)	3,590 (250)	4,800 (280)	+6.8	+42.9

[a] psi; (std. dev.)

[b] $\Delta\% = \frac{\text{bonded or unbonded-control}}{\text{control}}$

hardboard matrix is acknowledged. The greatest enhancement of MOE and MOR is effected by creation of a wood fiber/glass fiber adhesive bond.

DYNAMIC MECHANICAL PROPERTIES OF GLASS FIBER REINFORCED HARDBOARD

Introduction

The flexural dynamic mechanical properties of free-free glass fiber reinforced hardboard beams were determined from the fundamental resonant frequency of vibration observed under conditions of forced oscillation. Dynamic modulus of elasticity (also called storage modulus), logarithmic decrement and loss tangent were calculated directly from empirical data. The complex and loss moduli, and angle of phase lag between stress and strain were determined from the above using existing theoretical relationships.

Theoretical

The dynamic modulus of elasticity, or storage modulus, of a free-free rectangular beam vibrating at its fundamental resonant frequency is given by (Read and Dean 1978):

$$E' = \frac{0.00245\ f_r^2 w L^3}{b d^3} \qquad [28]$$

(Units in Equation [28] are consistent with English units.)

In viscoelastic materials, part of the applied excitation energy is dissipated acoustically or thermally via internal friction. The logarithmic decrement, a measure of a material's internal friction or damping capacity, is determined from the width of the resonance peak at an amplitude $1/\sqrt{2}$ times the maximum amplitude (Figure 14):

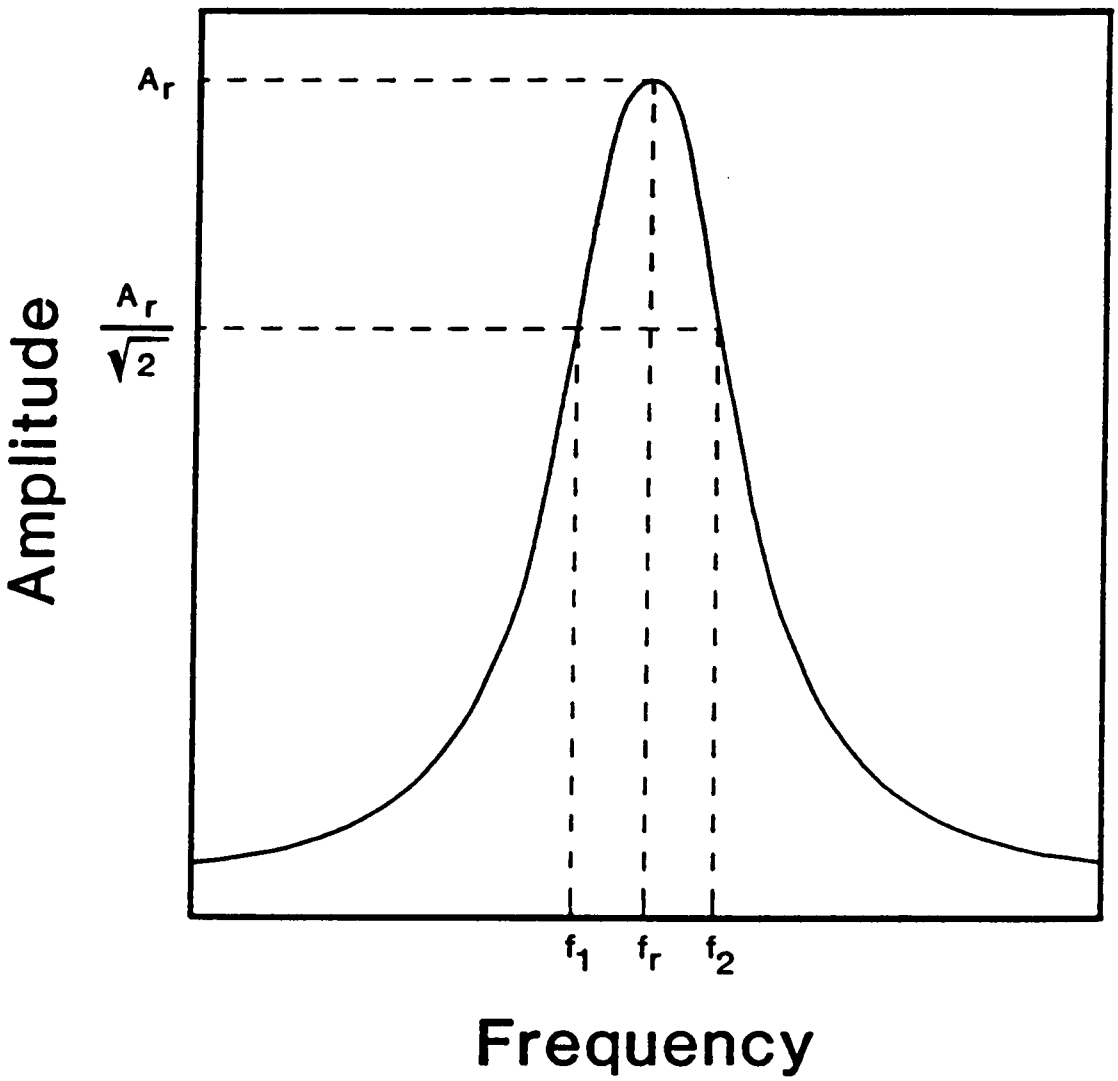

Figure 14. Amplitude of vibration versus frequency of vibration for a free-free beam vibrating at its fundamental resonant frequency under forced oscillation.

$$\Delta = \frac{\pi (f_2 - f_1)}{f_r} \qquad [29]$$

The loss tangent, also a measure of internal friction, is related to the logarithmic decrement:

$$\tan \delta = \frac{\Delta}{\pi} \qquad [30]$$

Under dynamic conditions, an alternating strain (or stress) lags behind the corresponding alternating stress (or strain). This reflects the finite time required for a material to respond to an applied stress (or strain). The angle of phase lag between stress and strain is:

$$\delta = \arctan \frac{\Delta}{\pi} \qquad [31]$$

The dynamic modulus of elasticity or storage modulus, E', represents the ratio of the amplitude of the in-phase component of stress to the strain amplitude. The ratio of the amplitude of the out-of-phase component of stress to the strain amplitude is termed the loss modulus, E". The complex modulus, E*, is used to express the storage and loss moduli as a complex number:

$$E^* = E' + iE'' \qquad [32]$$

The three moduli of Equation [32] are vector quantities. Thus, the complex modulus can be represented geometrically as the resultant (hypoteneuse) of a right triangle formed by the loss and storage

moduli, which act normal to one another. The angle of phase lag, δ, lies between the complex modulus and the adjacent storage modulus. Thus, the complex, storage and loss moduli are related as:

$$E'' = E' \tan \delta \qquad [33]$$

and

$$E^* = \frac{E'}{\cos \delta} \qquad [34]$$

Dynamic mechanical properties are generally highly correlated with mechanical properties determined under static conditions. Thus, dynamic mechanical testing affords a reliable nondestructive means of estimating static mechanical properties.

Assumptions

Underscoring the use of Equation [28] for calculating the dynamic modulus of elasticity, is the assumption that sections plane before bending remain plane after bending. Shear deformation effects are significant only at the higher modes of resonant vibration, and only for low span-to-depth ratios. Hence they are ignored. Air and specimen support damping losses are considered insignificant. Dynamic mechanical properties are dependent upon the frequency of excitation, and ambient temperature. For hygroscopic materials, dynamic properties vary with moisture content. The dynamic properties reported herein were obtained under conditions of constant temperature

and specimen moisture content, at the fundamental resonant frequency only.

Experimental

The dynamic mechanical properties of 9 specimens at each effective reinforcement volume fraction were determined under forced vibration using the test apparatus shown in Figure 15. The specimen was excited with an amplified audio signal of known frequency emanating from a loudspeaker mounted beneath it. Flexural compressive and tensile strains induced in the specimen surface were transduced into an electric signal by the piezoelectric effect of a diamond stylus resting upon it. At constant audio signal gain, the amplitude of the transduced signal was monitored with a voltmeter as the exciting frequency was varied. Maximum signal amplitude was attained when the specimen was driven at its natural fundamental resonant frequency. A frequency counter in series with the audio signal generator allowed the resonant frequency of vibration to be measured to 0.1 Hz. The width of the resonance peak was determined by identifying the exciting frequency, both above and below the resonant frequency, at which the signal amplitude dropped to $1/\sqrt{2}$ times the maximum amplitude.

The specimen was supported at its nodal points, the points at which no vertical displacement occurs. Nodal points are located at a distance of 0.2242L from each end of the specimen when it is vibrated in its fundamental resonant mode. The diamond transducer contacted

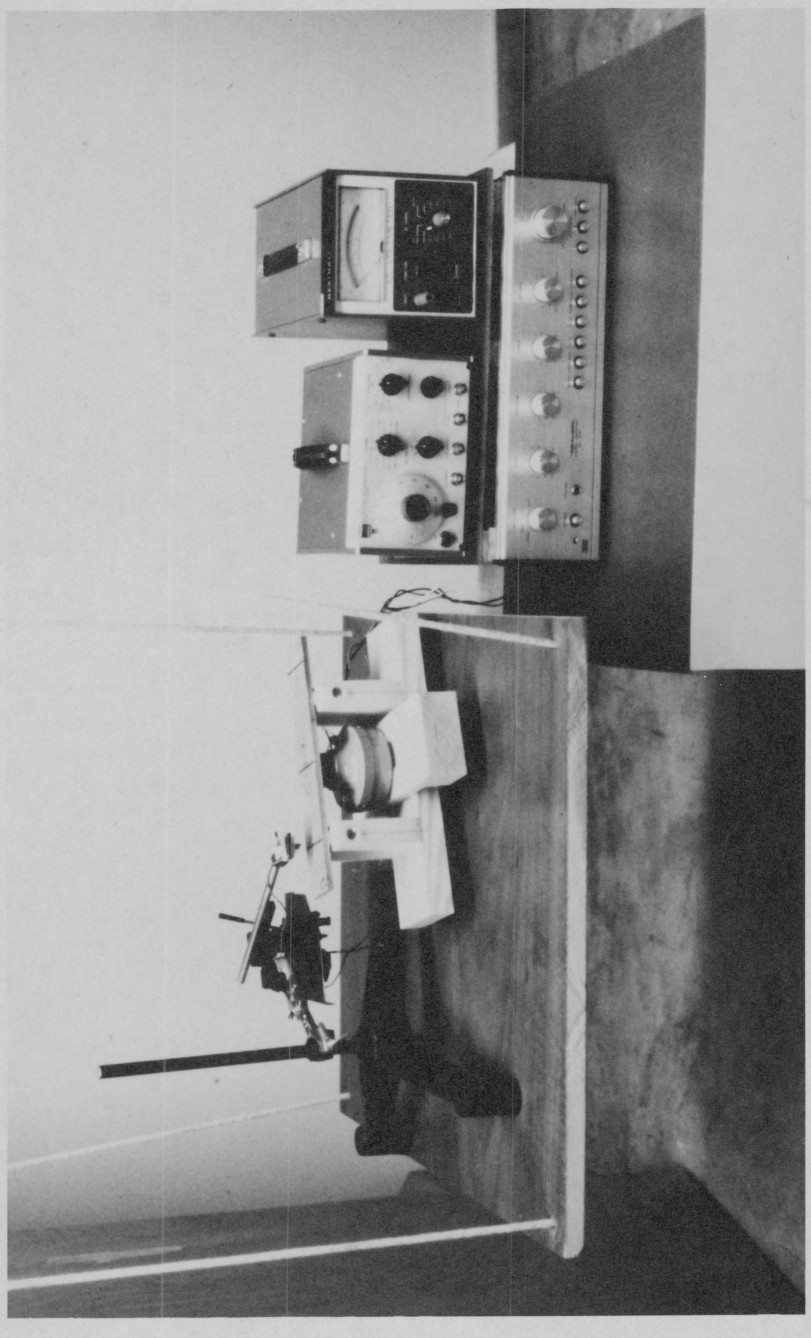

Figure 15. Dynamic modulus of elasticity test apparatus.

the specimen at one of the nodes. Thus, only the alternating contraction and elongation of the surface during flexure was sensed; vertical displacement was not detected. The arm supporting the transducer was counterweighted such that only the force required to maintain contact with the specimen was exerted upon its surface. The test apparatus was suspended from overhead to isolate it from stray vibrations present in the testing area.

Following dynamic property determination, specimens were tested in static bending as outlined previously. The relationship between the dynamic and static mechanical properties of glass fiber reinforced hardboard is discussed in the following chapter.

Results and Discussion

The fundamental resonant frequency of vibration, and hence, the dynamic modulus of elasticity, or storage modulus, of glass fiber reinforced hardboard increased with increasing effective reinforcement volume fraction in a curvilinear relationship (Table 9). The mean and range of observed values of E', and the 95 percent confidence interval for each mean are plotted versus effective reinforcement volume fraction in Figure 16. Individual observed values of f_r and E' are listed in Appendix 3. Inequality among the means over all effective reinforcement volume fractions was shown at $\alpha = 0.01$ via ANOVA. Each mean was shown to be unique, also at $\alpha = 0.01$, using DMRT. A summary of ANOVA and DMRT results is presented in Appendix 7.

Table 9. Dynamic mechanical properties of glass fiber reinforced hardboard.

Effective V_f	f_r [a]	E' [b]	Δ	tan δ	E'' [b]	E^* [b]
0	311	554,300	0.0703	0.0224	12,400	554,500
0.0073	337	671,200	0.0663	0.0211	14,200	671,400
0.0158	349	741,000	0.0643	0.0205	15,200	741,200
0.0260	363	808,600	0.0612	0.0195	15,800	808,800

[a] Hz

[b] psi

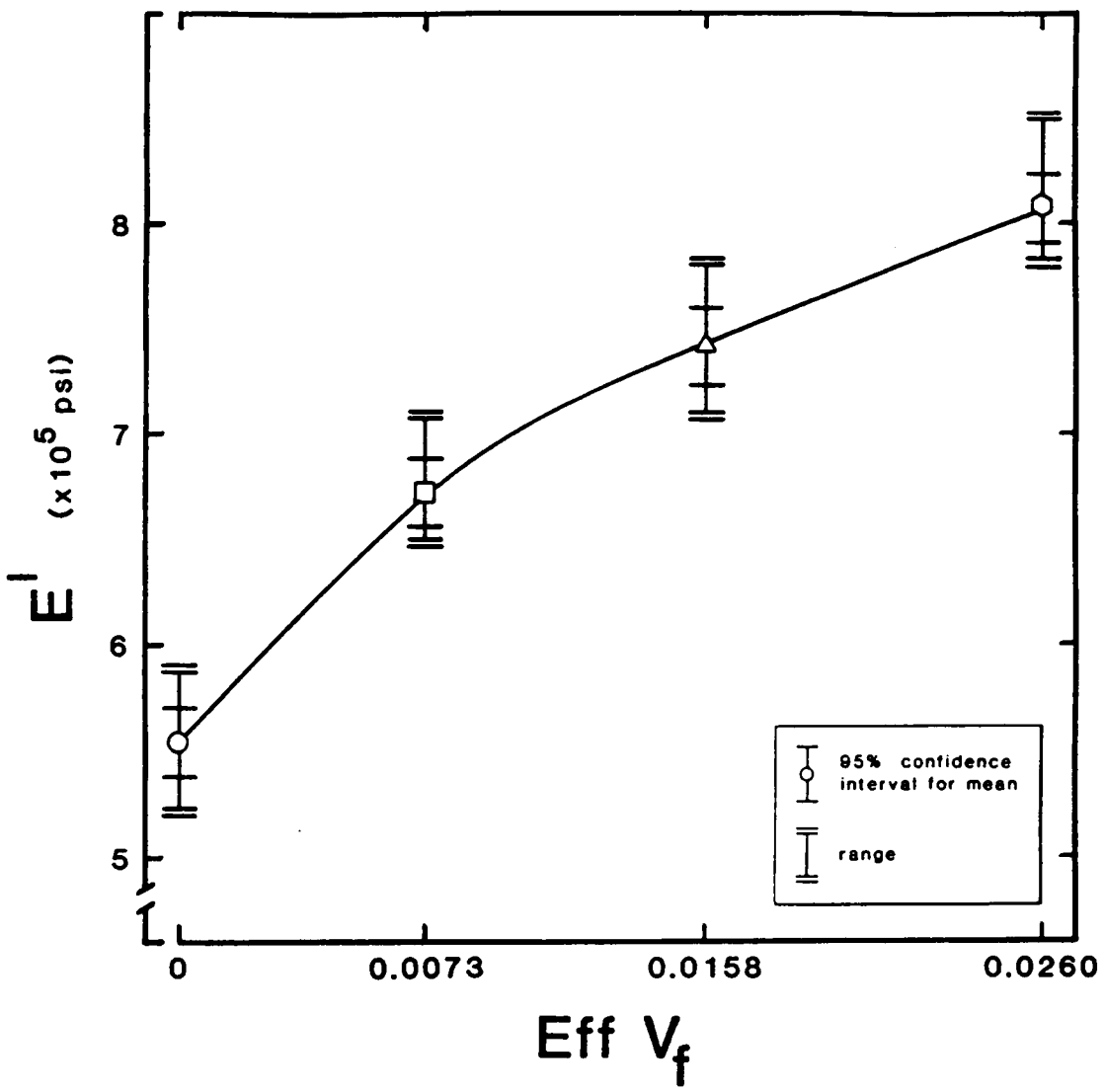

Figure 16. Influence of effective reinforcement volume fraction (Eff V_f) on the flexural dynamic modulus of elasticity (E') of glass fiber reinforced hardboard.

The logarithmic decrement of glass fiber reinforced hardboard was observed to decrease with increasing effective reinforcement volume fraction (Table 9). The mean and range of observed values, and the 95 percent confidence interval for each mean are plotted versus effective reinforcement volume fraction in Figure 17. Mean values for the associated loss tangent are also plotted in Figure 17. Individual observed values for the logarithmic decrement are listed in Appendix 3. ANOVA performed on the means showed inequality among them at $\alpha = 0.01$ (Appendix 8). The mean logarithmic decrements at an effective reinforcement volume fraction of 0 and 0.0260 are shown to be unique at $\alpha = 0.05$ using DMRT. DMRT could not distinguish between the means at an effective reinforcement volume fraction of 0.0073 and 0.0158. The inability of DMRT to distinguish between the means is due to the inclusion of outliers among the data at an effective reinforcement volume fraction of 0.0158.

The logarithmic decrement may be viewed as representing the percentage of energy applied to a material that is dissipated internally rather than being transmitted through it. It follows that a stiff, high modulus material has a low damping capacity, and a small logarithmic decrement. Since glass fiber reinforcement increases the modulus of elasticity of hardboard, a concurrent decrease in the logarithmic decrement is anticipated.

The loss tangent observed for the nonreinforced hardboard controls compares favorably with that reported by Moslemi (1967):

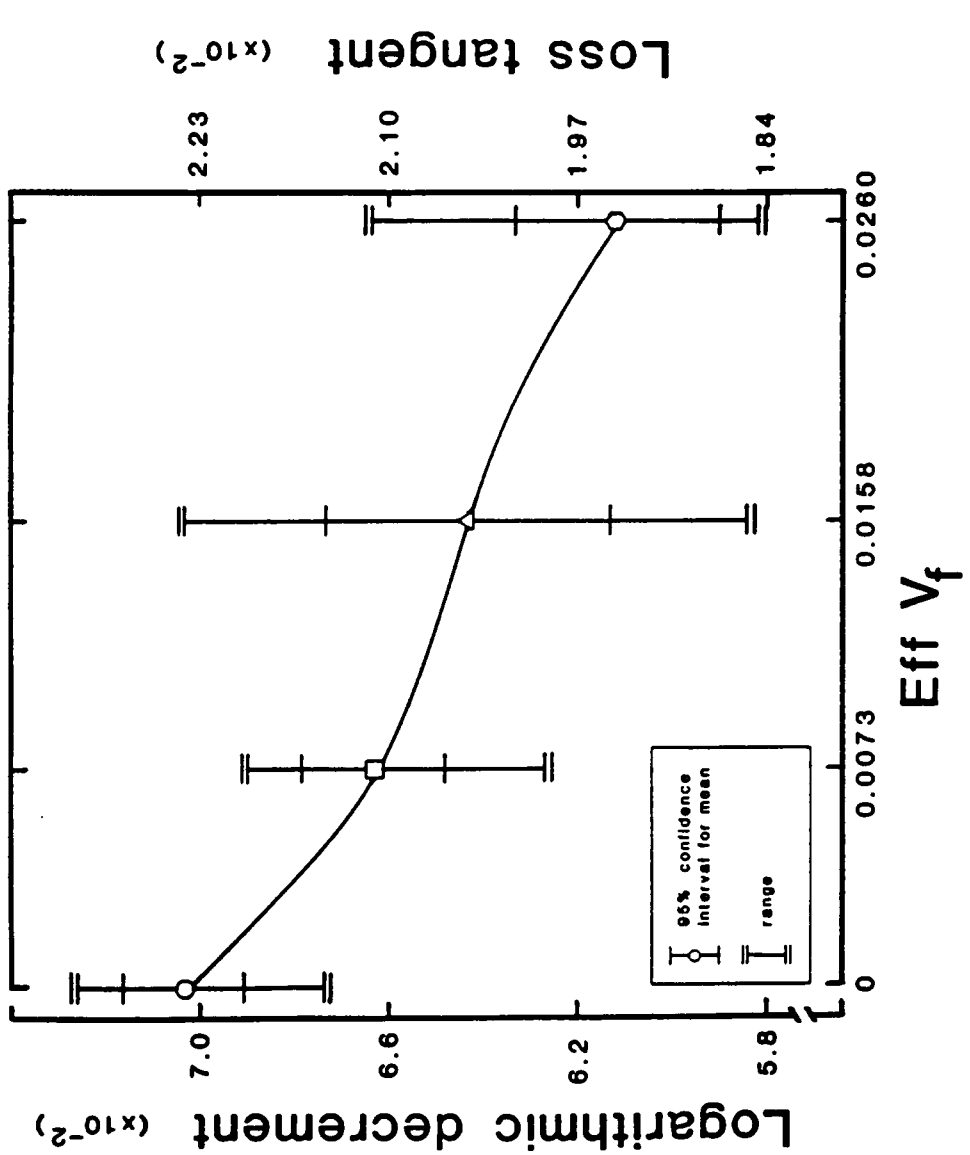

Figure 17. Influence of effective reinforcement volume fraction (Eff V_f) on the loss tangent and logarithmic decrement of glass fiber reinforced hardboard.

0.0224 and 0.0206, respectively. The associated angles of phase lag are 1.28° and 1.18°, respectively.

The loss tangent, and therefore the damping capacity, of hardboard is large relative to most materials, and comparable to that of solid wood. The magnitude of the loss tangent for rubbery polymers is 10^{0} to 10^{-1}, for example, while that for glassy polymers is 10^{-2} to 10^{-4}, and 10^{-4} to 10^{-6} for metals (Read and Dean 1978).

The complex and storage moduli of glass fiber reinforced hardboard also increased with effective reinforcement volume fraction as per Equations [33] and [34]. The complex and storage moduli differ by less than 2 percent, owing to the small values of loss tangent.

Conclusions

The fundamental resonant frequency of vibration and the flexural dynamic modulus of elasticity of free-free glass fiber reinforced hardboard beams increased in a curvilinear fashion with increasing effective reinforcement volume fraction. The mean observed dynamic modulus of elasticity at each effective reinforcement volume fraction was statistically unique at $\alpha = 0.01$. The logarithmic decrement, and loss tangent of glass fiber reinforced hardboard decreased with increasing effective reinforcement volume fraction, also in a non-linear manner.

CORRELATION OF THE DYNAMIC AND STATIC MECHANICAL PROPERTIES OF GLASS FIBER REINFORCED HARDBOARD

Introduction

Relationships among the dynamic flexural modulus of elasticity, the static flexural modulus of elasticity and the modulus of rupture of glass fiber reinforced hardboard were examined. The intention was to identify empirical relationships between flexural properties obtained from nondestructive dynamic and destructive static test methods.

Experimental

As noted in the preceding chapter, the dynamic modulus of elasticity was determined for 9 specimens at each effective reinforcement volume fraction. The static flexural MOE and MOR for each were subsequently evaluated as previously described. Static bending tests alone were conducted on 6 additional specimens at each effective reinforcement volume fraction. Thus, dynamic and static moduli of elasticity and modulus of rupture data were known for each of 9 specimens at each effective reinforcement volume fraction, while static modulus of elasticity and modulus of rupture data were known for each of 15 specimens at each effective reinforcement volume fraction.

Correlations between paired values of dynamic modulus of elasticity and static modulus of elasticity, dynamic modulus of elasticity and modulus of rupture, and static modulus of elasticity and modulus of rupture were identified using the least squares method. With this technique, both quantities considered are assumed to be random variables. A linear relationship between the variables is required. The strength of linear association is measured by the correlation coefficient, r, which ranges from -1 to +1. As the value of r approaches the extremes of its range, linear association between data pairs becomes more perfect.

Thirty-six paired data points were used in correlating the dynamic modulus of elasticity and static modulus of elasticity, and dynamic modulus of elasticity and modulus of rupture. Correlation of static modulus of elasticity and modulus of rupture was performed with 60 data point pairs.

Results and Discussion

Excellent correlation exists between the dynamic and static moduli of elasticity, the dynamic modulus of elasticity and the modulus of rupture, and the static modulus of elasticity and modulus of rupture of glass fiber reinforced hardboard. The criterion of a linear relationship between paired random variables is met in all cases.

The static modulus of elasticity is plotted versus the dynamic modulus of elasticity in Figure 18. The estimated least squares regression equation relating the two is:

$$MOE = 0.85818\ E' - 37983 \qquad [35]$$

A correlation coefficient of 0.99 demonstrates that the static modulus of elasticity of glass fiber reinforced hardboard can be accurately predicted from the dynamic modulus of elasticity. Values for E' were on average, 25 percent greater than the corresponding values of MOE. The departure between E' and MOE ranged from 18 to 29 percent.

Enhanced values for the flexural modulus obtained under dynamic versus static test conditions is attributed to the rapid rate of loading employed in the former method. McNatt (1970), for example, reported that the observed bending strength of hardboard increased 8 percent for each tenfold decrease in time to maximum load. The modulus of elasticity of hardboard should be similarly affected, as hardboard is not perfectly elastic, but rather viscoelastic. Under ramp loading in static bending, the proportional limit for the hardboard control was reached in about 35 seconds. During dynamic testing, the control at resonance was being driven at a rate of 311 Hz, or about 10,000 times faster.

The modulus of rupture is plotted versus the dynamic modulus of elasticity in Figure 19. The estimated least squares regression equation expressing MOR as a function of E' is:

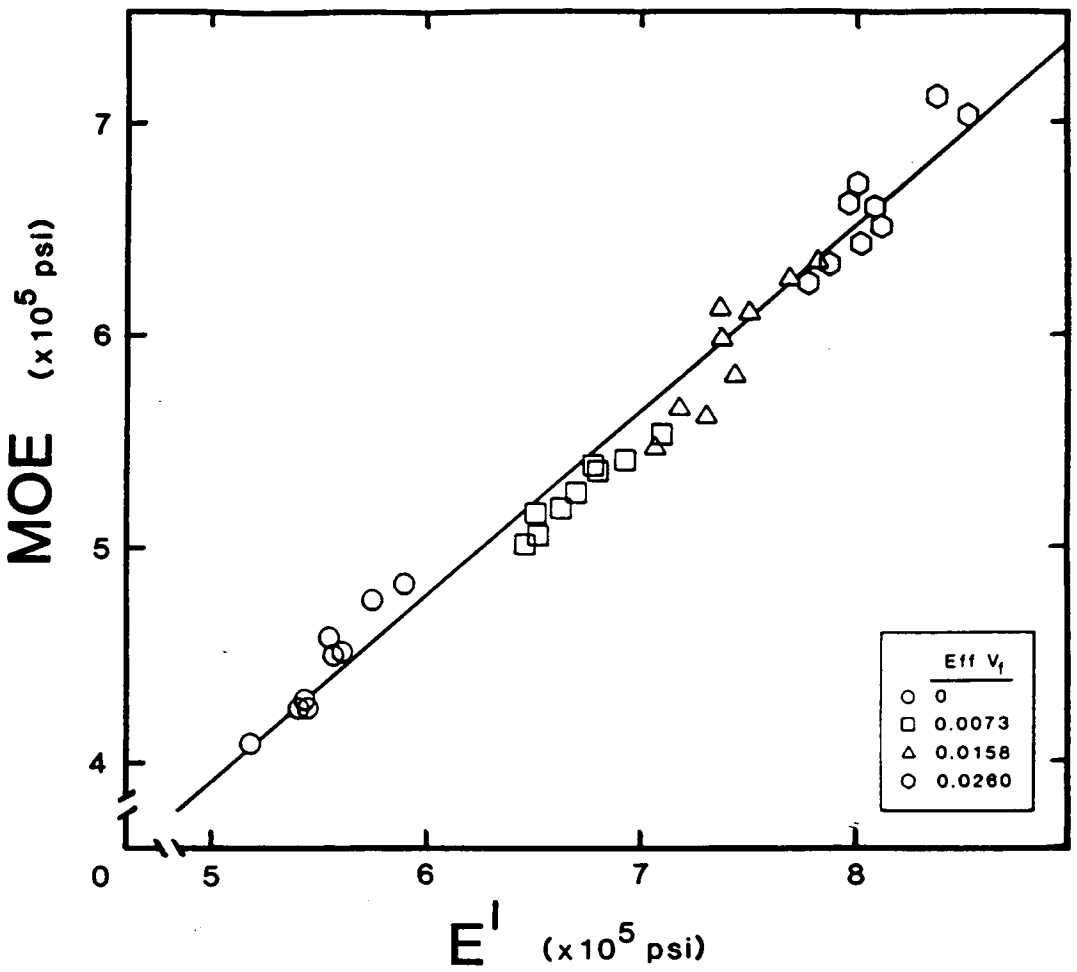

Figure 18. Relationship between the static bending modulus of elasticity (MOE) and the dynamic modulus of elasticity (E') of glass fiber reinforced hardboard by effective reinforcement volume fraction (Eff V_f).

MOE = 0.85818 E' - 37983 r = 0.99

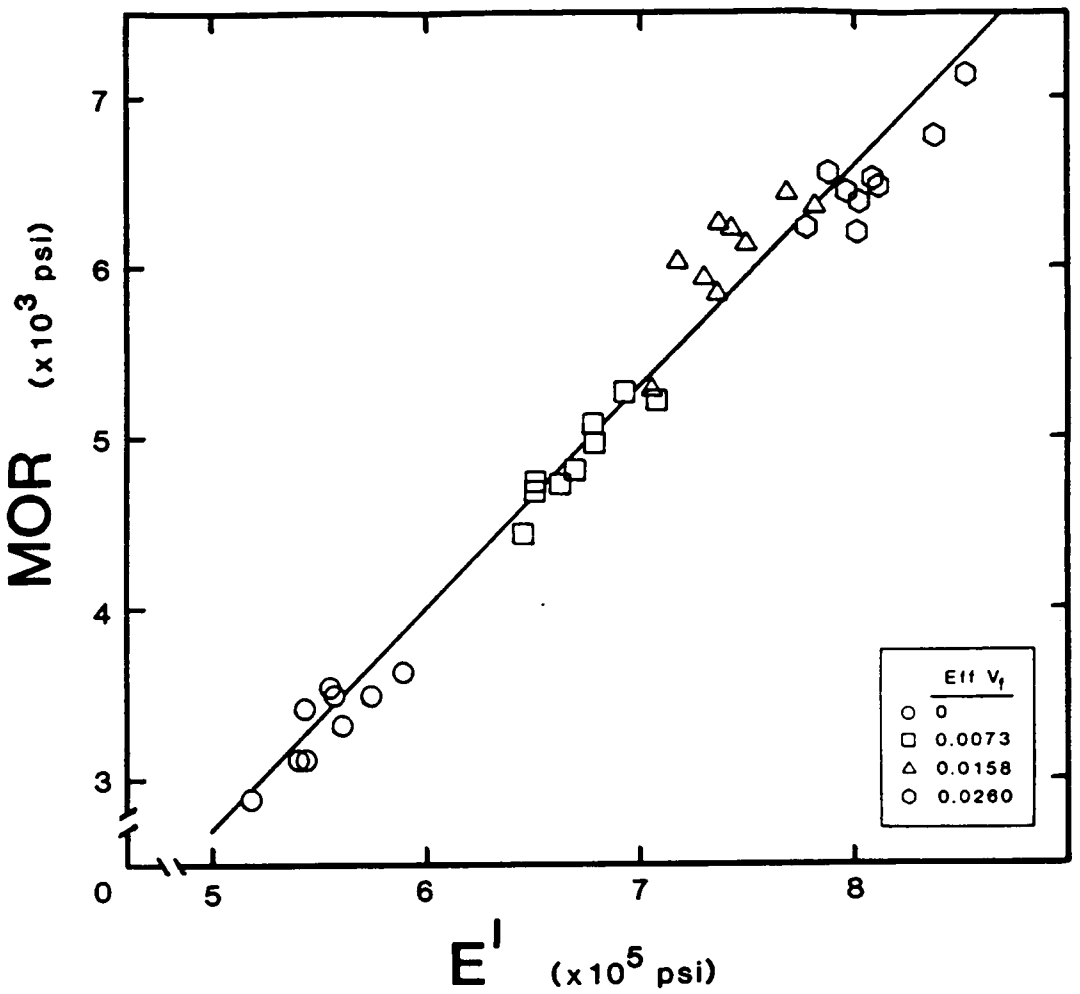

Figure 19. Relationship between the static bending modulus of rupture (MOR) and the dynamic modulus of elasticity (E') of glass fiber reinforced hardboard by effective reinforcement volume fraction (Eff V_f).

MOR = 0.01291 E' - 3760 r = 0.99

$$MOR = 0.01291\ E' - 3760 \qquad [36]$$

Modulus of rupture of glass fiber reinforced hardboard can be reliably estimated from the dynamic modulus of elasticity as evidenced by a correlation coefficient of 0.99.

The modulus of rupture is plotted versus the static modulus of elasticity in Figure 20. The estimated least squares regression line relating the two is:

$$MOR = 0.01467\ MOE - 2945 \qquad [37]$$

A correlation coefficient of 0.98 demonstrates that the modulus of rupture of glass fiber reinforced hardboard can be reliably estimated from the static modulus of elasticity.

Strong correlation found among the dynamic and static moduli of elasticity and the modulus of rupture owes to the similar dependence of each on the effective reinforcement volume fraction. The mean observed dynamic and static modulus of elasticity and modulus of rupture were shown previously to be unique at $\alpha = 0.01$ for each effective reinforcement volume fraction. Inspection of Figures 18, 19 and 20 shows that a slight overlapping of the range of values about each mean occurs at its extremes for all effective reinforcement volume fractions. The tight clustering of observed data point pairs about each estimated regression line further bolsters the confidence with which property estimates may be made using estimated regression Equations [35], [36] and [37].

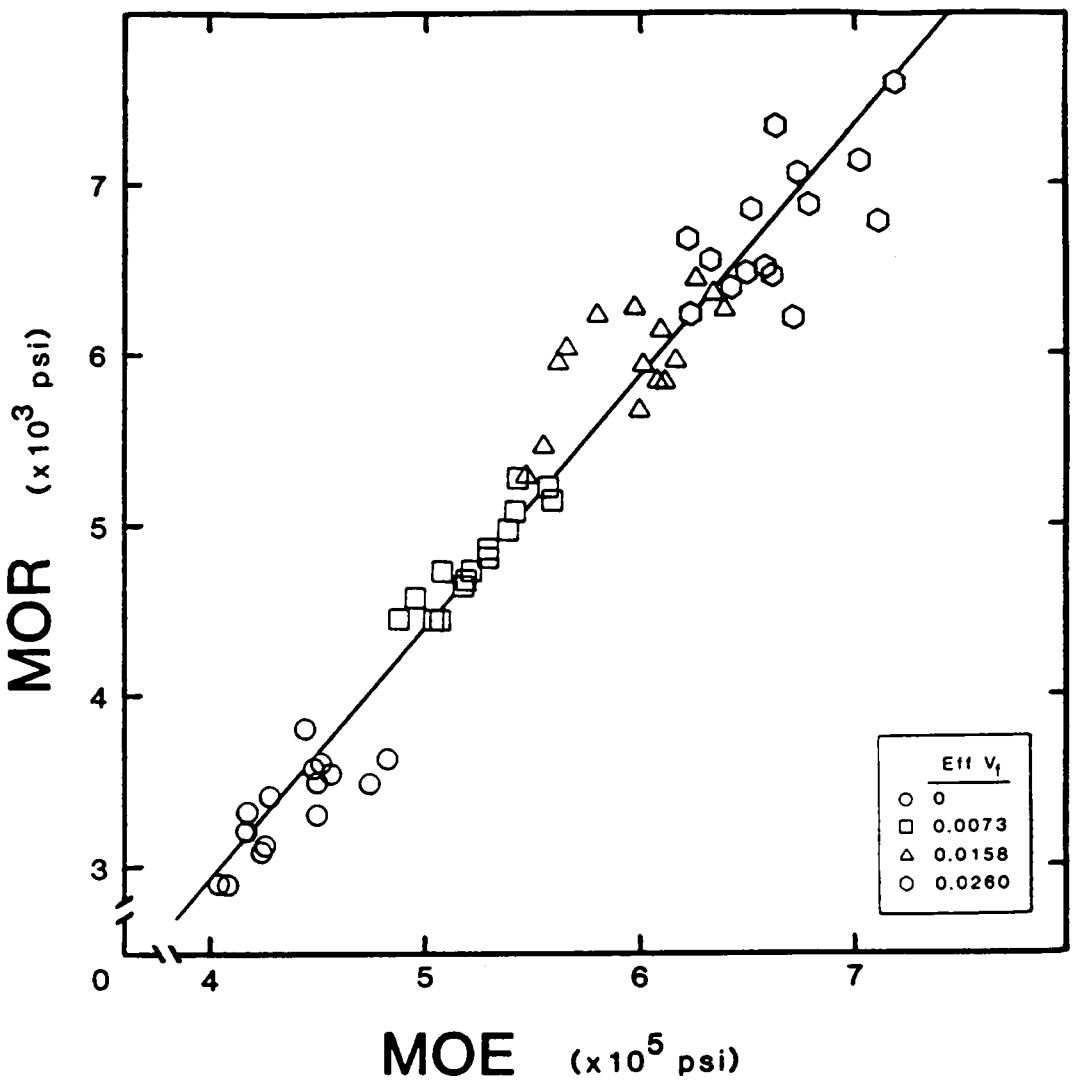

Figure 20. Relationship between the static bending modulus of rupture (MOR) and the static bending modulus of elasticity (MOE) of glass fiber reinforced hardboard by effective reinforcement volume fraction (Eff V_f).

MOR = 0.01467 MOE - 2945 r = 0.98

Conclusions

Excellent correlation existed among the dynamic modulus of elasticity, the static modulus of elasticity, and the modulus of rupture of glass fiber reinforced hardboard. The static modulus of elasticity, and the modulus of rupture can be reliably estimated from the dynamic modulus of elasticity using empirical regression equations derived via the method of least squares. Modulus of rupture can be reliably estimated from the static modulus of elasticity in the same manner. Strong linear association between flexural properties determined in destructive static tests and nondestructive dynamic tests demonstrated the usefulness of dynamic test methods for flexural property evaluation. The dynamic modulus of elasticity is on average, 25 percent greater than the static modulus of elasticity, owing to rate of loading effects.

CREEP BEHAVIOR OF GLASS FIBER REINFORCED HARDBOARD

Introduction

The short-term flexural creep behavior of glass fiber reinforced hardboard within the elastic limit was investigated. Creep deflection data were fitted to the numerical analog of a 4-element mechanical model comprising elastic, viscoelastic and viscous components. Model parameters were estimated using nonlinear regression analysis. The creep behavior of glass fiber reinforced hardboard at constant ambient temperature and relative humidity is well described by the model.

Theoretical

The flexural creep behavior of a linear viscoelastic material can be described mechanistically by the 4-element Burger model shown in Figure 21a. The lone spring and dashpot represent, respectively, the instantaneous elastic and viscous responses; the spring and dashpot paired in parallel represent the delayed elastic, or viscoelastic response.

The mathematical analog of the Burger model expresses the total axial strain developed during bending as the sum of the strains developed in its elastic, viscoelastic and viscous components with respect to time under load (Flugge 1975):

$$\varepsilon(t) = \frac{\sigma}{E_e} + \frac{\sigma}{E_d}\left(1 - \exp\ \frac{-t}{\tau}\right) + \frac{\sigma t}{\eta_v} \qquad [38]$$

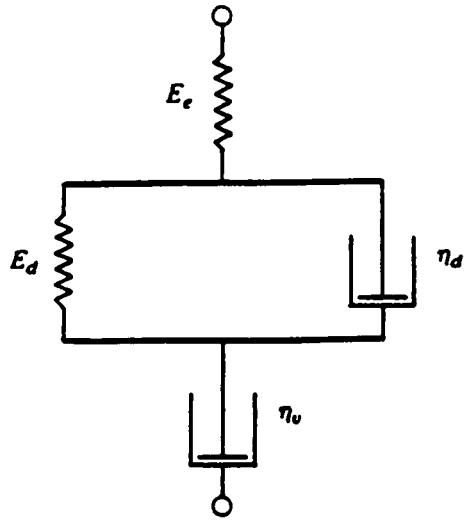

a.

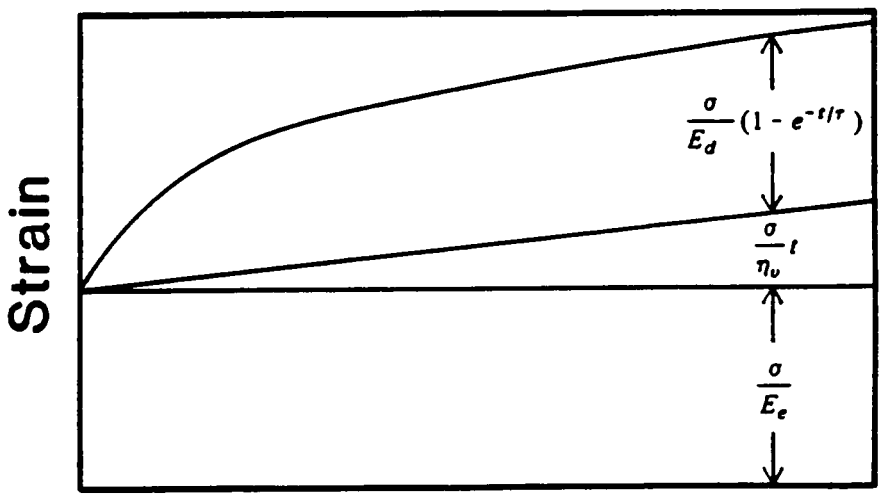

b.

Figure 21a. Four-element Burger model for creep of linear viscoelastic materials.

21b. Flexural creep strain versus time as per the Burger model.

The retardation time, τ, is equal to the ratio of the delayed coefficient of viscosity to the delayed modulus of elasticity, η_d/E_d. The parameters of the numerical model can be graphically estimated from a plot of creep strain versus time (Figure 21b). Since deflection, and not strain, is routinely measured during creep testing, creep deflection must be transformed to creep strain through the observed instantaneous modulus of elasticity, E_e.

A plot of $\varepsilon(t)$ versus t becomes linear for large values of t. The constant slope of the creep curve in the viscous deformation region is σ/η_v, allowing for estimation of the viscous coefficient of viscosity, η_v. In this region, it is assumed that all viscoelastic deformation has occurred. Equation [38] may be rewritten to reflect this:

$$\varepsilon(t) = \frac{\sigma}{E_e} + \frac{\sigma}{E_d} + \frac{\sigma t}{\eta_v} \qquad [39]$$

Creep strain is now expressed as a linear function of time.

A line drawn tangent to $\varepsilon(t)$ versus t in the region of viscous deformation intercepts the strain axis at:

$$\varepsilon(t) = \frac{\sigma}{E_e} + \frac{\sigma}{E_d} \qquad [40]$$

The delayed modulus of elasticity, E_d, can be estimated from $\varepsilon(t)$, σ and E_e. The retardation time, τ, is estimated empirically when known values of $\varepsilon(t)$, t, σ and E_e, and the estimated values of E_d and η_v are substituted into Equation [38]. When a value of τ that

satifies Equation [38] is found, an estimate of the delayed coefficient of viscosity, η_d, is given by τ times E_d.

Estimates of Burger model parameters using graphic techniques have been made by Moslemi (1964a), and Szabo and Ifju (1970), for hardboard and solid wood in flexure, respectively. Senft and Suddarth (1971) employed nonlinear regression techniques to estimate model parameters for compression creep of wood. Nonlinear regression analysis was employed by Pierce and Dinwoodie (1977), and Pierce, et al. (1979, 1985) to estimate creep model parameters of flakeboard in flexure.

Assumptions

It is assumed that glass fiber reinforced hardboard behaves as a linear viscoelastic material (see Results and Discussion section). The estimated model describes the creep behavior of glass fiber reinforced hardboard within the elastic range only. Deflection due to shear is assumed insignificant, and therefore ignored, given the low load levels employed and the use of two-point loading. Creep deflection of hardboard is influenced by specimen moisture content, and fluctuating ambient temperature and relative humidity. Estimates for the model parameters given herein, are valid only for short-term loading under conditions of constant specimen moisture content, and ambient temperature and relative humidity.

Experimental

The mid-point creep deflection of 3 glass fiber reinforced hardboard beams at each effective reinforcement volume fraction was monitored over 4 hours' time under two load levels within the elastic range. The test apparatus accommodated a 2 inch by 10 inch specimen simply-supported over an 8 inch span. The load was applied at two points 2 inches apart, and symmetric about the mid-point of the specimen. As shown in Figure 22, the two-point loading head was supported on its underside by an overhead bracket which straddled the specimen. The bracket was manually lowered with a gear-and-rack mechanism, and descended from beneath the loading head once contact was made with the specimen. The mass of the loading head accounted for only part of the applied load. A weight suspended from it by wire comprised the remainder. With this system, the specimen was loaded or unloaded instantaneously in a smooth and highly controlled manner.

Creep specimens were stressed in flexure at a nominal 650 or 1110 psi, under a load of 9.09 or 15.5 pounds, respectively. The former value is nominally 50 percent of the load at proportional limit for the hardboard control; the latter is nominally 50 percent of the load at proportional limit for hardboard reinforced with the greatest glass fiber volume fraction. Load level is expressed as a percentage of the load at proportional limit for each effective reinforcement volume fraction in Table 10.

Mid-point creep deflection was measured to 0.0001 inch with a DC-powered linear variable differential transducer (LVDT) in contact with

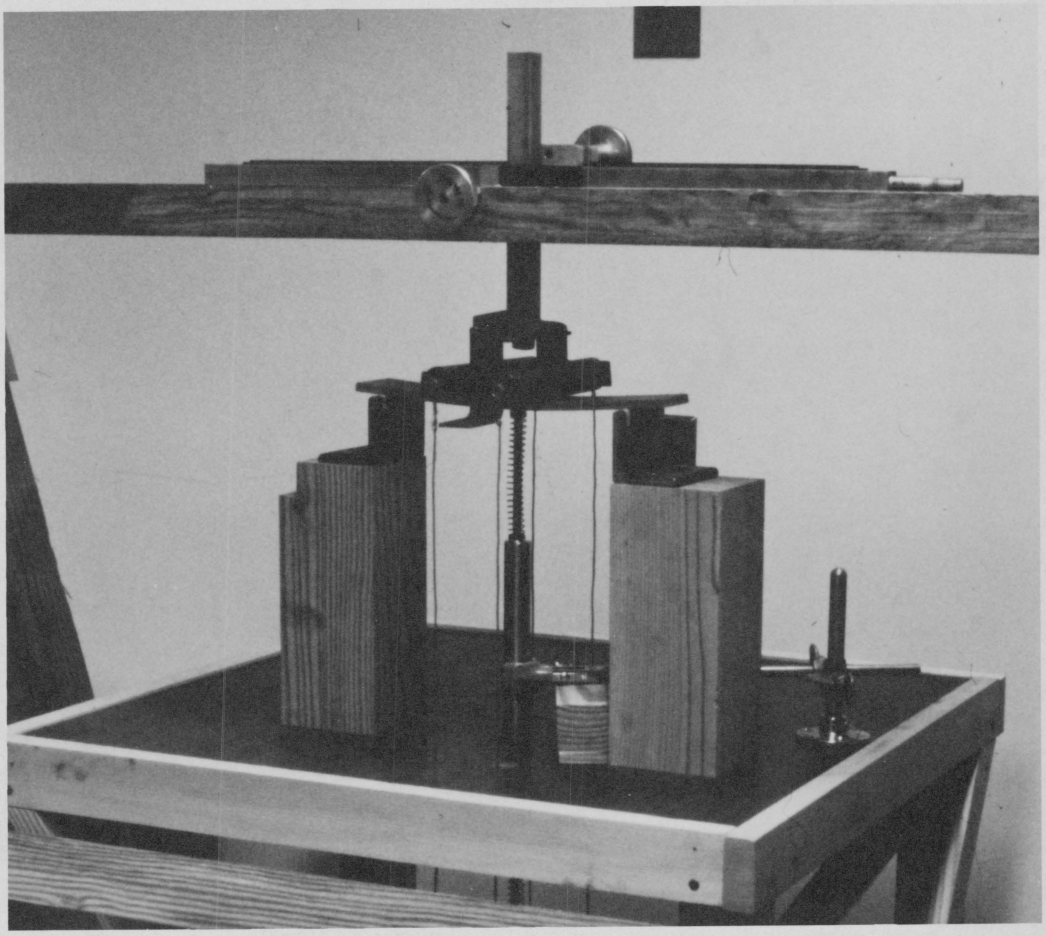

Figure 22. Creep test apparatus.

Table 10. Creep test load levels expressed as a percentage of mean observed load at proportional limit in static bending.

Effective V_f	P[a]	% of P	
		9.09[b]	15.5[b]
0	18.65	48.7	83.3
0.0073	23.44	38.8	66.3
0.0158	28.11	32.3	55.3
0.0260	31.83	28.5	48.8

[a] mean observed load at proportional limit in static bending (lbs)

[b] creep test load level (lbs)

the underside of the specimen. The LVDT was interfaced with a Hewlett-Packard multimeter, calculator/controller and printer that comprised an automated data collection system. Briefly, deflection of the specimen induced a DC voltage in the LVDT which was displayed on the multimeter. An internal clock in the calculator/controller triggered execution of a program in which the displayed DC voltage was converted to deflection using an initial voltage and the LVDT calibration constant stored in its memory. The deflection and the time under load were then printed. The internal clock triggered program execution upon expiration of a user-specified interval of time.

The time capability of the calculator/controller allowed for measurement of the instantaneous elastic deflection with minimal experimental error. The internal clock was allowed to trigger the deflection/time program before the load was applied. The time of execution was noted. The load was then applied one second before the user-specified time interval elapsed, so that load application was concurrent with program execution.

Moslemi (1964a, 1964b) and Sauer and Haygreen (1968) have shown that creep deflection of hardboard becomes approximately linear with time after only 2 hours under moderate loads. In this study, deflection/time data were recorded for a minimum of 4 hours. During the first 20 minutes under load, creep deflection accrued rapidly, and was measured every 60 seconds. By 20 minutes' time, the rate of creep

deflection had slowed considerably. Henceforth, creep deflection was measured every 5 minutes.

Creep deflection/time data were fitted to the Burger model using nonlinear least squares regression (Department of Biomathematics 1981). Graphic estimates taken from high resolution creep deflection/time plots served as initial estimates for the model parameters. Two regression analyses were performed on the data for each specimen. In the first analysis, CREEP I, the instantaneous modulus of elasticity, E_e, was fixed at its observed value. The values of E_d, η_v, and τ were continuously adjusted within user-specified limits until the residual sum of squares attained a minimum value. Limits were defined as $\pm$ 10 percent of the initial estimates. Estimates of all model parameters, including E_e, were adjusted within the same limits in the second analysis, CREEP II. Again, a minimum value for the residual sum of squares indicated a best fit.

The proportion of the variation in creep strain with time which is explained by the regression model is given by the coefficient of determination, R^2, or by the multiple correlation coefficient, $R = + \sqrt{R^2}$. The more closely R approximates +1, the greater the accuracy of prediction afforded by the model.

Results and Discussion

Mean observed values for the modulus of elasticity of the composite determined from creep and static bending test data are in good agreement at all effective reinforcement volume fractions (Table

11). With one exception, values calculated from the instantaneous elastic deflection observed in the former method, on average, exceed those calculated with the latter method by 5 percent. A difference in loading arrangement, and rate of loading accounts for the departure.

Use of the 4-element Burger model presupposes linear viscoelastic behavior. When subjected to load P, for example, the creep deflection of a simply supported beam at time t is y(t). If the load is doubled to 2P, and the test repeated, the creep deflection of a linear viscoelastic material will also be doubled to 2y(t), for the same elapsed time t. If upon doubling the load, creep deflection over the same time interval differs significantly from 2y(t), then nonlinear viscoelastic behavior is indicated.

At all effective reinforcement volume fractions, glass fiber reinforced hardboard exhibited linear viscoelastic behavior. As seen in Figure 23, the ratio of creep deflection under a 15.5 pound load to that under a 9.09 pound load is essentially constant over the duration of the test, and approximates the ideal value, 1.71.

The creep behavior of glass fiber reinforced hardboard was influenced by the magnitude of the applied load, and the effective reinforcement volume fraction. As the applied load was increased, total creep deflection increased at each effective reinforcement volume fraction. The rate of creep was unaffected, due to the material's linear viscoelastic nature. Increasing the effective reinforcement volume fraction reduced both total creep deflection and creep rate at a given load level. Mean observed instantaneous elastic

Table 11. Comparison of modulus of elasticity of glass fiber reinforced hardboard determined from load and deflection at proportional limit in static bending, and load and instantaneous elastic deflection during creep testing.

Effective V_f	MOE[a,b]	Creep MOE[a,c]	
		9.09[d]	15.5[d]
0	439,500	458,100	463,700
0.0073	524,900	563,400	557,700
0.0158	597,300	651,900	607,400
0.0260	664,800	693,900	655,400

[a] psi

[b] static bending

[c] based on instantaneous elastic deflection

[d] creep test load level (lbs)

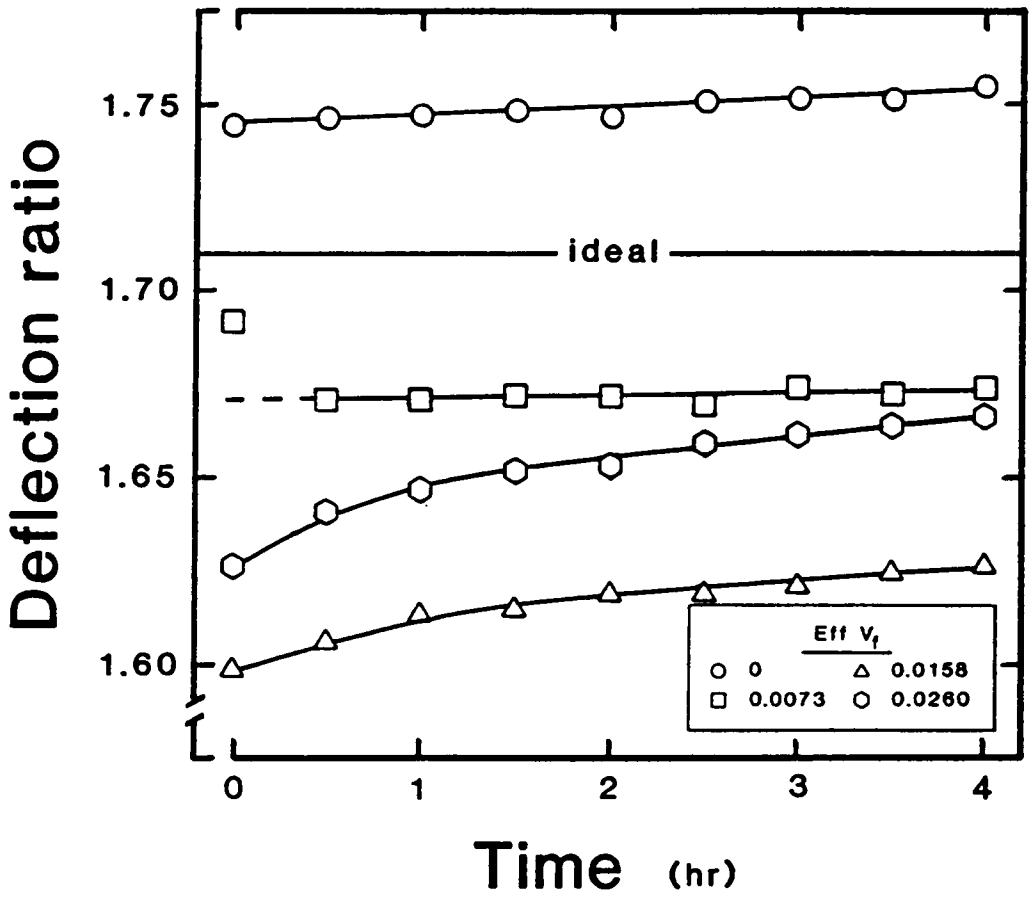

Figure 23. Influence of effective reinforcement volume fraction (Eff V_f) on the creep deflection ratio of glass fiber reinforced hardboard with time. The deflection ratio is equal to the deflection observed under a load of 15.5 lbs. divided by the deflection observed under a load of 9.09 lbs. A deflection ratio of 15.5/9.09 = 1.71 represents ideal linear viscoelastic behavior.

deflection and total deflection data are presented in Table 12 in evidence of these generalizations. Graphic support is provided in Figures 24 and 25 for all effective reinforcement volume fractions. Mean observed creep deflection divided by the instantaneous elastic deflection of the control is plotted versus time, under a load of 9.09 and 15.5 pounds, respectively. Observed and predicted creep deflection for individual specimens at all effective reinforcement volume fractions and load levels are listed in Appendix 9.

Mean estimates of creep model parameters obtained with the CREEP I regression analysis, in which the instantaneous modulus of elasticity parameter, E_e, is fixed at its observed value, are summarized in Tables 13 and 14 for loads of 9.09 and 15.5 pounds, respectively. Parameter estimates and multiple correlation coefficients for individual specimens at all effective reinforcement volume fractions and load levels are listed in Appendix 10. A plot of mean observed and predicted creep deflection, divided by the observed instantaneous elastic deflection, versus time for the composite at an effective reinforcement volume fraction of 0.0073 under 9.09 pounds is shown in Figure 26. An equivalent relationship between mean observed and predicted creep deflection exists at all effective reinforcement volume fractions for both load levels. The following discussion, although referenced to Figure 26, applies equally to all other effective reinforcement volume fraction/load level combinations.

Excellent agreement existed between observed and predicted creep deflections at all effective reinforcement volume fractions for both

Table 12. Mean observed creep deflection of glass fiber reinforced hardboard.

Effective V_f	Deflection[a]					
	9.09[b]			15.5[b]		
	Initial[c]	Final	Creep	Initial[c]	Final	Creep
0	0.0725	0.0856	0.0131	0.1265	0.1502	0.0237
0.0073	0.0587	0.0679	0.0092	0.0993	0.1136	0.0143
0.0158	0.0553	0.0623	0.0070	0.0884	0.1013	0.0129
0.0260	0.0511	0.0560	0.0049	0.0831	0.0933	0.0102

[a] mean observed (in)

[b] creep test load level (lbs)

[c] instantaneous elastic deflection

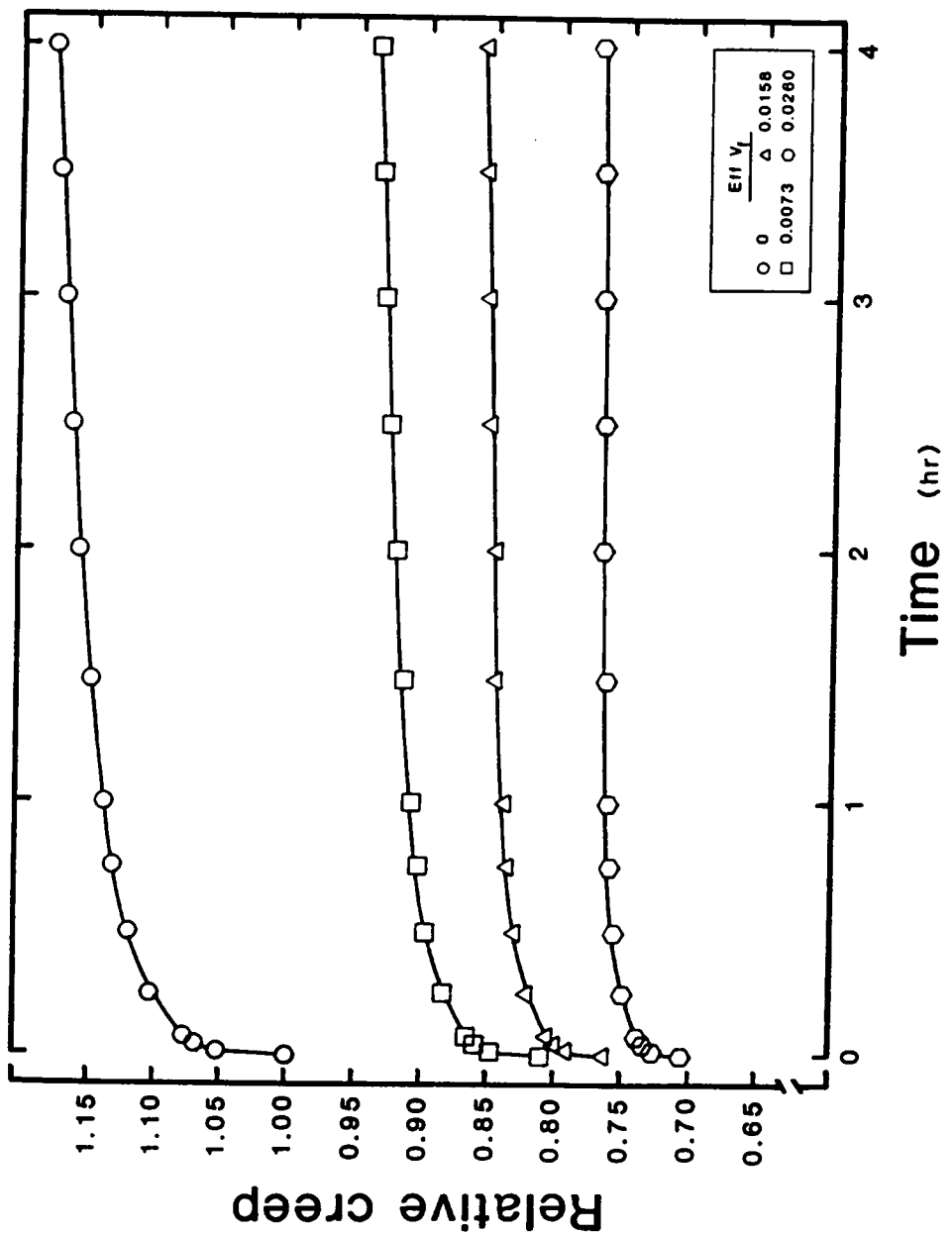

Figure 24. Influence of effective reinforcement volume fraction (Eff V_f) on the relative creep deflection of glass fiber reinforced hardboard under a load of 9.09 lbs.

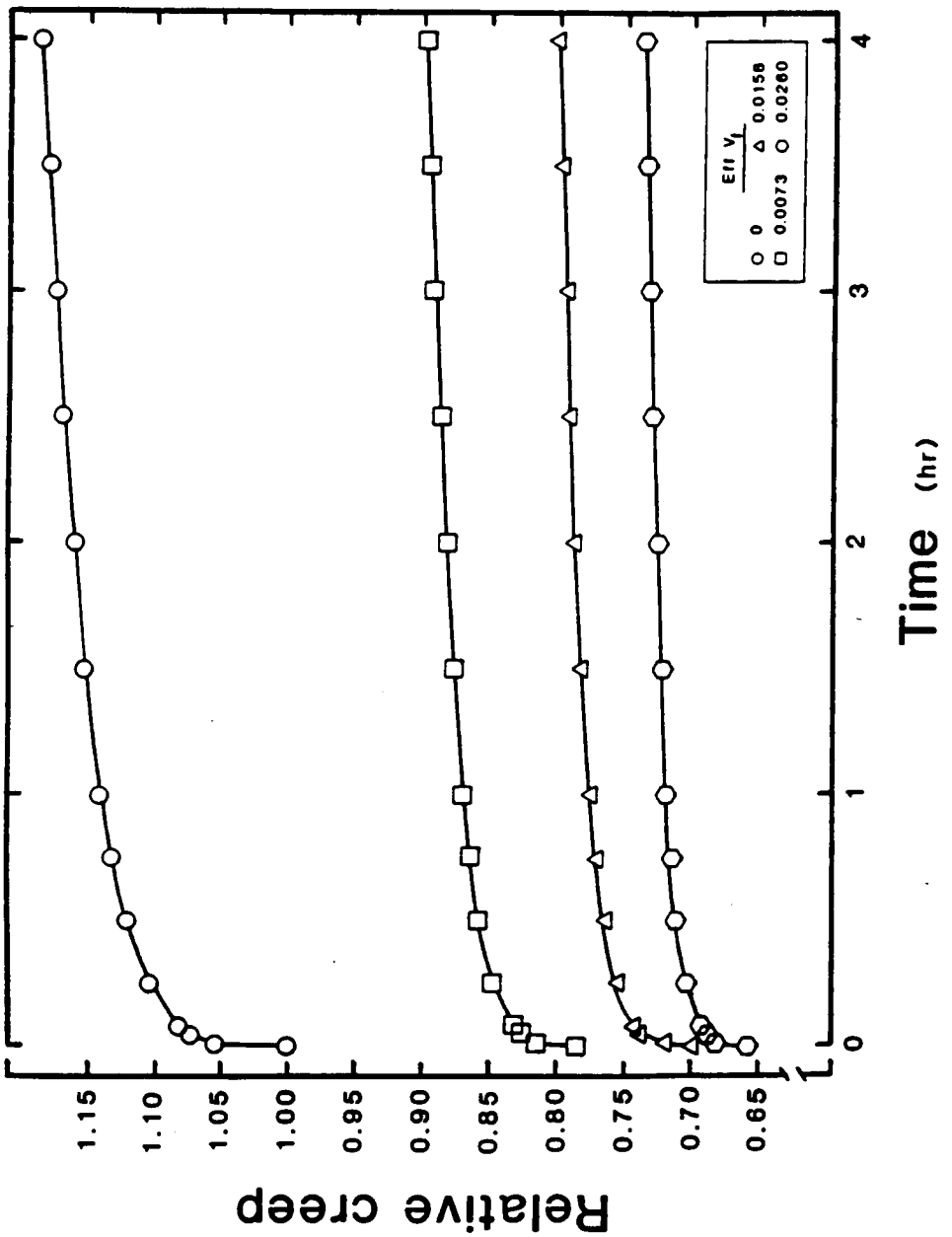

Figure 25. Influence of effective reinforcement volume fraction (Eff V_f) on the relative creep deflection of glass fiber reinforced hardboard under a load of 15.5 lbs.

Table 13. Estimated Burger model creep parameters for glass fiber reinforced hardboard under 9.09 lbs load using CREEP I analysis.

Effective V_f	E_e [a]	E_d [a]	η_d [b]	τ [c]	η_v [b]
0	463,700	3,452,700	483,400	0.14	49,000,000
0.0073	557,700	4,718,500	660,600	0.14	76,667,000
0.0158	607,400	6,630,600	862,000	0.13	82,000,000
0.0260	655,400	8,989,200	1,078,700	0.12	113,500,000

[a] psi

[b] psi-hr

[c] hr

Table 14. Estimated Burger model creep parameters for glass fiber reinforced hardboard under 15.5 lbs load using CREEP I analysis.

Effective V_f	E_e [a]	E_d [a]	η_d [b]	τ [c]	η_v [b]
0	458,100	3,566,900	392,300	0.11	35,000,000
0.0073	563,400	5,428,400	760,000	0.14	68,333,000
0.0158	651,900	6,149,300	922,400	0.15	83,333,000
0.0260	693,900	7,828,900	939,500	0.12	95,000,000

[a] psi

[b] psi-hr

[c] hr

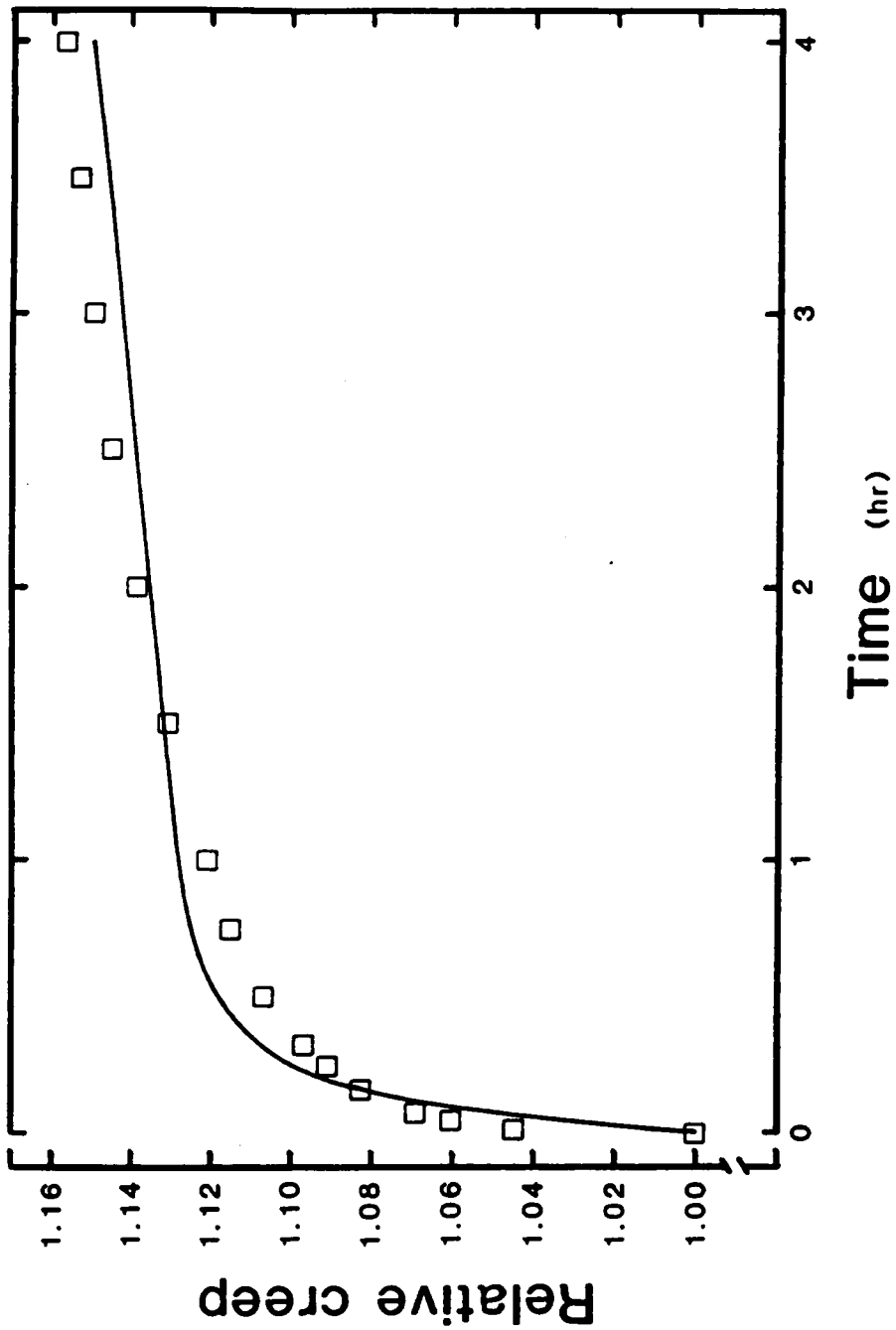

Figure 26. Relative observed (□) and predicted (—) creep deflection of glass fiber reinforced hardboard at an effective reinforcement volume fraction of 0.0073 under 9.09 lbs. load using CREEP I analysis.

load levels (Appendix 9). The multiple correlation coefficient, R, ranged from 0.95 to 0.97 for all 24 CREEP I regression analyses performed (Appendix 10). With the exception of the instantaneous elastic deflection, which was fixed at its observed value, predicted deflections underestimated measured deflections by at most 3 percent for t less than 15 minutes. At this time, and continuing to about 1.5 hours, predicted values exceeded observed values by at most 1 percent. For t greater than 1.5 hours, predicted values underestimated observed values by less than 1 percent.

The delayed modulus of elasticity and the delayed coefficient of viscosity increased with effective reinforcement volume fraction at both load levels (Tables 13 and 14). The retardation time, τ, is equal to the ratio η_d / E_d, and represents the time required for the delayed elastic strain to decay to 1/e times its value at removal of the applied stress. Retardation time decreased with effective reinforcement volume fraction owing to a concurrent increase in restorative force, E_d. The trend in retardation time is most apparent at a load level of 9.09 pounds (Table 13). Retardation times estimated with the CREEP I regression analysis are quite low, and range from 0.11 to 0.15 hours.

The viscous coefficient of viscosity increased with effective reinforcement volume fraction. Given their magnitude (10^7), parameter estimates at both load levels are approximately equal at each effective reinforcement volume fraction. The rate of creep deflection

is thus unaffected by load level for a given effective reinforcement volume fraction, and linear viscoelastic behavior is indicated.

Fixing the instantaneous modulus of elasticity at its observed value, as in CREEP I, forced τ to assume artificially small values. A second nonlinear regression analysis was performed in which the observed instantaneous modulus of elasticity was instead, varied between user-specified limits. The analysis is designated CREEP II, and allows for experimental error possibly present in the measured instantaneous elastic deflection.

Mean estimates of creep model parameters using the CREEP II regression analysis are presented in Tables 15 and 16, for loads of 9.09 and 15.5 pounds, respectively. Parameter estimates and multiple correlation coefficients for individual specimens at each effective reinforcement volume fraction/load level combination are listed in Appendix 11. A plot of mean observed and predicted creep deflection, divided by the observed instantaneous elastic deflection, versus time for the composite at an effective reinforcement volume fraction of 0.0073 under 9.09 pounds is shown in Figure 27. Although referenced to Figure 27, the following discussion may be generalized to all effective reinforcement volume fraction/load level combinations.

Excellent agreement existed between observed and predicted creep deflections at all effective reinforcement volume fractions for both load levels (Appendix 9). The multiple correlation coefficient, R, ranged from 0.96 to 0.99 for all 24 CREEP II regression analyses performed (Appendix 11). Predicted values for the instantaneous

Table 15. Estimated Burger model creep parameters for glass fiber reinforced hardboard under 9.09 lbs load using CREEP II analysis.

Effective V_f	E_e [a]	E_d [a]	η_d [b]	τ [c]	η_v [b]
0	444,900	4,856,400	1,262,700	0.26	49,000,000
0.0073	538,100	6,521,800	1,826,100	0.28	75,667,000
0.0158	591,400	8,990,300	1,977,900	0.22	82,000,000
0.0260	643,800	11,473,300	2,179,900	0.19	113,500,000

[a] psi

[b] psi-hr

[c] hr

Table 16. Estimated Burger model creep parameters for glass fiber reinforced hardboard under 15.5 lbs load using CREEP II analysis.

Effective V_f	E_e [a]	E_d [a]	η_d [b]	τ [c]	η_v [b]
0	439,300	5,141,000	1,131,000	0.22	35,000,000
0.0073	545,700	7,593,800	2,050,300	0.27	68,333,000
0.0158	630,200	8,679,200	2,690,500	0.31	83,333,000
0.0260	675,400	10,954,500	2,410,000	0.22	95,000,000

[a] psi

[b] psi-hr

[c] hr

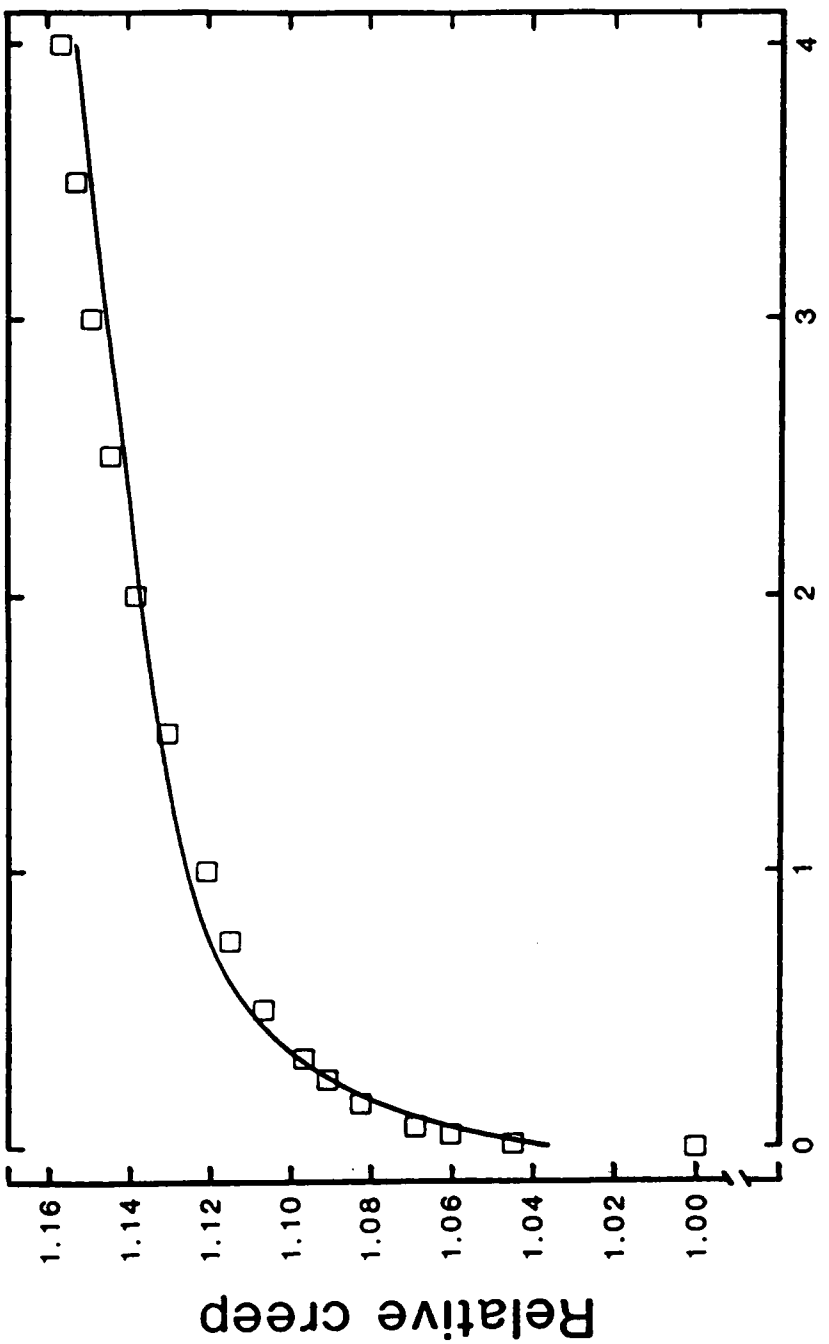

Figure 27. Relative observed (□) and predicted (—) creep deflection of glass fiber reinforced hardboard at an effective reinforcement volume fraction of 0.0073 under 9.09 lbs. load using CREEP II analysis.

elastic deflection exceeded observed values by at most 4.5 percent. Owing to the inverse relationship between deflection and elastic modulus, the predicted instantaneous modulus of elasticity also underestimated observed values by 4.5 percent. A near-perfect relationship existed between predicted and observed creep deflection. At all times greater than zero, the departure is less than 1 percent.

The delayed modulus of elasticity and the delayed coefficient of viscosity increased with effective reinforcement volume fraction at both load levels (Tables 15 and 16). Parameter estimates for E_d and η_d at 9.09 and 15.5 pounds are, on average, 41 and 36, and 175 and 140 percent greater than those of CREEP I, respectively. Estimates for the retardation time were more reasonable than those of CREEP I, and ranged from 0.19 to 0.31 hours. Retardation time decreased with effective reinforcement volume fraction. The trend is best seen at a load level of 9.09 pounds (Table 15).

Estimates of the viscous coefficient of viscosity in CREEP II were identical to those of CREEP I. In both cases, the user-specified limiting value was attained.

Burger model parameter estimates for the hardboard control using CREEP II confirm those reported by Moslemi (1964a). Estimates of 60 and 62 lbs in^{-1} for the spring constant of the elastic element were made in the former and latter studies, respectively. In the present investigation the retardation time was estimated to be 0.26 and 0.22 hours, under 9.09 and 15.5 pounds, respectively. A value of 0.25 hours was reported by Moslemi. The viscous coefficient of viscosity

was estimated by Moslemi to be 6.3×10^6 lbs s in^{-1}. In this study, an average value of 4.0×10^7 lbs s in^{-1} was found.

Conclusions

The short-term flexural creep behavior of glass fiber reinforced hardboard within the elastic range is well described by a 4-element linear viscoelastic model. Total creep deflection increased with increasing load at each effective reinforcement volume fraction; creep rate was unaffected. For a given load, total creep deflection and creep rate decreased with increasing effective reinforcement volume fraction.

Creep deflections predicted from Burger model parameters estimated using nonlinear regression were in excellent agreement with observed values. The delayed modulus of elasticity, the delayed coefficient of viscosity and the viscous coefficient of viscosity of the composite increased with increasing effective reinforcement volume fraction. The retardation time decreased with increasing effective reinforcement volume fraction. The most reliable parameter estimates were generated with the CREEP II regression analysis detailed previously. Burger model parameter estimates for the hardboard control confirmed prior published values.

SUMMARY OF CONCLUSIONS

The effect of reinforcement volume fraction on the static and dynamic flexural behavior of glass fiber reinforced hardboard has been investigated. The following conclusions were based on the results of experiments performed in fulfillment of the objectives of this study:

1. The static modulus of elasticity, modulus of rupture, and dynamic modulus of elasticity of glass fiber reinforced hardboard increased with increasing effective reinforcement volume fraction in a curvilinear fashion. The mean observed MOE, MOR and E' at each effective reinforcement volume fraction examined was statistically unique at $\alpha = 0.01$.

2. The logarithmic decrement of glass fiber reinforced hardboard decreased with increasing effective reinforcement volume fraction in a curvilinear manner. The mean observed logarithmic decrement was statistically unique at $\alpha = 0.05$ at an effective reinforcement volume fraction of 0 and 0.0260.

3. The work-to-failure of glass fiber reinforced hardboard increased in a curvilinear fashion with increasing effective reinforcement volume fraction.

4. When modelled as a sandwich composite, the static flexural MOE of glass fiber reinforced hardboard could be successfully predicted from the static flexural MOE of the hardboard matrix, and the tensile MOE and effective volume fraction of the glass fiber reinforcement.

5. When modelled as a sandwich composite, the MOR of glass fiber reinforced hardboard could be predicted from the static flexural MOE and stress at ultimate load of the hardboard matrix, and the tensile MOE and effective volume fraction of the glass fiber reinforcement. The composite MOR was predicted with limited success on this basis.

6. Excellent linear empirical correlation existed between the static modulus of elasticity and dynamic modulus of elasticity, the modulus of rupture and dynamic modulus of elasticity, and the modulus of rupture and static modulus of elasticity of glass fiber reinforced hardboard.

7. At a given load, both the total flexural creep deflection and the rate of creep deflection of glass fiber reinforced hardboard decreased with increasing effective reinforcement volume fraction.

8. At a given effective reinforcement volume fraction, the flexural creep deflection of glass fiber reinforced hardboard increased with increasing load level. The rate of creep was unaffected.

9. Creep deflection of glass fiber reinforced hardboard could be successfully predicted from empirical estimates of the parameters of a 4-element linear viscoelastic creep model.

10. At all effective reinforcement volume fractions, the apparent failure of glass fiber reinforced hardboard in flexure occurred as a tensile fracture of the extreme fiber of the hardboard core.

11. Significant stress transfer between the hardboard matrix and the glass fiber reinforcement of the composite occurred only when the reinforcement was bonded to the matrix.

RECOMMENDATIONS

In this investigation, the effect of a single variable, viz., reinforcement volume fraction, on the flexural properties of glass fiber reinforced hardboard was examined. Recommendations for future research listed below will aid in the identification of other factors that may affect the properties of glass fiber reinforced hardboard.

1. The effect of hardboard matrix equilibrium moisture content on the flexural properties and creep behavior of glass fiber reinforced hardboard.

2. The effect of moisture content cycling on the flexural properties and creep behavior of glass fiber reinforced hardboard.

3. The effect of other organic or inorganic fiber reinforcements and reinforcement volume fractions on the mechanical properties of glass fiber reinforced hardboard.

4. The effect of reinforcement volume fraction on the tensile and compressive properties of glass fiber reinforced hardboard.

5. The effect of hardboard matrix specific gravity on the flexural properties of glass fiber reinforced hardboard.

6. The effect of cyclic loading on the flexural properties of glass fiber reinforced hardboard.

7. Refinement of the predictive equations relating constituent properties and composite performance.

LITERATURE CITED

Adams, S., M. Maiti and R. Mark. 1967. Three-dimensional elasticity solution of a composite beam. J. Composite Materials 1(2):122-135.

Agarwal, B. and L. Broutman. 1980. Analysis and Performance of Fiber Composites. John Wiley and Sons. New York, NY. 355 pp.

Ali, M. and F. Grimer. 1969. Mechanical properties of glass fiber-reinforced gypsum. J. of Materials Science 4(5):389-395.

Allen, H. 1971. Stiffness and strength of two glass-fiber reinforced cement laminates. J. Composite Materials 5:194-207.

American Plywood Association. 1972. Plywood Overlaid with Fiberglass-Reinforced Plastic. Basic Panel Properties. APA Laboratory Report 119, Part 1. Amer. Plywood Assn. Tacoma, WA.

American Society for Testing and Materials. 1981. Standard Methods of Evaluating the Properties of Wood-Base Fiber and Particle Panel Materials. Annual Book of ASTM Standards. Part 22, Wood; Adhesives. ASTM. Philadelphia, PA. pp. 300-342.

Armstrong, L. and P. Grossman. 1972. The behavior of particle board and hardboard beams during moisture cycling. Wood Science and Technology 6(2):128-137.

Aveston, T., G. Cooper and A. Kelly. 1972. Single and multiple fracture. In The Properties of Fiber Composites, IPC Science and Technology Press Ltd. Guildford, England. 90 pp.

Biblis, E. 1965. Analysis of wood-fiberglass composite beams within and beyond the elastic region. For. Prod. J. 15(2):81-88.

Bodig, J. and B. Jayne. 1982. Mechanics of Wood and Wood Composites. Van Nostrand Reinhold Co. New York, NY. 712 pp.

Boehme, C. and U. Schulz. 1974. The constructive behavior of GFK-wood sandwiches. Holz als Roh-und Werkstoff 32(7):250-256.

Boehme, C. 1976a. The constructive behavior of GFK-wood sandwiches - Comparison of experimental results with various computation methods. Holz als Roh-und Werkstoff 34(5):155-161.

Boehme, C. 1976b. Improvement in creep behavior of wood based materials by glass fiber reinforced plastic coating. Holz als Roh-und Werkstoff 34(12):453-458.

Bulleit, W. 1981. Models for fiberglass reinforced particleboard in flexure. In Proceedings 15th International Particleboard Symposium, T. Maloney (ed.). Washington State Univ. Pullman, WA. pp. 289-308.

Bulleit, W. 1984. Reinforcement of wood materials: A review. Wood and Fiber Science 16(3):391-397.

Cavlin, S. and E. Back. 1968. The effect of sheet density and glass fiber addition on the dimensional stability of fiber building boards. Svensk Papperstidning 71(24):883-889.

Chan, W. 1979. Strength properties and structural use of tempered hardboard. J. of the Inst. of Wood Science 8(4):147-160.

Chow, P. and R. Hanson. 1979. Effects of load level, core density, and shelling ratio on creep behavior of hardboard composites. Wood and Fiber 11(1):57-65.

Department of Biomathematics. 1981. BMDP Statistical Software, W. Dixon (ed.). Univ. of California Press. Los Angeles, CA. 726 pp.

Dietz, A. 1949. Engineering Laminates. J. Wiley & Sons. New York, New York. 797 pp.

Flugge, W. 1975. Viscoelasticity. Springer-Verlag. New York, NY. 194 pp.

Forest Products Laboratory. 1974. Wood Handbook. USDA Forest Service Agriculture Handbook No. 72. Forest Products Laboratory, Madison WI. 415 pp.

Goldfein, S. 1960. General formula for creep and rupture in plastics. Modern Plastics 37:127-132.

Grossman, P. 1976. Requirements for a model that exhibits mechano-sorptive behavior. Wood Science and Technology 10(3):163-168.

Hansen, T. 1964. Estimating stress relaxation from creep data. Materials Research and Standards 4(1):12-14.

Haygreen, J. and D. Sauer. 1969. Prediction of flexural creep and stress rupture in hardboard by use of a time-temperature relationship. Wood Science 1(4):241-249.

Hofstrand, A. 1958. Relationship of specific gravity to moduli of rupture and elasticity in commercial hardboard. For. Prod. J. 8(6):177-180.

Klinga, L. and E. Back. 1964. Drying stresses in hardboard and the introduction of cross-linking stresses by a heat treatment. For. Prod. J. 14(9):425-429.

Koran, Z. 1970. Surface structure of thermomechanical pulp fibers studied by electron microscopy. Wood and Fiber 2(3):247-258.

Kuenzi, E. 1959. Structural sandwich design criteria. FPL Report No. 2161. Madison, WI.

Laufenberg, T., R. Rowlands and G. Krueger. 1984. Economic feasibility of synthetic fiber reinforced laminated veneer lumber (LVL). For. Prod. J. 34(4):15-22.

Lundgreen, S. 1957. Hardboard as construction material - A viscoelastic body. Holz als Roh-und Werkstoff 15(1):19-23.

Lundgreen, S. 1969. Wood-based sheet as a structural material. Part I. Swedish Wallboard Manufacturers Association. Stockholm, Sweden. 252. pp.

Maloney, T. 1977. Modern Particleboard and Dry-Process Fiberboard Manufacturing. Miller Freeman Publications, Inc. San Francisco, CA. 672 pp.

Mark, R. and B. Zuckerman. 1958. Reinforced plastics as protective coatings for wood. For. Prod. J. 8(7):25A-26A.

Mark, R., S. Adams and M. Maiti. 1968. Design of a composite pole laminate. For. Prod. J. 18(4):23-28.

Mataki, Y. 1972. Internal structure of fiberboard and its relation to mechanical properties. In Theory and Design of Wood and Fiber Composite Materials, B. Jayne (ed.). Syracuse Univ. Press. Syracuse, NY. pp 219-253.

McNatt, J. 1970. Design stresses for hardboard - Effect of rate, duration and repeated loading. For. Prod. J. 20(1):53-60.

McNatt, J. 1973. Buckling due to linear expansion of hardboard siding. For. Prod. J. 23(1):37-43.

McNatt, J. 1974. Effects of equilibrium moisture content changes on hardboard properties. For. Prod. J. 24(2):29-35.

McNatt, J. 1980. Hardboard-webbed beams: Research and application. For. Prod. J. 30(10):57-64.

McNatt, J. and M. Superfesky. 1983. Long-term performance of hardboard I-beams. Research Paper FPL 441. Forest Products Laboratory. Madison, WI.

Mitzner, R. 1973. Plywood overlaid with fiberglass-reinforced plastic. Durability and Maintenance. APA Lab Report 119, Part 3. Amer. Plywood Assn. Tacoma, WA.

Moslemi, A. 1964a. Some aspects of viscoelastic behavior of hardboard. For. Prod. J. 14(8):337-342.

Moslemi, A. 1964b. Effect of moisture content, the process of manufacture and load on the creep and relaxation of hardboard. Quarterly Bull. of the Michigan State Univ. Agr. Exp. Sta. 47(2):271-291.

Moslemi, A. 1967. Dynamic viscoelasticity in hardboard. For. Prod. J. 17(1):25-33.

Myers, G. 1977. How fiber acidity affected functional properties of dry-formed hardboards. USDA Forest Service Research Paper FPL 282. Forest Products Laboratory. Madison, WI.

Nelson, N. 1973. Effects of wood and pulp properties on medium-density dry-formed hardboard. For. Prod. J. 23(9):72-80.

Nishikawa, K., A. Matsumoto and O. Niiro. 1974. Studies on the manufacture of fiberboards mixed with mineral fibers - The effect of mixing ratio of glass chopped strand and kinds of phenolic resin. J. of the Hokkaido For. Prod. Res. Inst. 10:11-15.

Nishikawa, K., A. Matsumoto and O. Niiro. 1975. Studies on the manufacture of fiberboards mixed with mineral fibers - The effects of kinds of glass and other mineral fibers. J. of the Hokkaido For. Prod. Res. Inst. 1:8-12.

Pierce, C. and J. Dinwoodie. 1977. Creep in chipboard. J. of Materials Science 12:1955-1960.

Pierce, C., J. Dinwoodie and B. Paxton. 1979. Creep in chipboard. Wood Science and Technology 13(4):262-285.

Pierce, C., J. Dinwoodie and B. Paxton. 1985. Creep in chipboard. Wood Science and Technology. 19(1):83-91.

Poplis, J. and R. Mitzner. 1973. Plywood overlaid with fiberglass-reinforced plastic. Fastener Tests. APA Lab Report 119, Part 2. Amer. Plywood Assn. Tacoma, WA.

Read, B. and G. Dean. 1978. The Determination of Dynamic Properties of Polymers and Composites. Adam Hilger Ltd. Bristol, England. 207 pp.

Rowlands, R., R. Van Deweghe, G. Krueger and T. Laufenberg. 1982. Fiber-reinforced wood composites. Unpublished report from the Department of Mechanics, Univ. of Wisconsin. Madison, WI.

Saucier, J. and J. Holman. 1975. Structural particleboard reinforced with glass fiber - Progress in its development. For. Prod. J. 25(9):67-72.

Sauer, D. and J. Haygreen. 1968. Effects of sorption on the flexural creep behavior of hardboard. For. Prod. J. 18(10):57-63.

Senft, J. and S. Suddarth. 1971. An analysis of creep - inducing stress in Sitka spruce. Wood and Fiber 2(4):321-327.

Short, P. 1981. Scanning electron microscopy of -60/+80 mesh fiberboard furnish. Wood Science 14(1):32-40.

Spalt, H. and R. Sutton. 1968. Buckling of thin surface materials due to restrained hygroexpansion. For. Prod. J. 18(4):53-57.

Spalt, H. 1977. Chemical changes in wood associated with wood fiberboard manufacture. In Wood Technology: Chemical Aspects, I. S. Goldstein (ed.). ACS Symposium Series No. 43. Amer. Chem. Soc. Washington, D.C. pp. 193-219.

Spaun, F. 1981. Reinforcement of wood with fiberglass. For. Prod. J. 31(4):26-35.

Steinmetz, P. and D. Fahey. 1968. Resin treatments for improving dimensional stability of structural fiberboards. For. Prod. J. 18(9):71-75.

Steinmetz, P. and C. Polley. 1974. Influence of fiber alignment on stiffness and dimensional stability of high-density dry-formed hardboard. For. Prod. J. 24(5):45-50.

Steinmetz, P. 1977. Resin systems and glass reinforcements to improve dry-formed hardboards. USDA Forest Service Research Paper FPL 284. Forest Products Laboratory. Madison, WI.

Stillinger, J. and W. Coggan. 1956. Relationship of moisture content and flexural properties in 25 commercial hardboards. For. Prod. J. 6(5):179-186.

Suchsland, O. 1964. Swelling stresses and swelling deformations in hardboard. Quarterly Bull. of the Michigan State Univ. Agr. Exp. Sta. 47(4):591-605.

Superfesky, M. and T. Ramaker. 1978. Hardboard-webbed I-beams: Effects of long-term loading and loading environment. Research Paper FPL 306. Forest Products Lab. Madison, WI.

Sutula, P. and A. Moslemi. 1973. Effects of three cyclic constant levels of moisture content on creep deflection in hardboard. For. Prod. J. 23(3):50-55.

Szabo, T. and G. Ifju. 1970. Influence of stress on creep and moisture distribution in wooden beams under sorption conditions. Wood Science 2(3):159-167.

Tang, R. and S. Adams. 1973. Applications of reinforced plastics for laminated transmission poles. For. Prod. J. 23(10):42-46.

Theakston, F. 1965. A feasibility study for strengthening timber beams with fiberglass. Canadian Agricultural Engineering, January 1965.

Timoshenko, S. and J. Gere. 1972. Mechanics of Materials. D. Van Nostrand Co. New York, NY. 552 pp.

Ulrich, A. 1981. U.S. timber production, trade, consumption, and price statistics 1950-80. USDA Forest Service Miscellaneous Publication No. 1408. Forest Resources Economic Research Staff. Washington, D.C.

Wangaard, F. 1964. Elastic deflection of wood-fiberglass composite beams. For. Prod. J. 14(6):256-260.

Werren, F. and J. McNatt. 1975. Basic properties and their variability in twenty commercial hardboards. Unpublished report. Forest Products Laboartory. Madison, WI.

Woodson, G. 1977. Density profile and fiber alignment in fiberboard from three southern hardwoods. For. Prod. J. 27(8):29-34.

Appendix 1. Glass fiber fabric tensile stress-strain curve.

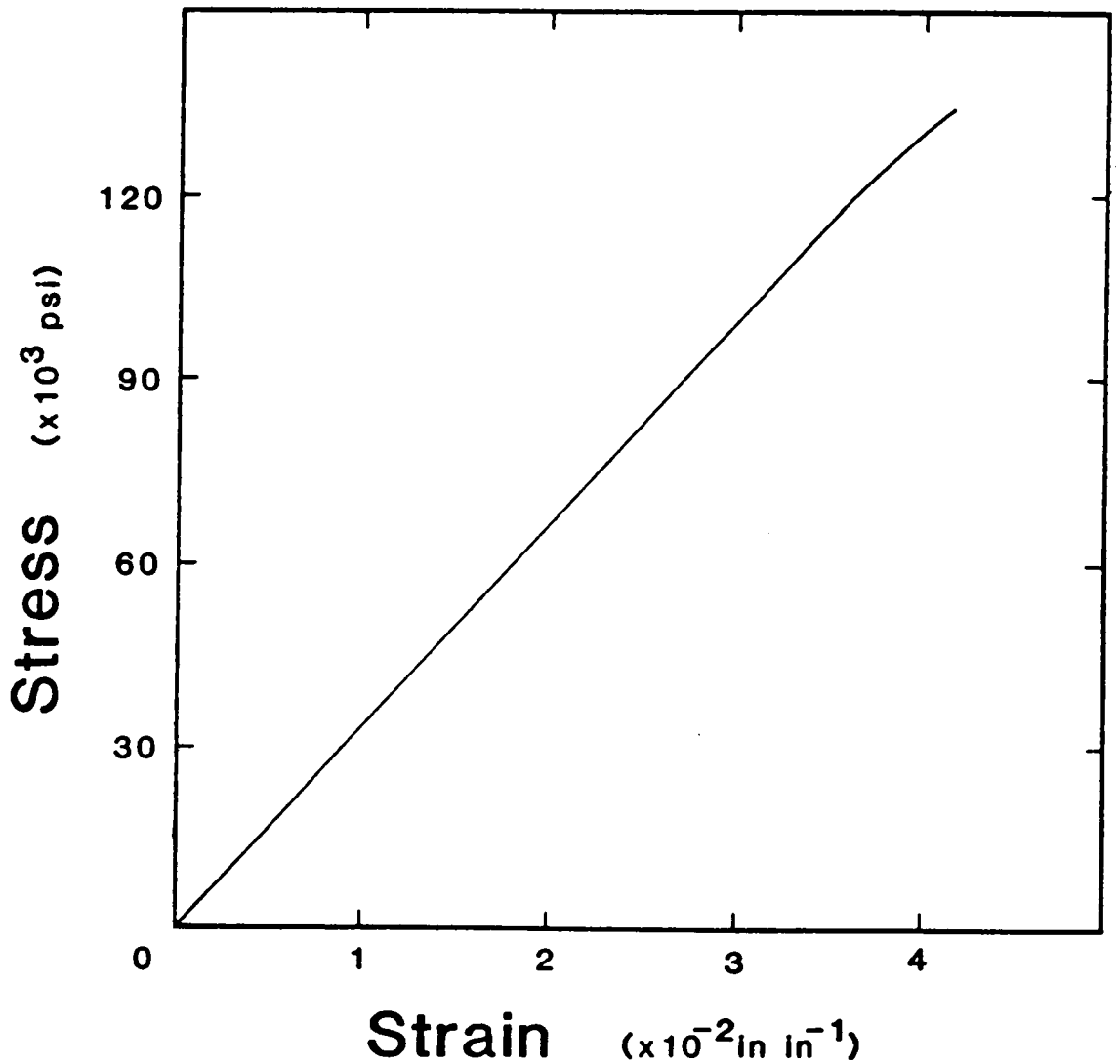

Appendix 2. Phenolic resin product information sheet.

Georgia-Pacific

Resin Division

P.O. Box 105605, Atlanta, Georgia 30348 (404) 521-4000

Product Information

PARAC® Powdered Phenolic Resin GP-5520

PARAC® GP-5520 powdered phenolic resin is a general purpose two-step novolac resin with a moderate cure rate. It has been specifically formulated for applications where a moderately high melt viscosity and moderate flow during cure are required.

Uses and Application

PARAC GP-5520 powdered resin is used as delivered. It is usually added to the customer mix in powder form from a storage hopper or powder bin.

Curing takes place on heating in the presence of the hexamethylenetetramine catalyst that is already part of the GP-5520 resin formulation.

Typical Properties

Type	phenol-formaldehyde novolac
Form supplied	powder
Color	off-white to tan
Hexamethylenetetra-mine, %	7.5-9.5
Inclined plate flow at 125°C, mm	35-60
Hot plate cure time at 150°C, sec 302 °F	65-85
Screen analysis, % retained on 200 mesh (maximum)	5
Storage life at 70-75°F	6 months maximum

Appendix 3. Observed static modulus of elasticity, modulus of rupture, dynamic modulus of elasticity and logarithmic decrement of glass fiber reinforced hardboard by effective reinforcement volume fraction.

Eff V_f=0

No.	MOE	MOR	E'	Δ
01	474818	3497	575222	0.0714
02	483162	3637	589957	0.0694
03	457142	3540	555233	0.0692
04	425096	3107	541523	0.0720
05	451376	3303	561191	0.0705
06	426067	3116	544975	0.0727
07	428223	3410	543969	0.0698
08	450899	3496	557808	0.0703
09	408323	2888	519061	0.0672
10	445044	3800		
11	452492	3597		
12	405007	2890		
13	417905	3314		
14	449152	3581		
15	417905	3216		
$\bar{X}$	439507	3359	554327	0.0703
S	23358	273	20518	0.00165

Eff V_f=0.0073

16	520117	4678	651497	0.0625
17	545326	5264	692405	0.0665
18	539442	4960	679788	0.0670
19	508429	4736	651592	0.0660
20	557151	5217	709366	0.0691
21	542212	5076	677846	0.0650
22	521918	4720	663178	0.0681
23	529217	4801	669692	0.0649
24	505179	4445	645750	0.0678
25	488485	4444		
26	529955	4857		
27	511408	4441		
28	519338	4658		
29	559743	5134		
30	495381	4565		
$\bar{X}$	524887	4800	671235	0.0663
S	21262	279	20950	0.00200

Appendix 3. Observed static modulus of elasticity, modulus of rupture, dynamic modulus of elasticity and logarithmic decrement of glass fiber reinforced hardboard by effective reinforcement volume fraction.

Eff V_f=0.0158

No.	MOE	MOR	E'	Δ
31	611488	5839	735977	0.0620
32	626416	6444	768695	0.0616
33	598305	6264	736941	0.0649
34	610065	6140	749413	0.0629
35	634277	6348	782537	0.0698
36	562248	5945	729787	0.0704
37	565195	6023	717373	0.0641
38	580310	6222	742872	0.0645
39	547668	5288	705570	0.0582
40	616608	5964		
41	602497	5925		
42	555623	5457		
43	609115	5830		
44	639044	6252		
45	600245	5671		
$\bar{X}$	597274	5974	741018	0.0643
S	28809	326	23842	0.00387

Eff V_f=0.0260

46	671435	6193	801035	0.0641
47	711841	6767	838063	0.0580
48	649569	6477	811721	0.0665
49	661424	6449	796361	0.0585
50	703276	7134	852548	0.0597
51	659666	6511	809134	0.0603
52	624032	6221	777591	0.0631
53	642685	6384	803254	0.0598
54	633363	6548	788100	0.0609
55	679467	6868		
56	674886	7061		
57	623076	6669		
58	664004	7334		
59	720221	7605		
60	653106	6854		
$\bar{X}$	664805	6738	808645	0.0612
S	29777	408	23524	0.00280

Appendix 3. Data for static modulus of elasticity, modulus of rupture, dynamic modulus of elasticity and logarithmic decrement of glass fiber reinforced hardboard by effective reinforcement volume fraction.

	No.	b	d	y	P	P	f_r	f_1	f_2	w
Eff V_f=0	01	2.038	0.248	0.075	20.5	48.7	316.8	313.2	320.4	64.425
	02	2.028	0.247	0.064	17.5	50.0	316.6	313.3	320.3	65.041
	03	2.038	0.248	0.076	20.0	49.3	313.2	309.9	316.8	63.624
	04	2.030	0.248	0.080	19.5	43.1	309.4	306.3	313.4	63.339
	05	2.032	0.247	0.064	21.5	45.5	311.9	308.6	315.6	63.874
	06	2.029	0.248	0.086	21.0	43.2	310.6	307.4	314.6	63.218
	07	2.037	0.246	0.084	20.2	46.7	305.8	302.5	309.3	63.786
	08	2.036	0.246	0.081	20.5	47.8	308.0	305.0	311.9	64.446
	09	2.037	0.248	0.083	19.5	40.2	303.6	300.5	307.0	63.269
	10	1.973	0.245	0.069	16.5	50.0				
	11	1.967	0.244	0.071	17.0	46.8				
	12	1.997	0.246	0.074	16.5	38.8				
	13	1.966	0.245	0.073	16.5	43.9				
	14	1.975	0.243	0.070	16.5	46.4				
	15	1.986	0.245	0.073	16.5	42.6				
Eff V_f=0.0073	16	2.059	0.247	0.087	26.0	65.3	331.2	328.4	335.0	66.636
	17	2.051	0.245	0.087	26.5	72.0	335.1	331.7	338.8	67.252
	18	2.069	0.246	0.078	24.0	69.0	337.6	334.1	341.3	66.430
	19	2.059	0.247	0.069	26.0	66.1	333.4	329.9	336.9	65.769
	20	2.044	0.246	0.080	27.0	71.7	340.2	337.2	344.7	67.440
	21	2.072	0.247	0.074	25.2	71.3	337.8	334.6	341.6	67.069
	22	2.036	0.249	0.079	24.0	66.2	336.9	333.3	340.6	66.410
	23	2.035	0.249	0.076	23.4	67.3	336.6	333.3	342.3	66.358
	24	2.044	0.250	0.082	24.5	63.1	338.2	334.6	341.9	65.200
	25	1.985	0.247	0.085	23.0	59.8				
	26	1.969	0.246	0.073	21.0	64.3				
	27	1.966	0.246	0.075	21.0	59.3				
	28	1.970	0.246	0.078	22.0	61.7				
	29	1.977	0.245	0.073	22.0	67.7				
	30	1.997	0.246	0.066	18.0	61.3				
Eff V_f=0.0158	31	2.059	0.247	0.074	26.0	81.5	344.5	340.4	353.3	67.600
	32	2.080	0.245	0.093	33.0	89.4	341.4	338.5	355.4	68.856
	33	2.063	0.247	0.090	31.0	87.6	348.4	344.9	352.1	68.249
	34	2.042	0.246	0.099	34.0	84.3	348.8	345.8	352.8	67.711
	35	2.085	0.246	0.096	35.0	89.0	354.7	351.5	359.4	69.611
	36	2.062	0.247	0.102	33.0	83.1	347.9	344.2	352.0	67.748
	37	2.065	0.248	0.091	30.0	85.0	348.0	344.5	352.6	67.407
	38	2.065	0.247	0.093	31.1	87.1	350.3	347.1	354.3	68.120
	39	2.056	0.249	0.073	23.5	74.9	345.3	342.1	348.5	67.920
	40	1.982	0.244	0.073	24.0	78.2				
	41	1.968	0.243	0.073	23.0	76.5				
	42	1.989	0.244	0.074	22.0	71.8				
	43	1.983	0.245	0.076	25.0	77.1				
	44	1.990	0.244	0.076	26.0	82.3				
	45	1.990	0.247	0.075	25.0	76.5				
Eff V_f=0.0260	46	2.056	0.249	0.081	32.0	87.8	362.2	359.0	366.4	70.150
	47	2.083	0.249	0.092	39.0	97.1	368.2	365.2	372.0	71.863
	48	2.092	0.248	0.099	38.0	92.6	362.9	359.9	367.6	71.118
	49	2.054	0.247	0.091	34.5	89.8	359.7	356.6	363.3	68.889
	50	2.070	0.247	0.096	39.0	100.1	366.2	363.1	372.1	70.952
	51	2.081	0.248	0.098	38.0	92.6	364.2	361.0	366.0	70.016
	52	2.063	0.248	0.099	36.0	87.7	356.4	353.1	362.3	68.881
	53	2.076	0.249	0.097	37.0	91.3	362.0	358.8	365.7	71.038
	54	2.064	0.249	0.099	37.0	93.1	360.9	357.7	364.7	69.718
	55	1.991	0.245	0.076	28.0	91.2				
	56	1.989	0.244	0.072	26.0	92.9				
	57	1.996	0.246	0.070	24.0	89.5				
	58	1.975	0.245	0.070	25.0	96.6				
	59	1.982	0.243	0.058	22.0	98.9				
	60	1.995	0.245	0.062	22.0	91.2				

Appendix 3. Data for static modulus of elasticity and modulus of rupture of glass fiber reinforced hardboard with unbonded glass fiber. Eff V_f=0.0073.

No.	b	d	y	P	P	MOE	MOR
1	1.997	0.252	0.073	20.0	50.4	462936	3577
2	1.999	0.252	0.074	21.0	53.0	479035	3758
3	1.995	0.254	0.075	19.5	44.8	429460	3133
4	1.999	0.247	0.088	23.7	51.1	482787	3771
5	1.998	0.248	0.087	22.6	49.9	460291	3655
6	1.997	0.248	0.085	21.0	45.5	437987	3334
7	1.998	0.247	0.087	22.0	48.7	453535	3596
8	1.999	0.246	0.085	22.6	53.5	482464	3980
9	1.994	0.248	0.090	22.5	48.4	443868	3552
					$\bar{X}$	459151	3595
					S	19710	248

Appendix 4. Static Modulus of Elasticity ANOVA.

i. Hypotheses H_o: $\mu_1 = \mu_2 = \mu_3 = \mu_4 = \mu$

H_1: $\mu_i \neq \mu$

ii. ANOVA Table

Source	df	Sum of Squares	Mean Square	F_{obs}
Between	3	421185347064	140395115355	207
Within	56	38000004955	67857 15 17	
Total	59	459185352019		

iii. Conclusion

Reject H_o as $F_{obs} = 207 > 4.13 = F_{(3,60)0.99}$; inequality among means at $\alpha = 0.01$.

Appendix 4. Static Modulus of Elasticity DMRT.

Rank Ordering of Means.

1	2	3	4
439507	524887	597274	664805

i. Hypotheses H_o: $\mu_i = \mu_j$

H_1: $\mu_i \neq \mu_j$

ii. Test Statistic

$$W_r = q'_\alpha(r,v) \frac{MSW}{n}$$

at $\alpha = 0.01$:

$W_4 = 27105$

$W_3 = 26366$

$W_2 = 25290$

r = no. steps between means

$v = df_{within}$

$q'_\alpha(r,v)$ = tabulated percentage point

MSW = mean square within

n = no. of observations

iii. Results

4 step

$|\bar{y}_4 - \bar{y}_1| = 255298 > W_4$; reject H_o

3 step

$|\bar{y}_4 - \bar{y}_2| = 139918$

$|\bar{y}_3 - \bar{y}_1| = 157767$

$\Big\} > W_3$; reject H_o

2 step

$|\bar{y}_4 - \bar{y}_3| = 67531$

$|\bar{y}_3 - \bar{y}_2| = 72387$

$|\bar{y}_2 - \bar{y}_1| = 85380$

$\Big\} > W_2$; reject H_o

iv. Conclusions

$\bar{y}_1 \neq \bar{y}_2 \neq \bar{y}_3 \neq \bar{y}_4$ at $\alpha = 0.01$

Appendix 5. Modulus of Rupture ANOVA.

i. Hypotheses H_o: $\mu_1 = \mu_2 = \mu_3 = \mu_4 = \mu$

H_1: $\mu_i \neq \mu$

ii. ANOVA Table

Source	df	Sum of Squares	Mean Square	F_{obs}
Between	3	97707113	32569038	307
Within	56	5946520	106188	
Total	59	103653633		

iii. Conclusion

Reject H_o as $F_{obs} = 307 > 4.13 = F_{(3,60)\ 0.99}$; inequality among means at $\alpha = 0.01$.

Appendix 5. Modulus of Rupture DMRT.

Rank Ordering of Means.

1	2	3	4
3359	4800	5974	6738

i. Hypotheses H_o: $\mu_i = \mu_j$

H_1: $\mu_i \neq \mu_j$

ii. Test Statistic (see Appendix 4)

at $\alpha = 0.01$:

$W_4 = 339$

$W_3 = 330$

$W_2 = 316$

iii. Results

4 step

$|\bar{y}_4 - \bar{y}_1| = 3379 > W_4$; reject H_o

3 step

$$\left.\begin{aligned} |\bar{y}_4 - \bar{y}_2| &= 1938 \\ |\bar{y}_3 - \bar{y}_1| &= 2615 \end{aligned}\right\} > W_3; \text{ reject } H_o$$

2 step

$$\left.\begin{aligned} |\bar{y}_4 - \bar{y}_3| &= 764 \\ |\bar{y}_3 - \bar{y}_2| &= 1174 \\ |\bar{y}_2 - \bar{y}_1| &= 1441 \end{aligned}\right\} > W_2; \text{ reject } H_o$$

iv. Conclusions

$\bar{y}_1 \neq \bar{y}_2 \neq \bar{y}_3 \neq \bar{y}_4$ at $\alpha = 0.01$

Appendix 6. t-Test for Static Bending MOE and MOR of Control Versus Unbonded Glass Fiber at Eff $V_f = 0.0073$.[a]

i. Hypotheses H_o: $\mu_{control} = \mu_{unbonded}$

H_1: $\mu_{control} < \mu_{unbonded}$

ii. Test Statistic

$df = n_c + n_u - 2$

$$s_p^2 = \frac{(n_c-1)s_c^2 + (n_u-1)s_u^2}{n_c + n_u - 2}$$

$$t_{obs} = \frac{|\bar{x}_c - \bar{x}_u|}{s_p\sqrt{\frac{1}{n_c} + \frac{1}{n_u}}}$$

n = no. observations

s = standard deviation

$\bar{x}$ = mean

s_p = pooled standard deviation

$t_{(df)_{1-\alpha}}$ = tabulated percentage point

at $\alpha = 0.05$, $t_{(22)0.95} = 1.717$

iii. Results

as MOE $t_{obs} = 2.111 > 1.717$, reject H_o at $\alpha = 0.05$

as MOR $t_{obs} = 2.098 > 1.717$, reject H_o at $\alpha = 0.05$

iv. Conclusions

$MOE_{unbonded} > MOE_{control}$ at $\alpha = 0.05$

$MOR_{unbonded} > MOR_{control}$ at $\alpha = 0.05$

---

[a] using data from Table 8

Appendix 7. Dynamic Modulus of Elasticity ANOVA.

i. Hypotheses H_o: $\mu_1 = \mu_2 = \mu_3 = \mu_4 = \mu$

H_1: $\mu_i \neq \mu$

ii. ANOVA Table

Source	df	Sum of Squares	Mean Square	F_{obs}
Between	3	3 184239785 15	106 14 1326 172	214
Within	32	158538663 00	495433322	
Total	35	334 27784481 5		

iii. Conclusion

Reject H_o as $F_{obs} = 214 > 4.51 = F_{(3,30)0.99}$; inequality among means at $\alpha = 0.01$.

Appendix 7. Dynamic Modulus of Elasticity DMRT.

Rank Ordering of Means.

1	2	3	4
554330	671236	741018	808645

i. Hypotheses H_o: $\mu_i = \mu_j$

H_1: $\mu_i \neq \mu_j$

ii. Test Statistic (see Appendix 4)

at $\alpha = 0.01$:

$W_4 = 30865$

$W_3 = 30123$

$W_2 = 28882$

iii. Results

4 step

$|\bar{y}_4 - \bar{y}_1| = 254315 > W_4$; reject H_o

3 step

$|\bar{y}_4 - \bar{y}_2| = 137409$

$|\bar{y}_3 - \bar{y}_1| = 186688$

$\Big\} > W_3$; reject H_o

2 step

$|\bar{y}_4 - \bar{y}_3| = 67627$

$|\bar{y}_3 - \bar{y}_2| = 69782$

$|\bar{y}_2 - \bar{y}_1| = 116906$

$\Big\} > W_2$; reject H_o

iv. Conclusions

$\bar{y}_1 \neq \bar{y}_2 \neq \bar{y}_3 \neq \bar{y}_4$ at $\alpha = 0.01$

Appendix 8. Logarithmic Decrement ANOVA.

i. Hypotheses H_o: $\mu_1 = \mu_2 = \mu_3 = \mu_4 = \mu$

H_1: $\mu_i \neq \mu$

ii. ANOVA Table

Source	df	Sum of Squares	Mean Square	F_{obs}
Between	3	0.00039159	0.000130530	17.7
Within	32	0.00023597	0.000007374	
Total	35	0.00062756		

iii. Conclusion

Reject H_o as $F_{obs} = 17.7 > 4.51 = F_{(3,30)0.99}$; inequality among means at $\alpha = 0.01$.

Appendix 8. Logarithmic Decrement DMRT.

Rank Ordering of Means.

1	2	3	4
0.0703	0.0663	0.0643	0.0612

i. Hypotheses H_o: $\mu_i = \mu_j$

H_1: $\mu_i \neq \mu_j$

ii. Test Statistic (see Appendix 4)

at $\alpha = 0.01$:	at $\alpha = 0.05$:
$W_4 = 0.003765$	0.002824
$W_3 = 0.003675$	0.002752
$W_2 = 0.003521$	0.002616

iii. Results

4 step

$|\bar{y}_4 - \bar{y}_1| = 0.0091 > W_4$; reject H_o at $\alpha = 0.01$

3 step

$\left.\begin{array}{l} |\bar{y}_4 - \bar{y}_2| = 0.0051 \\ |\bar{y}_3 - \bar{y}_1| = 0.0060 \end{array}\right\} > W_3$; reject H_o at $\alpha = 0.01$

2 step

$|\bar{y}_4 - \bar{y}_3| = 0.0031 > W_2$; reject H_o at $\alpha = 0.05$

$|\bar{y}_3 - \bar{y}_2| = 0.0020 < W_2$; cannot reject H_o

$|\bar{y}_2 - \bar{y}_1| = 0.0040 > W_2$; reject H_o at $\alpha = 0.01$

iv. Conclusions

$\bar{y}_2 = \bar{y}_3$

$\bar{y}_1 \neq \bar{y}_2$ at $\alpha = 0.01$

$\bar{y}_3 \neq \bar{y}_4$ at $\alpha = 0.05$

Appendix 9. Observed and predicted creep deflection of glass fiber reinforced hardboard. CREEP I; Eff V_f=0; 9.09 lbs; hr; in.

	1		2		3	
Time	Obs	Prd	Obs	Prd	Obs	Prd
0.00000	.0728	.07280	.0734	.07340	.0712	.07120
.01666	.0762	.07383	.0775	.07477	.0746	.07219
.03333	.0770	.07475	.0748	.07595	.0755	.07308
.05000	.0775	.07557	.0748	.07695	.0760	.07389
.06666	.0779	.07631	.0782	.07783	.0764	.07462
.08333	.0782	.07697	.0785	.07858	.0767	.07528
.10000	.0785	.07757	.0798	.07923	.0770	.07588
.11666	.0787	.07810	.0800	.07978	.0772	.07642
.13333	.0789	.07858	.0802	.08026	.0774	.07691
.15000	.0791	.07900	.0804	.08067	.0775	.07735
.16666	.0793	.07939	.0805	.08102	.0776	.07775
.18333	.0794	.07973	.0807	.08133	.0780	.07812
.20000	.0795	.08004	.0808	.08159	.0781	.07844
.21666	.0798	.08032	.0810	.08182	.0783	.07874
.23333	.0799	.08057	.0811	.08202	.0784	.07901
.25000	.0801	.08079	.0812	.08219	.0785	.07925
.26666	.0802	.08100	.0813	.08233	.0786	.07948
.28333	.0803	.08118	.0814	.08245	.0787	.07968
.30000	.0804	.08134	.0815	.08258	.0788	.07986
.31666	.0805	.08149	.0816	.08267	.0790	.08002
.33333	.0806	.08163	.0817	.08276	.0791	.08017
.41666	.0810	.08210	.0820	.08305	.0795	.08074
.50000	.0814	.08243	.0824	.08323	.0798	.08110
.58333	.0817	.08266	.0827	.08334	.0802	.08134
.66666	.0820	.08282	.0830	.08343	.0804	.08149
.75000	.0823	.08295	.0832	.08351	.0807	.08160
.83333	.0825	.08305	.0833	.08357	.0809	.08169
.91666	.0827	.08315	.0835	.08364	.0811	.08175
1.00000	.0829	.08323	.0836	.08370	.0812	.08181
1.08333	.0831	.08332	.0837	.08377	.0814	.08186
1.16666	.0833	.08340	.0838	.08383	.0815	.08191
1.25000	.0835	.08348	.0839	.08389	.0817	.08195
1.33333	.0836	.08356	.0840	.08396	.0818	.08200
1.41666	.0838	.08363	.0841	.08402	.0819	.08204
1.50000	.0839	.08371	.0842	.08408	.0820	.08209
1.58333	.0840	.08379	.0843	.08414	.0822	.08213
1.66666	.0842	.08387	.0844	.08421	.0823	.08217
1.75000	.0842	.08395	.0845	.08427	.0824	.08221
1.83333	.0844	.08403	.0847	.08433	.0825	.08226
1.91666	.0845	.08410	.0848	.08440	.0826	.08230
2.00000	.0847	.08418	.0849	.08446	.0825	.08234
2.16666	.0849	.08434	.0850	.08459	.0828	.08242
2.33333	.0850	.08449	.0851	.08471	.0829	.08251
2.50000	.0851	.08465	.0853	.08484	.0830	.08259
2.66666	.0853	.08481	.0854	.08496	.0832	.08268
2.83333	.0855	.08496	.0855	.08509	.0833	.08276
3.00000	.0856	.08512	.0857	.08521	.0834	.08285
3.16666	.0857	.08528	.0858	.08534	.0835	.08293
3.33333	.0859	.08543	.0860	.08547	.0836	.08302
3.50000	.0860	.08559	.0861	.08559	.0837	.08310
3.66666	.0861	.08574	.0862	.08572	.0838	.08319
3.83333	.0863	.08590	.0863	.08584	.0839	.08327
4.00000	.0863	.08606	.0864	.08597	.0840	.08335
4.16666	.0864	.08621	.0865	.08609	.0841	.08344
4.33333	.0866	.08637	.0866	.08622	.0842	.08352
4.50000	.0868	.08653	.0867	.08635	.0842	.08361
4.66666	.0870	.08668	.0868	.08647	.0843	.08369
4.83333	.0871	.08684	.0870	.08660	.0844	.08378
5.00000			.0871	.08672	.0844	.08386

Appendix 9. Observed and predicted creep deflection of glass fiber reinforced hardboard. CREEP I; Eff V_f=0.0073; 9.09 lbs; hr; in.

	4		5		6	
Time	Obs	Prd	Obs	Prd	Obs	Prd
0.00000	.0591	.05610	.0640	.06400	.0559	.05590
.01666	.0594	.05697	.0646	.06458	.0565	.05697
.03333	.0598	.05758	.0672	.06531	.0590	.05794
.05000	.0597	.05821	.0676	.06598	.0594	.05855
.06666	.0600	.05979	.0678	.06640	.0595	.05913
.08333	.0603	.05929	.0681	.06638	.0598	.05960
.10000	.0605	.05976	.0683	.06732	.0600	.05998
.11666	.0607	.06018	.0685	.06772	.0601	.06030
.13333	.0609	.06055	.0686	.06808	.0603	.06055
.15000	.0610	.06089	.0687	.06841	.0604	.06076
.16666	.0612	.06120	.0689	.06872	.0605	.06093
.18333	.0613	.06148	.0690	.06900	.0606	.06107
.20000	.0614	.06173	.0691	.05925	.0607	.06119
.21666	.0615	.06195	.0692	.05948	.0607	.06129
.23333	.0617	.06216	.0693	.05970	.0608	.06136
.25000	.0618	.06234	.0694	.05989	.0609	.06143
.26666	.0619	.06251	.0695	.07007	.0609	.06148
.28333	.0620	.06265	.0696	.07024	.0610	.06152
.30000	.0621	.06280	.0697	.07039	.0610	.06156
.31666	.0622	.06293	.0697	.07052	.0611	.06159
.33333	.0623	.06304	.0698	.07065	.0611	.06162
.41666	.0627	.06347	.0701	.07114	.0613	.06177
.50000	.0630	.06374	.0704	.07146	.0616	.06181
.58333	.0632	.06391	.0706	.07168	.0617	.06184
.66666	.0634	.06404	.0708	.07183	.0618	.06188
.75000	.0636	.06413	.0710	.07193	.0620	.06191
.83333	.0638	.06420	.0712	.07201	.0621	.06194
.91666	.0639	.06426	.0713	.07207	.0621	.06198
1.00000	.0641	.06431	.0715	.07212	.0621	.06201
1.08333	.0642	.06436	.0715	.07217	.0622	.06205
1.16666	.0643	.06441	.0718	.07221	.0622	.06208
1.25000	.0644	.06446	.0719	.07225	.0623	.06211
1.33333	.0645	.06450	.0720	.07228	.0623	.06215
1.41666	.0645	.06454	.0721	.07232	.0623	.06218
1.50000	.0646	.06459	.0722	.07235	.0624	.06221
1.58333	.0647	.06463	.0723	.07238	.0624	.06225
1.66666	.0648	.06468	.0724	.07242	.0624	.06228
1.75000	.0649	.06472	.0725	.07245	.0624	.06231
1.83333	.0649	.06476	.0726	.07248	.0625	.06235
1.91666	.0650	.06481	.0726	.07252	.0625	.06238
2.00000	.0651	.06485	.0728	.07255	.0627	.06243
2.16666	.0652	.06494	.0729	.07261	.0627	.06251
2.33333	.0653	.06503	.0731	.07268	.0628	.06258
2.50000	.0655	.06512	.0732	.07274	.0629	.06265
2.66666	.0656	.06520	.0733	.07281	.0629	.06271
2.83333	.0657	.06529	.0734	.07288	.0630	.06278
3.00000	.0658	.06538	.0735	.07294	.0631	.06285
3.16666	.0659	.06547	.0736	.07301	.0631	.06291
3.33333	.0659	.06555	.0737	.07307	.0632	.06299
3.50000	.0660	.06564	.0738	.07314	.0632	.06305
3.66666	.0661	.06573	.0738	.07320	.0633	.06312
3.83333	.0662	.06582	.0739	.07327	.0633	.06318
4.00000	.0663	.06591	.0740	.07333	.0634	.06325
4.16666	.0663	.06599	.0740	.07340	.0635	.06332
4.33333	.0664	.06608	.0741	.07346	.0635	.06338
4.50000	.0665	.06617	.0741	.07353	.0637	.06345
4.66666	.0666	.06626	.0742	.07359	.0637	.06352
4.83333			.0743	.07366	.0634	.06359
5.00000						

Appendix 9. Observed and predicted creep deflection of glass fiber reinforced hardboard. CREEP I; Eff V_f=0.0158; 9.09 lbs; hr; in.

	7		8		9	
Time	Obs	Prd	Obs	Prd	Obs	Prd
0.00000	.0591	.05910	.0527	.05270	.0541	.05410
.01666	.0615	.05979	.0544	.05327	.0559	.05483
.03333	.0621	.06042	.0548	.05376	.0564	.05544
.05000	.0624	.06099	.0550	.05420	.0566	.05595
.06666	.0627	.06151	.0552	.05457	.0568	.05637
.09333	.0630	.06198	.0554	.05490	.0569	.05672
.10000	.0632	.06241	.0555	.05519	.0571	.05702
.11666	.0634	.06281	.0556	.05544	.0572	.05726
.13333	.0635	.06316	.0557	.05566	.0573	.05746
.15000	.0637	.06349	.0558	.05585	.0574	.05763
.16666	.0638	.06378	.0559	.05602	.0575	.05778
.18333	.0640	.06405	.0559	.05616	.0576	.05789
.20000	.0641	.06430	.0560	.05629	.0577	.05799
.21666	.0642	.06452	.0560	.05640	.0577	.05808
.23333	.0643	.06473	.0561	.05650	.0578	.05815
.25000	.0644	.06491	.0562	.05659	.0578	.05820
.26666	.0645	.06508	.0562	.05666	.0579	.05825
.28333	.0646	.06524	.0563	.05673	.0579	.05829
.30000	.0647	.06538	.0563	.05679	.0580	.05833
.31666	.0648	.06551	.0564	.05685	.0580	.05836
.33333	.0649	.06563	.0564	.05689	.0580	.05839
.41666	.0655	.06636	.0566	.05706	.0582	.05846
.50000	.0657	.06655	.0569	.05717	.0583	.05850
.58333	.0659	.06669	.0570	.05724	.0584	.05852
.66666	.0661	.06678	.0571	.05730	.0585	.05854
.75000	.0663	.06685	.0572	.05734	.0585	.05856
.83333	.0664	.06691	.0573	.05739	.0585	.05857
.91666	.0666	.06695	.0574	.05743	.0585	.05858
1.00000	.0667	.06699	.0574	.05747	.0585	.05860
1.08333	.0668	.06703	.0575	.05751	.0585	.05861
1.16666	.0669	.06706	.0575	.05755	.0586	.05862
1.25000	.0670	.06710	.0576	.05759	.0587	.05864
1.33333	.0671	.06713	.0577	.05763	.0588	.05865
1.41666	.0672	.06716	.0578	.05767	.0589	.05866
1.50000	.0672	.06719	.0578	.05771	.0589	.05867
1.58333	.0673	.06722	.0579	.05775	.0590	.05869
1.66666	.0673	.06725	.0579	.05779	.0588	.05870
1.75000	.0674	.06728	.0580	.05783	.0588	.05871
1.83333	.0675	.06731	.0581	.05787	.0589	.05873
1.91666	.0675	.06734	.0581	.05791	.0588	.05874
2.00000	.0676	.06740	.0582	.05795	.0589	.05875
2.16666	.0677	.06746	.0582	.05804	.0589	.05878
2.33333	.0679	.06752	.0583	.05812	.0589	.05880
2.50000	.0679	.06758	.0584	.05820	.0590	.05883
2.66666	.0680	.06765	.0585	.05828	.0590	.05886
2.83333	.0681	.06771	.0587	.05836	.0590	.05888
3.00000	.0682	.06777	.0587	.05844	.0591	.05891
3.16666	.0683	.06783	.0587	.05852	.0591	.05893
3.33333	.0684	.06789	.0587	.05860	.0591	.05896
3.50000	.0684	.06795	.0588	.05868	.0592	.05899
3.66666	.0685	.06801	.0589	.05876	.0592	.05901
3.83333	.0686	.06807	.0589	.05884	.0592	.05904
4.00000	.0686	.06813	.0591	.05892	.0592	.05907
4.16666	.0687	.06819	.0592	.05900	.0593	.05909
4.33333	.0687	.06825	.0592	.05908	.0593	.05912
4.50000			.0593	.05916	.0593	.05914
4.66666					.0593	.05917
4.83333					.0594	.05920
5.00000					.0594	.05922

Appendix 9. Observed and predicted creep deflection of glass fiber reinforced hardboard. CREEP I; Eff V_f=0.0260; 9.09 lbs; hr; in.

	10		11		12	
Time	Obs	Prd	Obs	Prd	Obs	Prd
0.00000	.0506	.05060	.0519	.05189	.0507	.05070
.01666	.0521	.05116	.0535	.05285	.0523	.05123
.03333	.0525	.05165	.0538	.05350	.0527	.05171
.05000	.0528	.05208	.0540	.05393	.0529	.05213
.06666	.0530	.05246	.0541	.05421	.0531	.05250
.08333	.0532	.05278	.0542	.05440	.0533	.05283
.10000	.0533	.05306	.0543	.05453	.0534	.05311
.11666	.0534	.05331	.0544	.05462	.0535	.05337
.13333	.0535	.05352	.0544	.05468	.0537	.05359
.15000	.0536	.05371	.0544	.05472	.0538	.05379
.16666	.0537	.05387	.0545	.05474	.0539	.05396
.18333	.0538	.05401	.0545	.05476	.0539	.05412
.20000	.0539	.05414	.0545	.05478	.0540	.05425
.21666	.0540	.05425	.0545	.05479	.0541	.05437
.23333	.0540	.05434	.0546	.05480	.0542	.05448
.25000	.0541	.05442	.0546	.05480	.0542	.05459
.26666	.0542	.05450	.0546	.05481	.0543	.05466
.28333	.0542	.05456	.0546	.05481	.0544	.05473
.30000	.0543	.05462	.0547	.05481	.0544	.05480
.31666	.0543	.05467	.0547	.05482	.0545	.05486
.33333	.0543	.05471	.0547	.05482	.0545	.05491
.41666	.0545	.05496	.0547	.05484	.0547	.05510
.50000	.0547	.05495	.0548	.05485	.0549	.05521
.58333	.0548	.05501	.0549	.05486	.0550	.05528
.66666	.0549	.05505	.0549	.05488	.0552	.05533
.75000	.0550	.05509	.0549	.05489	.0553	.05536
.83333	.0550	.05512	.0550	.05491	.0553	.05539
.91666	.0551	.05514	.0550	.05492	.0554	.05542
1.00000	.0551	.05517	.0550	.05494	.0554	.05545
1.08333	.0552	.05520	.0550	.05495	.0555	.05547
1.16666	.0553	.05522	.0550	.05496	.0556	.05549
1.25000	.0554	.05525	.0550	.05498	.0556	.05552
1.33333	.0554	.05528	.0551	.05499	.0556	.05554
1.41666	.0554	.05530	.0551	.05501	.0556	.05556
1.50000	.0555	.05533	.0551	.05502	.0557	.05559
1.58333	.0555	.05536	.0551	.05503	.0557	.05561
1.66666	.0556	.05538	.0551	.05505	.0558	.05563
1.75000	.0556	.05541	.0551	.05506	.0558	.05566
1.83333	.0556	.05544	.0552	.05508	.0558	.05568
1.91666	.0557	.05546	.0552	.05509	.0558	.05570
2.00000	.0557	.05549	.0552	.05510	.0558	.05572
2.16666	.0557	.05554	.0552	.05513	.0559	.05577
2.33333	.0558	.05559	.0552	.05516	.0560	.05582
2.50000	.0558	.05565	.0553	.05519	.0560	.05586
2.66666	.0558	.05570	.0553	.05522	.0560	.05591
2.83333	.0559	.05575	.0553	.05524	.0561	.05595
3.00000	.0559	.05580	.0555	.05527	.0561	.05600
3.16666	.0560	.05586	.0555	.05530	.0561	.05605
3.33333	.0560	.05591	.0555	.05533	.0562	.05609
3.50000	.0560	.05596	.0555	.05536	.0563	.05614
3.66666	.0561	.05601	.0556	.05539	.0563	.05619
3.83333	.0561	.05607	.0556	.05541	.0563	.05623
4.00000	.0562	.05612	.0556	.05544	.0563	.05628
4.16666	.0562	.05617	.0557	.05547	.0564	.05632
4.33333	.0563	.05622	.0557	.05550	.0565	.05637
4.50000	.0563	.05628	.0557	.05553	.0566	.05642
4.66666			.0557	.05555	.0566	.05646
4.83333					.0566	.05651
5.00000					.0566	.05655

Appendix 9. Observed and predicted creep deflection of glass fiber reinforced hardboard. CREEP I; Eff V_f=0; 15.5 lbs; hr; in.

	13		14		15	
Time	Obs	Prd	Obs	Prd	Obs	Prd
0.00000	.1302	.13020	.1275	.12750	.1218	.12180
.01666	.1391	.13281	.1348	.13001	.1275	.12352
.03333	.1396	.13505	.1362	.13214	.1288	.12505
.05000	.1405	.13696	.1370	.13395	.1296	.12642
.06666	.1412	.13860	.1377	.13548	.1302	.12763
.08333	.1417	.14000	.1382	.13679	.1307	.12871
.10000	.1421	.14120	.1386	.13790	.1311	.12967
.11666	.1425	.14222	.1390	.13884	.1314	.13053
.13333	.1429	.14310	.1393	.13965	.1317	.13129
.15000	.1432	.14385	.1396	.14033	.1320	.13198
.16666	.1435	.14450	.1399	.14092	.1323	.13258
.18333	.1438	.14505	.1402	.14142	.1326	.13312
.20000	.1441	.14553	.1404	.14184	.1328	.13361
.21666	.1443	.14594	.1406	.14221	.1330	.13404
.23333	.1445	.14630	.1409	.14252	.1332	.13443
.25000	.1447	.14660	.1410	.14279	.1334	.13477
.26666	.1449	.14687	.1412	.14303	.1336	.13509
.28333	.1451	.14710	.1414	.14323	.1338	.13536
.30000	.1452	.14730	.1415	.14340	.1340	.13561
.31666	.1454	.14747	.1417	.14356	.1341	.13584
.33333	.1455	.14763	.1418	.14369	.1343	.13604
.41666	.1460	.14799	.1428	.14433	.1352	.13700
.50000	.1466	.14837	.1433	.14456	.1357	.13741
.58333	.1471	.14862	.1437	.14474	.1362	.13770
.66666	.1476	.14880	.1442	.14490	.1367	.13793
.75000	.1480	.14896	.1446	.14505	.1371	.13811
.83333	.1483	.14911	.1448	.14519	.1375	.13827
.91666	.1487	.14925	.1452	.14533	.1379	.13843
1.00000	.1490	.14938	.1455	.14547	.1382	.13857
1.08333	.1492	.14952	.1458	.14561	.1385	.13871
1.16666	.1495	.14966	.1460	.14575	.1387	.13886
1.25000	.1499	.14979	.1463	.14589	.1390	.13900
1.33333	.1502	.14993	.1465	.14603	.1393	.13913
1.41666	.1504	.15006	.1467	.14617	.1395	.13927
1.50000	.1506	.15020	.1468	.14631	.1397	.13941
1.58333	.1509	.15033	.1470	.14645	.1400	.13955
1.66666	.1511	.15047	.1471	.14659	.1402	.13969
1.75000	.1514	.15060	.1473	.14673	.1404	.13983
1.83333	.1516	.15074	.1474	.14687	.1405	.13997
1.91666	.1518	.15087	.1477	.14701	.1407	.14010
2.00000	.1520	.15101	.1479	.14715	.1408	.14024
2.16666	.1523	.15128	.1481	.14743	.1411	.14052
2.33333	.1526	.15155	.1484	.14771	.1416	.14079
2.50000	.1530	.15182	.1488	.14799	.1419	.14107
2.66666	.1533	.15209	.1490	.14827	.1421	.14135
2.83333	.1535	.15236	.1493	.14855	.1425	.14162
3.00000	.1537	.15263	.1496	.14883	.1428	.14190
3.16666	.1540	.15290	.1500	.14911	.1431	.14218
3.33333	.1543	.15317	.1502	.14939	.1433	.14245
3.50000	.1545	.15344	.1504	.14967	.1435	.14273
3.66666	.1547	.15371	.1508	.14995	.1437	.14301
3.83333	.1550	.15398	.1510	.15023	.1439	.14328
4.00000	.1552	.15425	.1512	.15051	.1442	.14356
4.16666	.1555	.15452	.1515	.15079	.1444	.14384
4.33333	.1557	.15479	.1517	.15107	.1446	.14411
4.50000	.1559	.15506	.1519	.15135	.1448	.14439
4.66666			.1521	.15149	.1450	.14467
4.83333					.1452	.14494
5.00000						

Appendix 9. Observed and predicted creep deflection of glass fiber reinforced hardboard. CREEP I; Eff V_f=0.0073; 15.5 lbs; hr; in.

	16		17		18	
Time	Obs	Prd	Obs	Prd	Obs	Prd
0.00000	.1003	.10030	.1019	.10190	.0957	.09570
.01666	.1039	.10144	.1056	.10292	.0997	.09714
.03333	.1048	.10246	.1065	.10386	.1006	.09838
.05000	.1054	.10337	.1071	.10470	.1012	.09943
.06666	.1058	.10419	.1075	.10548	.1016	.10033
.08333	.1062	.10491	.1078	.10618	.1020	.10110
.10000	.1065	.10556	.1081	.10681	.1022	.10175
.11666	.1068	.10614	.1084	.10739	.1025	.10231
.13333	.1070	.10666	.1086	.10792	.1027	.10279
.15000	.1072	.10713	.1088	.10840	.1029	.10320
.16666	.1074	.10754	.1090	.10883	.1030	.10355
.18333	.1076	.10792	.1091	.10923	.1032	.10385
.20000	.1078	.10825	.1093	.10959	.1033	.10411
.21666	.1080	.10855	.1094	.10992	.1034	.10433
.23333	.1081	.10882	.1095	.11022	.1036	.10452
.25000	.1083	.10906	.1097	.11049	.1037	.10468
.26666	.1084	.10928	.1098	.11074	.1038	.10482
.28333	.1085	.10947	.1099	.11097	.1039	.10494
.30000	.1087	.10965	.1100	.11117	.1040	.10504
.31666	.1088	.10981	.1102	.11136	.1041	.10513
.33333	.1089	.10995	.1103	.11154	.1042	.10521
.41666	.1092	.11030	.1109	.11241	.1045	.10551
.50000	.1097	.11071	.1112	.11278	.1048	.10566
.58333	.1100	.11097	.1116	.11304	.1051	.10575
.66666	.1103	.11115	.1119	.11322	.1052	.10582
.75000	.1106	.11129	.1122	.11336	.1054	.10589
.83333	.1109	.11141	.1125	.11347	.1055	.10595
.91666	.1111	.11151	.1127	.11357	.1058	.10601
1.00000	.1113	.11160	.1130	.11366	.1059	.10606
1.08333	.1114	.11169	.1132	.11374	.1061	.10612
1.16666	.1116	.11178	.1134	.11381	.1062	.10618
1.25000	.1118	.11186	.1136	.11389	.1063	.10623
1.33333	.1120	.11195	.1138	.11396	.1063	.10629
1.41666	.1121	.11203	.1140	.11403	.1064	.10635
1.50000	.1122	.11211	.1141	.11410	.1065	.10640
1.58333	.1124	.11220	.1142	.11417	.1066	.10646
1.66666	.1125	.11228	.1144	.11424	.1067	.10652
1.75000	.1127	.11236	.1145	.11431	.1068	.10657
1.83333	.1128	.11244	.1146	.11438	.1069	.10663
1.91666	.1129	.11248	.1147	.11445	.1070	.10669
2.00000	.1130	.11261	.1149	.11452	.1071	.10674
2.16666	.1132	.11278	.1151	.11466	.1072	.10685
2.33333	.1134	.11294	.1153	.11480	.1073	.10697
2.50000	.1136	.11311	.1155	.11495	.1076	.10708
2.66666	.1138	.11327	.1157	.11509	.1078	.10719
2.83333	.1140	.11344	.1159	.11523	.1079	.10731
3.00000	.1143	.11361	.1161	.11537	.1080	.10742
3.16666	.1145	.11377	.1162	.11551	.1081	.10753
3.33333	.1147	.11394	.1164	.11565	.1082	.10765
3.50000	.1148	.11410	.1165	.11579	.1083	.10776
3.66666	.1149	.11427	.1167	.11593	.1084	.10787
3.83333	.1151	.11444	.1169	.11607	.1085	.10799
4.00000	.1152	.11460	.1170	.11621	.1086	.10810
4.16666			.1171	.11635	.1087	.10821
4.33333			.1172	.11649	.1088	.10832
4.50000			.1174	.11663	.1089	.10844
4.66666			.1175	.11677	.1090	.10855
4.83333			.1176	.11691	.1092	.10866
5.00000					.1093	.10878

Appendix 9. Observed and predicted creep deflection of glass fiber reinforced hardboard. CREEP I; Eff V_f=0.0158; 15.5 lbs; hr; in.

	19		20		21	
Time	Obs	Prd	Obs	Prd	Obs	Prd
0.00000	.0924	.09240	.0875	.08550	.0874	.08740
.01666	.0966	.09366	.0895	.08628	.0906	.08846
.03333	.0974	.09478	.0892	.08700	.0914	.08939
.05000	.0979	.09576	.0897	.08766	.0919	.09022
.06666	.0983	.09662	.0900	.08826	.0922	.09094
.08333	.0986	.09738	.0903	.08882	.0925	.09157
.10000	.0989	.09805	.0906	.08933	.0928	.09213
.11666	.0992	.09864	.0909	.08980	.0930	.09262
.13333	.0994	.09916	.0910	.09024	.0932	.09305
.15000	.0996	.09962	.0911	.09064	.0934	.09343
.16666	.0997	.10003	.0913	.09100	.0935	.09376
.18333	.0999	.10038	.0914	.09134	.0936	.09405
.20000	.1001	.10070	.0915	.09165	.0938	.09431
.21666	.1002	.10098	.0917	.09194	.0939	.09454
.23333	.1003	.10122	.0918	.09220	.0940	.09474
.25000	.1004	.10144	.0919	.09244	.0941	.09492
.26666	.1006	.10164	.0920	.09267	.0943	.09507
.28333	.1007	.10181	.0922	.09287	.0944	.09521
.30000	.1008	.10196	.0922	.09306	.0945	.09534
.31666	.1009	.10210	.0923	.09324	.0946	.09545
.33333	.1010	.10222	.0924	.09340	.0947	.09554
.41666	.1014	.10266	.0928	.09401	.0950	.09586
.50000	.1018	.10293	.0931	.09444	.0953	.09608
.58333	.1021	.10310	.0935	.09477	.0955	.09621
.66666	.1024	.10323	.0938	.09498	.0956	.09631
.75000	.1027	.10333	.0940	.09515	.0959	.09638
.83333	.1029	.10342	.0943	.09527	.0961	.09644
.91666	.1031	.10351	.0945	.09537	.0962	.09650
1.00000	.1033	.10358	.0947	.09545	.0963	.09655
1.08333	.1034	.10366	.0948	.09552	.0964	.09660
1.16666	.1036	.10374	.0949	.09559	.0965	.09665
1.25000	.1038	.10381	.0952	.09565	.0966	.09670
1.33333	.1039	.10389	.0953	.09571	.0967	.09675
1.41666	.1041	.10397	.0955	.09577	.0968	.09680
1.50000	.1043	.10404	.0957	.09582	.0969	.09685
1.58333	.1044	.10412	.0958	.09588	.0970	.09690
1.66666	.1045	.10419	.0960	.09593	.0970	.09695
1.75000	.1046	.10427	.0961	.09598	.0971	.09700
1.83333	.1047	.10434	.0963	.09604	.0972	.09705
1.91666	.1048	.10442	.0964	.09609	.0974	.09710
2.00000	.1049	.10449	.0964	.09614	.0974	.09715
2.16666	.1051	.10464	.0967	.09625	.0975	.09725
2.33333	.1054	.10479	.0969	.09636	.0977	.09735
2.50000	.1055	.10494	.0970	.09646	.0978	.09745
2.66666	.1057	.10510	.0971	.09657	.0979	.09755
2.83333	.1059	.10525	.0973	.09667	.0980	.09765
3.00000	.1060	.10540	.0974	.09678	.0982	.09775
3.16666	.1062	.10555	.0976	.09689	.0983	.09785
3.33333	.1063	.10570	.0977	.09699	.0984	.09795
3.50000	.1065	.10585	.0978	.09710	.0985	.09805
3.66666	.1066	.10600	.0980	.09721	.0987	.09815
3.83333	.1068	.10615	.0981	.09731	.0987	.09825
4.00000	.1069	.10630	.0982	.09742	.0989	.09835
4.16666	.1070	.10645	.0983	.09752	.0989	.09845
4.33333	.1072	.10660	.0985	.09763	.0990	.09854
4.50000	.1073	.10675	.0984	.09774	.0991	.09864
4.66666			.0986	.09784	.0992	.09874
4.83333					.0993	.09884
5.00000					.0994	.09894

Appendix 9. Observed and predicted creep deflection of glass fiber reinforced hardboard. CREEP I; Eff V_f=0.0260; 15.5 lbs; hr; in.

	22		23		24	
Time	Obs	Prd	Obs	Prd	Obs	Prd
0.00000	.0827	.08270	.0834	.08340	.0832	.08320
.01666	.0854	.08360	.0864	.08432	.0842	.08423
.03333	.0860	.08439	.0871	.08513	.0848	.08511
.05000	.0864	.08508	.0875	.08585	.0872	.08586
.06666	.0867	.08569	.0878	.08649	.0875	.08651
.08333	.0870	.08623	.0881	.08706	.0877	.08707
.10000	.0872	.08670	.0883	.08757	.0879	.08754
.11666	.0874	.08711	.0885	.08801	.0880	.08795
.13333	.0876	.08747	.0886	.08841	.0882	.08830
.15000	.0878	.08780	.0888	.08876	.0884	.08860
.16666	.0879	.08808	.0889	.08907	.0885	.08886
.18333	.0880	.08833	.0891	.08935	.0886	.08908
.20000	.0881	.08855	.0892	.08960	.0887	.08929
.21666	.0883	.08874	.0893	.08982	.0888	.08944
.23333	.0884	.08891	.0894	.09002	.0890	.08958
.25000	.0884	.08906	.0895	.09019	.0890	.08971
.26666	.0885	.08920	.0895	.09035	.0891	.08981
.28333	.0886	.08932	.0896	.09049	.0892	.08990
.30000	.0887	.08942	.0897	.09061	.0893	.08998
.31666	.0888	.08951	.0898	.09072	.0893	.09005
.33333	.0889	.08960	.0899	.09082	.0894	.09011
.41666	.0891	.08990	.0902	.09120	.0896	.09032
.50000	.0894	.09008	.0905	.09142	.0898	.09044
.58333	.0896	.09020	.0909	.09156	.0900	.09052
.66666	.0898	.09030	.0910	.09166	.0902	.09057
.75000	.0899	.09037	.0912	.09175	.0904	.09062
.83333	.0901	.09044	.0913	.09181	.0904	.09067
.91666	.0902	.09050	.0915	.09188	.0905	.09071
1.00000	.0904	.09056	.0916	.09193	.0906	.09075
1.08333	.0905	.09061	.0918	.09199	.0907	.09079
1.16666	.0906	.09067	.0918	.09205	.0909	.09083
1.25000	.0907	.09073	.0920	.09210	.0910	.09087
1.33333	.0908	.09078	.0921	.09216	.0910	.09091
1.41666	.0909	.09084	.0922	.09221	.0910	.09095
1.50000	.0910	.09090	.0923	.09227	.0911	.09099
1.58333	.0910	.09095	.0924	.09232	.0911	.09103
1.66666	.0911	.09101	.0925	.09238	.0912	.09107
1.75000	.0912	.09107	.0926	.09243	.0913	.09111
1.83333	.0913	.09112	.0927	.09248	.0914	.09115
1.91666	.0914	.09118	.0928	.09254	.0914	.09119
2.00000	.0915	.09124	.0929	.09259	.0914	.09123
2.16666	.0916	.09135	.0931	.09270	.0915	.09131
2.33333	.0918	.09146	.0932	.09281	.0916	.09139
2.50000	.0920	.09157	.0934	.09292	.0917	.09148
2.66666	.0921	.09169	.0934	.09303	.0918	.09156
2.83333	.0922	.09180	.0935	.09314	.0921	.09164
3.00000	.0923	.09191	.0937	.09325	.0921	.09172
3.16666	.0925	.09202	.0938	.09335	.0922	.09180
3.33333	.0925	.09214	.0939	.09346	.0923	.09188
3.50000	.0926	.09225	.0940	.09357	.0924	.09196
3.66666	.0927	.09236	.0941	.09368	.0924	.09204
3.83333	.0929	.09247	.0942	.09379	.0925	.09212
4.00000	.0930	.09259	.0944	.09390	.0926	.09220
4.16666	.0932	.09270	.0945	.09401	.0926	.09228
4.33333	.0932	.09281	.0946	.09412	.0927	.09236
4.50000	.0932	.09292	.0947	.09423	.0928	.09244
4.66666	.0933	.09299	.0948	.09433	.0929	.09252
4.83333			.0948	.09444	.0929	.09261
5.00000			.0949	.09455	.0930	.09269

Appendix 9. Observed and predicted creep deflection of glass fiber reinforced hardboard. CREEP II; Eff V_f=0; 9.09 lbs; hr; in.

	1		2		3	
Time	Obs	Prd	Obs	Prd	Obs	Prd
0.00000	.0728	.07564	.0734	.07646	.0712	.07443
.01666	.0762	.07609	.0775	.07701	.0748	.07480
.03333	.0770	.07649	.0783	.07751	.0755	.07515
.05000	.0775	.07687	.0798	.07798	.0760	.07543
.06666	.0779	.07724	.0792	.07841	.0764	.07590
.09333	.0782	.07758	.0795	.07880	.0767	.07610
.10000	.0785	.07790	.0798	.07917	.0770	.07639
.11666	.0787	.07821	.0800	.07951	.0772	.07656
.13333	.0789	.07849	.0802	.07982	.0774	.07692
.15000	.0791	.07875	.0804	.08011	.0775	.07717
.16666	.0793	.07901	.0805	.08037	.0778	.07740
.18333	.0794	.07925	.0807	.08062	.0780	.07759
.20000	.0796	.07948	.0808	.08084	.0781	.07784
.21666	.0798	.07969	.0810	.08105	.0783	.07804
.23333	.0799	.07989	.0811	.08125	.0784	.07823
.25000	.0801	.08008	.0812	.08143	.0785	.07842
.26666	.0802	.08026	.0813	.08159	.0786	.07959
.28333	.0803	.08043	.0814	.08175	.0787	.07876
.30000	.0804	.08059	.0815	.08189	.0788	.07892
.31666	.0805	.08074	.0816	.08202	.0790	.07907
.33333	.0806	.08088	.0817	.08215	.0791	.07921
.41666	.0810	.08144	.0820	.08262	.0795	.07983
.50000	.0814	.08191	.0824	.08297	.0798	.08033
.58333	.0817	.08228	.0827	.08323	.0802	.08072
.66666	.0820	.08257	.0830	.08342	.0804	.08103
.75000	.0823	.08280	.0832	.08357	.0807	.08128
.83333	.0825	.08300	.0833	.08368	.0809	.08148
.91666	.0827	.08316	.0835	.08378	.0811	.08165
1.00000	.0829	.08330	.0835	.08387	.0812	.08179
1.08333	.0831	.08342	.0837	.08395	.0814	.08190
1.16666	.0833	.08353	.0838	.08402	.0815	.08200
1.25000	.0835	.08363	.0839	.08409	.0817	.08209
1.33333	.0836	.08372	.0840	.08416	.0818	.08217
1.41666	.0838	.08381	.0841	.08423	.0819	.08224
1.50000	.0839	.08390	.0842	.08429	.0820	.08230
1.58333	.0840	.08399	.0843	.08436	.0822	.08236
1.66666	.0842	.08407	.0844	.08442	.0823	.08241
1.75000	.0842	.08415	.0845	.08448	.0824	.08246
1.83333	.0844	.08423	.0847	.08455	.0825	.08251
1.91666	.0845	.08431	.0848	.08461	.0826	.08256
2.00000	.0847	.08439	.0849	.08467	.0826	.08261
2.16666	.0849	.08455	.0850	.08480	.0828	.08270
2.33333	.0850	.08471	.0851	.08492	.0829	.08279
2.50000	.0851	.08486	.0853	.08505	.0830	.08287
2.66666	.0853	.08502	.0854	.08518	.0832	.08296
2.83333	.0855	.08518	.0855	.08530	.0833	.08304
3.00000	.0856	.08533	.0857	.08543	.0834	.08313
3.16666	.0857	.08549	.0858	.08555	.0835	.08321
3.33333	.0858	.08565	.0860	.08568	.0836	.08330
3.50000	.0860	.08580	.0861	.08580	.0837	.08339
3.66666	.0861	.08595	.0862	.08593	.0838	.08347
3.83333	.0863	.08611	.0863	.08606	.0839	.08355
4.00000	.0863	.08627	.0864	.08618	.0840	.08364
4.16666	.0864	.08643	.0865	.08631	.0841	.08372
4.33333	.0866	.08658	.0866	.08643	.0842	.08381
4.50000	.0868	.08674	.0867	.08656	.0843	.08389
4.66666	.0870	.08690	.0869	.08669	.0843	.08397
4.83333	.0871	.08705	.0870	.08681	.0844	.08406
5.00000			.0871	.08694	.0844	.08414

Appendix 9. Observed and predicted creep deflection of glass fiber reinforced hardboard. CREEP II; Eff V_f=0.0073; 9.09 lbs; hr; in.

	4		5		6	
Time	Obs	Prd	Obs	Prd	Obs	Prd
0.00000	.0591	.05927	.0640	.06672	.0559	.05748
.01666	.0593	.05962	.0666	.06693	.0585	.05798
.03333	.0593	.05995	.0672	.06713	.0590	.05842
.05000	.0597	.05925	.0676	.06732	.0594	.05881
.06666	.0600	.05954	.0679	.06751	.0595	.05916
.08333	.0603	.05982	.0681	.06769	.0599	.05946
.10000	.0605	.06007	.0683	.06786	.0600	.05973
.11666	.0607	.06032	.0685	.06803	.0601	.05997
.13333	.0609	.06055	.0686	.06819	.0603	.06019
.15000	.0610	.06076	.0687	.06834	.0604	.06037
.16666	.0612	.06097	.0689	.06849	.0605	.06054
.18333	.0613	.06115	.0690	.06864	.0606	.06069
.20000	.0614	.06134	.0691	.06877	.0607	.06082
.21666	.0615	.06151	.0692	.06891	.0607	.06094
.23333	.0617	.06167	.0693	.06904	.0609	.06104
.25000	.0618	.06182	.0694	.06916	.0609	.06113
.26666	.0619	.06197	.0695	.06928	.0609	.06121
.28333	.0620	.06210	.0696	.06940	.0610	.06129
.30000	.0621	.06223	.0697	.06951	.0610	.06135
.31666	.0622	.06235	.0697	.06962	.0611	.06141
.33333	.0623	.06247	.0698	.06972	.0611	.06146
.41666	.0627	.06295	.0701	.07019	.0615	.06178
.50000	.0630	.06332	.0704	.07058	.0618	.06196
.58333	.0632	.06360	.0706	.07091	.0617	.06191
.66666	.0634	.06382	.0709	.07119	.0618	.06196
.75000	.0636	.06400	.0710	.07143	.0620	.06200
.83333	.0638	.06414	.0712	.07163	.0621	.06204
.91666	.0639	.06425	.0713	.07180	.0621	.06207
1.00000	.0641	.06435	.0715	.07195	.0621	.06211
1.08333	.0642	.06443	.0716	.07207	.0622	.06214
1.16666	.0643	.06450	.0718	.07218	.0622	.06218
1.25000	.0644	.06456	.0719	.07228	.0623	.06221
1.33333	.0645	.06462	.0720	.07237	.0623	.06224
1.41666	.0645	.06468	.0721	.07245	.0623	.06228
1.50000	.0646	.06473	.0722	.07251	.0624	.06231
1.58333	.0647	.06478	.0723	.07258	.0624	.06234
1.66666	.0649	.06483	.0724	.07263	.0624	.06238
1.75000	.0649	.06488	.0725	.07269	.0624	.06241
1.83333	.0649	.06492	.0725	.07274	.0625	.06244
1.91666	.0650	.06497	.0726	.07278	.0625	.06249
2.00000	.0651	.06501	.0729	.07283	.0627	.06254
2.16666	.0652	.06510	.0729	.07291	.0627	.06261
2.33333	.0653	.06519	.0731	.07299	.0628	.06269
2.50000	.0655	.06528	.0732	.07306	.0628	.06275
2.66666	.0656	.06537	.0733	.07313	.0629	.06281
2.83333	.0657	.06545	.0734	.07320	.0630	.06288
3.00000	.0658	.06554	.0735	.07327	.0631	.06295
3.16666	.0659	.06563	.0736	.07334	.0631	.06301
3.33333	.0659	.06572	.0737	.07340	.0632	.06308
3.50000	.0660	.06581	.0738	.07347	.0632	.06315
3.66666	.0661	.06589	.0738	.07354	.0633	.06321
3.83333	.0662	.06598	.0739	.07360	.0633	.06329
4.00000	.0663	.06607	.0740	.07367	.0634	.06335
4.16666	.0663	.06616	.0740	.07373	.0635	.06341
4.33333	.0664	.06624	.0741	.07380	.0635	.06348
4.50000	.0665	.06633	.0741	.07386	.0637	.06355
4.66666	.0665	.06642	.0742	.07393	.0637	.06361
4.83333			.0743	.07399	.0638	.06368
5.00000						

Appendix 9. Observed and predicted creep deflection of glass fiber reinforced hardboard. CREEP II; Eff V_f=0.0158; 9.09 lbs; hr; in.

	7		8		9	
Time	Obs	Prd	Obs	Prd	Obs	Prd
0.00000	.0591	.06123	.0527	.05399	.0541	.05523
.01666	.0615	.06152	.0544	.05424	.0559	.05560
.03333	.0621	.06180	.0548	.05447	.0564	.05592
.05000	.0624	.06206	.0550	.05468	.0566	.05621
.06666	.0627	.06232	.0552	.05487	.0568	.05647
.08333	.0630	.06255	.0554	.05505	.0569	.05670
.10000	.0632	.06278	.0555	.05522	.0571	.05690
.11666	.0634	.06300	.0556	.05537	.0572	.05709
.13333	.0635	.06320	.0557	.05552	.0573	.05725
.15000	.0637	.06340	.0558	.05565	.0574	.05739
.16666	.0639	.06358	.0559	.05577	.0575	.05752
.18333	.0640	.06375	.0559	.05589	.0576	.05764
.20000	.0641	.06392	.0560	.05599	.0577	.05774
.21666	.0642	.06408	.0560	.05609	.0577	.05783
.23333	.0643	.06423	.0561	.05619	.0578	.05791
.25000	.0644	.06437	.0562	.05627	.0578	.05798
.26666	.0645	.06451	.0562	.05635	.0579	.05805
.28333	.0646	.06464	.0563	.05643	.0579	.05811
.30000	.0647	.06476	.0563	.05649	.0580	.05816
.31666	.0648	.06488	.0564	.05656	.0580	.05820
.33333	.0649	.06499	.0564	.05662	.0580	.05825
.41666	.0655	.06583	.0566	.05687	.0582	.05840
.50000	.0657	.06613	.0569	.05704	.0583	.05849
.58333	.0659	.06636	.0570	.05718	.0584	.05854
.66666	.0661	.06655	.0571	.05728	.0585	.05858
.75000	.0663	.06670	.0572	.05736	.0585	.05861
.83333	.0664	.06683	.0573	.05743	.0585	.05863
.91666	.0666	.06693	.0574	.05749	.0585	.05864
1.00000	.0667	.06701	.0574	.05754	.0585	.05866
1.08333	.0668	.06709	.0575	.05759	.0586	.05867
1.16666	.0669	.06715	.0575	.05764	.0586	.05869
1.25000	.0670	.06720	.0576	.05768	.0587	.05870
1.33333	.0671	.06725	.0577	.05772	.0588	.05871
1.41666	.0672	.06730	.0578	.05776	.0588	.05873
1.50000	.0672	.06734	.0578	.05781	.0588	.05874
1.58333	.0673	.06738	.0579	.05785	.0588	.05875
1.66666	.0673	.06741	.0579	.05789	.0588	.05877
1.75000	.0674	.06745	.0580	.05793	.0588	.05878
1.83333	.0675	.06748	.0581	.05797	.0588	.05879
1.91666	.0675	.06752	.0581	.05801	.0589	.05881
2.00000	.0676	.06758	.0582	.05805	.0589	.05882
2.16666	.0677	.06765	.0582	.05813	.0589	.05884
2.33333	.0679	.06771	.0583	.05821	.0589	.05887
2.50000	.0679	.06777	.0584	.05829	.0590	.05890
2.66666	.0680	.05783	.0585	.05837	.0590	.05892
2.83333	.0681	.06789	.0587	.05845	.0590	.05895
3.00000	.0682	.06795	.0587	.05853	.0591	.05897
3.16666	.0683	.06801	.0587	.05861	.0591	.05900
3.33333	.0684	.06807	.0588	.05869	.0591	.05903
3.50000	.0684	.06813	.0589	.05877	.0592	.05905
3.66666	.0685	.06819	.0589	.05885	.0592	.05908
3.83333	.0686	.06825	.0591	.05893	.0592	.05911
4.00000	.0686	.06831	.0592	.05901	.0592	.05913
4.16666	.0687	.06838	.0592	.05909	.0593	.05916
4.33333	.0687	.06844	.0593	.05917	.0593	.05918
4.50000				.05925	.0593	.05921
4.66666					.0593	.05924
4.83333					.0594	.05926
5.00000					.0594	.05929

Appendix 9. Observed and predicted creep deflection of glass fiber reinforced hardboard. CREEP II; Eff V_f=0.0260; 9.09 lbs; hr; in.

	10		11		12	
Time	Obs	Prd	Obs	Prd	Obs	Prd
0.00000	.0506	.05154	.0519	.05247	.0507	.05183
.01666	.0521	.05194	.0535	.05302	.0523	.05211
.03333	.0525	.05221	.0538	.05345	.0527	.05236
.05000	.0529	.05246	.0540	.05377	.0529	.05260
.06666	.0530	.05260	.0541	.05402	.0531	.05281
.08333	.0532	.05279	.0542	.05421	.0533	.05301
.10000	.0533	.05308	.0543	.05435	.0534	.05319
.11666	.0534	.05325	.0544	.05446	.0535	.05336
.13333	.0535	.05341	.0544	.05455	.0537	.05352
.15000	.0536	.05356	.0544	.05462	.0538	.05366
.16666	.0537	.05369	.0545	.05467	.0538	.05380
.18333	.0538	.05381	.0545	.05471	.0539	.05392
.20000	.0539	.05392	.0545	.05474	.0540	.05403
.21666	.0540	.05402	.0545	.05476	.0541	.05414
.23333	.0540	.05411	.0546	.05478	.0542	.05423
.25000	.0541	.05420	.0546	.05480	.0542	.05432
.26666	.0542	.05427	.0546	.05481	.0543	.05440
.28333	.0542	.05434	.0546	.05482	.0544	.05448
.30000	.0543	.05441	.0547	.05483	.0544	.05455
.31666	.0543	.05447	.0547	.05483	.0545	.05462
.33333	.0543	.05452	.0547	.05484	.0545	.05468
.41666	.0545	.05474	.0547	.05486	.0547	.05492
.50000	.0547	.05488	.0548	.05488	.0549	.05509
.58333	.0548	.05498	.0548	.05489	.0550	.05521
.66666	.0549	.05505	.0549	.05491	.0552	.05530
.75000	.0550	.05511	.0549	.05492	.0553	.05536
.83333	.0550	.05515	.0550	.05494	.0553	.05541
.91666	.0551	.05519	.0550	.05495	.0554	.05545
1.00000	.0551	.05522	.0550	.05496	.0554	.05549
1.08333	.0552	.05525	.0550	.05498	.0555	.05552
1.16666	.0553	.05528	.0550	.05499	.0556	.05555
1.25000	.0554	.05531	.0550	.05501	.0556	.05557
1.33333	.0554	.05534	.0551	.05502	.0556	.05560
1.41666	.0554	.05537	.0551	.05503	.0556	.05562
1.50000	.0555	.05539	.0551	.05505	.0557	.05565
1.58333	.0555	.05542	.0551	.05506	.0557	.05567
1.66666	.0556	.05545	.0551	.05508	.0558	.05570
1.75000	.0556	.05547	.0551	.05509	.0558	.05572
1.83333	.0556	.05550	.0552	.05510	.0558	.05574
1.91666	.0557	.05552	.0552	.05512	.0558	.05577
2.00000	.0557	.05555	.0552	.05513	.0558	.05579
2.16666	.0557	.05560	.0552	.05516	.0559	.05583
2.33333	.0558	.05566	.0552	.05519	.0560	.05588
2.50000	.0558	.05571	.0553	.05522	.0560	.05593
2.66666	.0558	.05576	.0553	.05525	.0560	.05597
2.83333	.0559	.05581	.0553	.05527	.0561	.05602
3.00000	.0559	.05587	.0555	.05530	.0561	.05607
3.16666	.0560	.05592	.0555	.05533	.0561	.05611
3.33333	.0560	.05597	.0555	.05536	.0562	.05616
3.50000	.0560	.05603	.0555	.05539	.0563	.05620
3.66666	.0561	.05608	.0556	.05541	.0563	.05625
3.83333	.0561	.05613	.0556	.05544	.0563	.05630
4.00000	.0562	.05618	.0556	.05547	.0563	.05634
4.16666	.0562	.05624	.0557	.05550	.0564	.05639
4.33333	.0563	.05629	.0557	.05553	.0565	.05643
4.50000	.0563	.05634	.0557	.05556	.0566	.05648
4.66666				.05558	.0566	.05653
4.83333					.0566	.05657
5.00000					.0566	.05662

Appendix 9. Observed and predicted creep deflection of glass fiber reinforced hardboard. CREEP II; Eff V_f=0; 15.5 lbs; hr; in.

	13		14		15	
Time	Obs	Prd	Obs	Prd	Obs	Prd
0.00000	.1302	.13634	.1275	.13285	.1218	.12661
.01666	.1381	.13727	.1348	.13381	.1405	.14032
.03333	.1396	.13812	.1362	.13470	.1407	.14046
.05000	.1405	.13893	.1370	.13554	.1408	.14060
.06666	.1412	.13966	.1377	.13627	.1411	.14088
.08333	.1417	.14034	.1382	.13696	.1416	.14116
.10000	.1421	.14097	.1386	.13760	.1419	.14143
.11666	.1425	.14156	.1390	.13818	.1421	.14171
.13333	.1429	.14211	.1393	.13872	.1425	.14199
.15000	.1432	.14262	.1396	.13922	.1428	.14226
.16666	.1435	.14309	.1399	.13968	.1431	.14254
.18333	.1438	.14353	.1402	.14010	.1433	.14282
.20000	.1441	.14394	.1404	.14049	.1435	.14310
.21666	.1443	.14432	.1406	.14084	.1437	.14337
.23333	.1445	.14468	.1408	.14117	.1439	.14365
.25000	.1447	.14500	.1410	.14148	.1442	.14392
.26666	.1449	.14531	.1412	.14176	.1444	.14420
.28333	.1451	.14560	.1414	.14202	.1446	.14448
.30000	.1452	.14586	.1415	.14226	.1448	.14475
.31666	.1454	.14611	.1417	.14249	.1450	.14503
.33333	.1455	.14634	.1418	.14269	.1452	.14531
.41666	.1460	.14695	.1423	.14388	.1275	.12729
.50000	.1466	.14774	.1433	.14437	.1288	.12792
.58333	.1471	.14831	.1437	.14474	.1296	.12852
.66666	.1476	.14874	.1442	.14503	.1302	.12908
.75000	.1480	.14908	.1446	.14526	.1307	.12962
.83333	.1483	.14935	.1448	.14546	.1311	.13012
.91666	.1487	.14958	.1452	.14564	.1314	.13059
1.00000	.1490	.14978	.1455	.14581	.1317	.13103
1.08333	.1492	.14996	.1458	.14597	.1320	.13145
1.16666	.1495	.15012	.1460	.14612	.1323	.13185
1.25000	.1499	.15027	.1463	.14627	.1326	.13222
1.33333	.1502	.15042	.1465	.14641	.1328	.13257
1.41666	.1504	.15057	.1467	.14655	.1330	.13291
1.50000	.1506	.15071	.1468	.14669	.1332	.13322
1.58333	.1509	.15085	.1470	.14684	.1334	.13352
1.66666	.1511	.15099	.1471	.14698	.1336	.13380
1.75000	.1514	.15112	.1473	.14712	.1338	.13406
1.83333	.1516	.15126	.1474	.14726	.1340	.13431
1.91666	.1518	.15139	.1477	.14740	.1341	.13455
2.00000	.1520	.15153	.1479	.14754	.1343	.13477
2.16666	.1523	.15180	.1481	.14782	.1352	.13600
2.33333	.1526	.15207	.1484	.14810	.1357	.13667
2.50000	.1530	.15234	.1488	.14838	.1362	.13720
2.66666	.1533	.15261	.1490	.14866	.1367	.13762
2.83333	.1535	.15288	.1493	.14994	.1371	.13797
3.00000	.1537	.15315	.1496	.14922	.1375	.13826
3.16666	.1540	.15342	.1500	.14950	.1379	.13851
3.33333	.1543	.15369	.1502	.14978	.1382	.13873
3.50000	.1545	.15396	.1504	.15006	.1385	.13892
3.66666	.1547	.15423	.1509	.15034	.1387	.13911
3.83333	.1550	.15450	.1510	.15062	.1390	.13928
4.00000	.1552	.15477	.1512	.15090	.1393	.13944
4.16666	.1555	.15504	.1515	.15118	.1395	.13959
4.33333	.1557	.15531	.1517	.15146	.1397	.13974
4.50000	.1559	.15559	.1519	.15174	.1400	.13989
4.66666			.1521	.15188	.1402	.14003
4.83333					.1404	.14018
5.00000						

Appendix 9. Observed and predicted creep deflection of glass fiber reinforced hardboard. CREEP II; Eff V_f=0.0073; 15.5 lbs; hr; in.

	16		17		18	
Time	Obs	Prd	Obs	Prd	Obs	Prd
0.00000	.1003	.10327	.1019	.10563	.0957	.09866
.01666	.1039	.10378	.1056	.10596	.0997	.09927
.03333	.1048	.10425	.1065	.10629	.1006	.09982
.05000	.1054	.10470	.1071	.10660	.1012	.10033
.06666	.1058	.10512	.1075	.10689	.1016	.10080
.08333	.1062	.10551	.1078	.10718	.1020	.10123
.10000	.1065	.10588	.1081	.10745	.1022	.10162
.11666	.1068	.10622	.1084	.10771	.1025	.10197
.13333	.1070	.10655	.1086	.10796	.1027	.10230
.15000	.1072	.10685	.1088	.10821	.1029	.10260
.16666	.1074	.10714	.1090	.10844	.1030	.10288
.18333	.1076	.10741	.1091	.10866	.1032	.10313
.20000	.1078	.10766	.1093	.10887	.1033	.10337
.21666	.1080	.10790	.1094	.10908	.1034	.10358
.23333	.1081	.10812	.1095	.10928	.1036	.10378
.25000	.1083	.10833	.1097	.10946	.1037	.10396
.26666	.1084	.10853	.1098	.10965	.1038	.10412
.28333	.1085	.10872	.1099	.10982	.1039	.10427
.30000	.1087	.10889	.1100	.10999	.1040	.10441
.31666	.1088	.10906	.1102	.11015	.1041	.10454
.33333	.1089	.10921	.1103	.11031	.1042	.10466
.41666	.1092	.10963	.1109	.11125	.1045	.10519
.50000	.1097	.11018	.1112	.11178	.1048	.10549
.58333	.1100	.11060	.1116	.11221	.1051	.10571
.66666	.1103	.11093	.1119	.11258	.1052	.10586
.75000	.1106	.11118	.1122	.11289	.1054	.10598
.83333	.1109	.11139	.1125	.11315	.1055	.10608
.91666	.1111	.11156	.1127	.11337	.1058	.10616
1.00000	.1113	.11171	.1130	.11356	.1059	.10624
1.08333	.1114	.11184	.1132	.11373	.1061	.10630
1.16666	.1116	.11195	.1134	.11388	.1062	.10637
1.25000	.1118	.11206	.1136	.11402	.1063	.10643
1.33333	.1120	.11216	.1138	.11414	.1063	.10649
1.41666	.1121	.11226	.1140	.11425	.1064	.10655
1.50000	.1122	.11235	.1141	.11436	.1065	.10660
1.58333	.1124	.11244	.1142	.11445	.1066	.10666
1.66666	.1125	.11253	.1144	.11455	.1067	.10672
1.75000	.1127	.11261	.1145	.11463	.1068	.10677
1.83333	.1128	.11270	.1146	.11472	.1069	.10683
1.91666	.1129	.11273	.1147	.11480	.1070	.10689
2.00000	.1130	.11287	.1149	.11488	.1071	.10694
2.16666	.1132	.11303	.1151	.11503	.1072	.10706
2.33333	.1134	.11320	.1153	.11518	.1073	.10717
2.50000	.1136	.11337	.1155	.11533	.1076	.10728
2.66666	.1138	.11353	.1157	.11547	.1078	.10740
2.83333	.1140	.11370	.1159	.11561	.1079	.10751
3.00000	.1143	.11386	.1161	.11575	.1080	.10762
3.16666	.1145	.11403	.1162	.11590	.1081	.10774
3.33333	.1147	.11420	.1164	.11604	.1082	.10785
3.50000	.1148	.11436	.1165	.11618	.1083	.10796
3.66666	.1149	.11453	.1167	.11632	.1084	.10808
3.83333	.1151	.11469	.1169	.11646	.1085	.10819
4.00000	.1152	.11486	.1170	.11660	.1086	.10830
4.16666			.1171	.11674	.1087	.10841
4.33333			.1172	.11688	.1088	.10853
4.50000			.1174	.11702	.1089	.10864
4.66666			.1175	.11716	.1090	.10875
4.83333			.1176	.11730	.1092	.10887
5.00000					.1093	.10898

Appendix 9. Observed and predicted creep deflection of glass fiber reinforced hardboard. CREEP II; Eff V_f=0.0158; 15.5 lbs; hr; in.

	19		20		21	
Time	Obs	Prd	Obs	Prd	Obs	Prd
0.00000	.0924	.09583	.0855	.08869	.0874	.08992
.01666	.0966	.09630	.0885	.08894	.0906	.09038
.03333	.0974	.09674	.0892	.08918	.0914	.09081
.05000	.0979	.09716	.0897	.08941	.0919	.09121
.06666	.0983	.09754	.0900	.08963	.0922	.09159
.08333	.0986	.09791	.0903	.08984	.0925	.09193
.10000	.0989	.09825	.0906	.09005	.0929	.09225
.11666	.0992	.09857	.0908	.09025	.0930	.09255
.13333	.0994	.09887	.0910	.09044	.0932	.09283
.15000	.0996	.09915	.0911	.09063	.0934	.09309
.16666	.0997	.09942	.0913	.09081	.0935	.09332
.18333	.0999	.09967	.0914	.09099	.0936	.09355
.20000	.1001	.09991	.0915	.09116	.0938	.09375
.21666	.1002	.10013	.0917	.09132	.0939	.09395
.23333	.1003	.10034	.0918	.09148	.0940	.09413
.25000	.1004	.10053	.0919	.09163	.0941	.09429
.26666	.1006	.10072	.0920	.09178	.0943	.09445
.28333	.1007	.10089	.0922	.09192	.0944	.09459
.30000	.1008	.10105	.0922	.09206	.0945	.09473
.31666	.1009	.10121	.0923	.09219	.0946	.09485
.33333	.1010	.10135	.0924	.09232	.0947	.09497
.41666	.1014	.10197	.0928	.09288	.0950	.09541
.50000	.1018	.10243	.0931	.09339	.0953	.09577
.58333	.1021	.10278	.0935	.09380	.0955	.09603
.66666	.1024	.10306	.0938	.09416	.0956	.09622
.75000	.1027	.10328	.0940	.09448	.0959	.09637
.83333	.1029	.10346	.0943	.09474	.0961	.09648
.91666	.1031	.10361	.0945	.09498	.0962	.09658
1.00000	.1033	.10374	.0947	.09518	.0963	.09666
1.08333	.1034	.10385	.0948	.09536	.0964	.09673
1.16666	.1036	.10395	.0949	.09552	.0965	.09679
1.25000	.1038	.10405	.0952	.09566	.0966	.09685
1.33333	.1039	.10414	.0953	.09579	.0967	.09691
1.41666	.1041	.10422	.0955	.09589	.0968	.09697
1.50000	.1043	.10431	.0957	.09600	.0969	.09702
1.58333	.1044	.10439	.0958	.09609	.0970	.09707
1.66666	.1045	.10447	.0960	.09618	.0970	.09712
1.75000	.1046	.10455	.0961	.09626	.0971	.09717
1.83333	.1047	.10462	.0963	.09634	.0972	.09722
1.91666	.1048	.10470	.0964	.09641	.0974	.09727
2.00000	.1049	.10478	.0964	.09648	.0974	.09732
2.16666	.1051	.10493	.0967	.09662	.0975	.09742
2.33333	.1054	.10508	.0969	.09674	.0977	.09752
2.50000	.1055	.10523	.0970	.09686	.0979	.09762
2.66666	.1057	.10538	.0971	.09697	.0979	.09772
2.83333	.1058	.10553	.0973	.09709	.0980	.09782
3.00000	.1060	.10568	.0974	.09720	.0982	.09792
3.16666	.1062	.10583	.0976	.09731	.0983	.09802
3.33333	.1063	.10598	.0977	.09741	.0984	.09812
3.50000	.1065	.10614	.0978	.09752	.0985	.09822
3.66666	.1066	.10629	.0980	.09763	.0987	.09832
3.83333	.1068	.10644	.0981	.09774	.0987	.09842
4.00000	.1069	.10659	.0982	.09784	.0989	.09852
4.16666	.1070	.10674	.0983	.09795	.0989	.09862
4.33333	.1072	.10689	.0983	.09806	.0990	.09872
4.50000	.1073	.10704	.0994	.09816	.0991	.09882
4.66666			.0986	.09827	.0992	.09891
4.83333					.0993	.09901
5.00000					.0994	.09911

Appendix 9. Observed and predicted creep deflection of glass fiber reinforced hardboard. CREEP II; Eff V_f=0.0260; 15.5 lbs; hr; in.

	22		23		24	
Time	Obs	Prd	Obs	Prd	Obs	Prd
0.00000	.0827	.08477	.0834	.08595	.0832	.08534
.01666	.0854	.08517	.0864	.08631	.0862	.08581
.03333	.0860	.08554	.0871	.08664	.0868	.08620
.05000	.0864	.08589	.0875	.08695	.0872	.08657
.06666	.0867	.08621	.0878	.08724	.0875	.08690
.08333	.0870	.08651	.0881	.08752	.0877	.08720
.10000	.0872	.08679	.0883	.08777	.0879	.08748
.11666	.0874	.08705	.0885	.08801	.0880	.08774
.13333	.0876	.08728	.0886	.08824	.0882	.08798
.15000	.0878	.08751	.0888	.08846	.0884	.08820
.16666	.0879	.08771	.0889	.08866	.0885	.08840
.18333	.0880	.08791	.0891	.08885	.0886	.08858
.20000	.0881	.08808	.0892	.08903	.0887	.08875
.21666	.0883	.08825	.0893	.08920	.0888	.08890
.23333	.0884	.08840	.0894	.08936	.0890	.08905
.25000	.0884	.08855	.0895	.08951	.0890	.08918
.26666	.0885	.08868	.0895	.08965	.0891	.08930
.28333	.0886	.08881	.0896	.08979	.0892	.08941
.30000	.0887	.08892	.0897	.08991	.0893	.08952
.31666	.0888	.08903	.0898	.09003	.0893	.08961
.33333	.0889	.08913	.0899	.09014	.0894	.08970
.41666	.0891	.08955	.0902	.09063	.0896	.09005
.50000	.0894	.08984	.0905	.09099	.0898	.09029
.58333	.0896	.09007	.0909	.09127	.0900	.09046
.66666	.0898	.09024	.0910	.09149	.0902	.09058
.75000	.0899	.09037	.0912	.09166	.0904	.09067
.83333	.0901	.09049	.0913	.09180	.0904	.09075
.91666	.0902	.09057	.0915	.09192	.0905	.09081
1.00000	.0904	.09065	.0916	.09202	.0906	.09087
1.08333	.0905	.09073	.0918	.09210	.0907	.09092
1.16666	.0906	.09080	.0919	.09218	.0909	.09097
1.25000	.0907	.09086	.0920	.09225	.0910	.09101
1.33333	.0909	.09092	.0921	.09232	.0910	.09105
1.41666	.0909	.09098	.0922	.09238	.0910	.09109
1.50000	.0910	.09104	.0923	.09245	.0911	.09114
1.58333	.0910	.09110	.0924	.09251	.0911	.09118
1.66666	.0911	.09116	.0925	.09256	.0912	.09122
1.75000	.0912	.09121	.0926	.09262	.0913	.09126
1.83333	.0913	.09127	.0927	.09268	.0914	.09130
1.91666	.0914	.09133	.0928	.09273	.0914	.09134
2.00000	.0915	.09138	.0929	.09279	.0914	.09138
2.16666	.0916	.09150	.0931	.09290	.0915	.09146
2.33333	.0918	.09161	.0932	.09301	.0916	.09154
2.50000	.0920	.09172	.0934	.09312	.0917	.09162
2.66666	.0921	.09183	.0934	.09323	.0918	.09170
2.83333	.0922	.09195	.0935	.09334	.0921	.09178
3.00000	.0923	.09206	.0937	.09344	.0921	.09186
3.16666	.0925	.09217	.0939	.09355	.0922	.09194
3.33333	.0925	.09228	.0939	.09366	.0923	.09203
3.50000	.0926	.09240	.0940	.09377	.0924	.09211
3.66666	.0927	.09251	.0941	.09388	.0924	.09219
3.83333	.0929	.09262	.0942	.09399	.0925	.09227
4.00000	.0930	.09273	.0944	.09410	.0926	.09235
4.16666	.0932	.09285	.0945	.09421	.0926	.09243
4.33333	.0932	.09296	.0946	.09431	.0927	.09251
4.50000	.0932	.09307	.0947	.09442	.0928	.09259
4.66666	.0933	.09314	.0948	.09453	.0929	.09267
4.83333			.0949	.09464	.0929	.09275
5.00000			.0949	.09475	.0930	.09283

Appendix 10. Estimated Burger model creep parameters for glass fiber reinforced hardboard using CREEP I analysis by effective reinforcement volume fraction and load level.

9.09 lbs

Eff V_f	No.	E_e	E_d	η_d	τ	η_v	R
	1	450804	3447882	513390	0.1489	35000000	0.971
0	2	462946	3555847	385809	0.1085	45000000	0.961
	3	477251	3354314	548766	0.1636	67000000	0.954
	4	572202	4166396	659124	0.1582	61000000	0.967
0.0073	5	526726	4339138	790591	0.1822	86000000	0.948
	6	574249	5649868	466114	0.0825	80000000	0.965
	7	584252	4590860	800646	0.1744	95000000	0.996
0.0158	8	630817	7738579	919343	0.1188	69000000	0.970
	9	607234	7562411	722210	0.0955	210000000	0.957
	10	655684	7787669	918166	0.1179	105000000	0.973
0.0260	11	644735	11636030	477077	0.0410	198000000	0.958
	12	665902	7543974	988260	0.1310	122000000	0.972

15.5 lbs

	13	435873	3220401	337498	0.1048	35000000	0.954
0	14	461386	3627235	363812	0.1003	35000000	0.964
	15	476967	3852950	537872	0.1396	35000000	0.970
	16	546074	5288480	765243	0.1447	55000000	0.967
0.0073	17	570114	5322442	910138	0.1710	69000000	0.960
	18	574042	5674378	588433	0.1037	81000000	0.960
	19	636018	5711747	733388	0.1284	65000000	0.958
0.0158	20	671045	6119387	1188385	0.1942	90000000	0.956
	21	648673	6616738	839664	0.1269	95000000	0.964
	22	694458	7986287	1008668	0.1263	85000000	0.970
0.0260	23	688974	7283007	991217	0.1361	88000000	0.963
	24	698253	8217473	877626	0.1068	120000000	0.959

Appendix 11. Estimated Burger model creep parameters for glass fiber reinforced hardboard using CREEP II analysis by effective reinforcement volume fraction and load level.

9.09 lbs

Eff V_f	No.	E_e	E_d	η_d	τ	η_v	R
	1	433838	4766305	1262118	0.2648	35000000	0.988
0	2	444396	5067340	1015495	0.2004	45000000	0.982
	3	456496	4735614	1535760	0.3243	67000000	0.982
	4	550827	5640635	1535381	0.2722	61000000	0.987
0.0073	5	505225	6265267	2736042	0.4367	86000000	0.980
	6	558381	7659592	1022556	0.1335	80000000	0.980
	7	563902	6194928	1950783	0.3149	95000000	0.984
0.0158	8	615658	10750710	2245823	0.2089	69000000	0.986
	9	594778	10025310	1419584	0.1416	210000000	0.977
	10	642475	10104130	1793483	0.1775	105000000	0.987
0.0260	11	637682	14389090	887807	0.0617	198000000	0.964
	12	651276	9926569	1998218	0.2013	122000000	0.988

15.5 lbs

	13	416220	4729469	1014944	0.2146	35000000	0.978
0	14	442803	5227242	998926	0.1911	35000000	0.983
	15	458833	5466257	1448011	0.2649	35000000	0.988
	16	530451	7170311	1801182	0.2512	55000000	0.986
0.0073	17	549973	7669478	2942012	0.3836	69000000	0.984
	18	556780	7941771	1470816	0.1852	81000000	0.979
	19	613212	8232299	2087711	0.2536	65000000	0.982
0.0158	20	646869	8686079	3984304	0.4587	90000000	0.984
	21	630478	9119236	2001672	0.2195	95000000	0.983
	22	677479	10905950	2354595	0.2159	85000000	0.986
0.0260	23	668383	10412260	2743631	0.2635	80000000	0.984
	24	680393	11545420	2197093	0.1903	120000000	0.980

The vita has been removed from the scanned document